



Sedimentological and tectonic studies in the Central Aquitaine basin: constraints on subsidence and deformation of a retro-foreland basin

Master 2 internship report

Supervisors: Mary Ford (CRPG, Nancy)

Frédéric Christophoul (OMP, Toulouse)

Anne-Gaëlle Bader (BRGM, Orléans)

Géraldine ROUGIER – Juin 2014

Master 2 – GPIR : Géosciences Pétrolières et Ingénierie des Réservoirs

Résumé

Le Bassin Aquitain constitue le bassin d'avant-pays du rétropisme nord pyrénéen. Il fait partie des bassins les plus explorés pour ses ressources pétrolières et gazières. Néanmoins, la déformation et la stratigraphie des dépôts syn-orogéniques sont peu documentées. L'interprétation des données de sub-surface (puits pétroliers et profils sismiques) permettent de reconstruire l'histoire sédimentaire pré-, syn- et post-orogénique. Nous présentons une nouvelle lithostratigraphie mésozoïque-cénozoïque complète le long d'un transect NNE-SSO de 120 km, de Saint-Gaudens à Montauban. La coupe est subdivisée en trois zones tectono-stratigraphiques : la plateforme nord, les Petites Pyrénées, la Zone Nord Pyrénéenne. Depuis le Crétacé supérieur, les épaisseurs des séries et la migration des faciès sont contrôlées par les variations de subsidence liées à l'orogenèse pyrénéenne. La chronologie de la déformation alpine et sa distribution sont affinées. La plate-forme au nord n'est pas déformée. Sa sédimentation migre vers l'avant-pays depuis l'Illerdien jusqu'à la base du Miocène et s'accompagne d'une nette diminution d'épaisseur des dépôts marins, devenant vers le nord détritiques et continentaux.

Les dépôts anté-albiens de la Zone Nord-Pyrénéenne très déformés pourraient être la signature d'une tectonique distensive avant la phase de déformation alpine, associée à un diapirisme actif dès le Jurassique. La déformation du bassin liée à l'orogenèse est concentrée sur trente kilomètres et constitue les Petites Pyrénées. C'est un dépôt-centre où reposent plusieurs kilomètres de dépôts turbiditiques crétacés impliqués dans des plis de croissance pluri-kilométriques d'axe SE-NO. La déformation se propage vers le nord au cours du temps et est aussi contrôlée par une activité diapirique probablement initiée dès le Jurassique. Nous montrons le rôle des structures crustales héritées des phases extensives mésozoïques. Par exemple, le Front des Petites Pyrénées, dont le jeu compressif s'échelonne du Crétacé supérieur à l'Oligocène, est scellé par les dépôts détritiques miocènes. Le Chevauchement Frontal Nord Pyrénéen correspond à l'inversion de la bordure nord du bassin albo-cénomanien qui contrôlait sa sédimentation. Les dépôts du Crétacé supérieur scellent son activité.

Ce projet rentre dans le cadre de l'ANR PYRAMID et est financé par le BRGM (RGF-Pyrénées).

Mots clés : rétro-bassin, Pyrénées, subsidence, lithostratigraphie

Abstract

The Aquitaine basin is the retro-foreland basin associated with the north Pyrenean retro-wedge. It is one of the most explored hydrocarbon retro-foreland basins in the world. However, the stratigraphy of syn-orogenic deposits and their deformation history are poorly documented in literature. Interpretations of subsurface data, such as seismic lines and well data, are used to reconstruct pre-, syn- and post-orogenic sedimentary history. In this study we provide a new lithostratigraphy along a 120 km transect, from Saint-Gaudens to Montauban. The section is divided into three tectonostratigraphic zones, the northern platform, the Petites Pyrenees and the North Pyrenean Zone. Since the Late Cretaceous, series thickness and facies migrations have been controlled by subsidence variations linked to Pyrenean orogenesis and halokinesis. Alpine deformation chronology and its distribution within the basin are here refined.

The northern platform is not deformed. Here, sedimentation migrated toward the north from Ilerdian to the base of Miocene. Marine deposits thin northwards and become pass progressively northward into detrital and continental facies.

The deformation of the basin linked to the orogeny constitutes a 30 km wide area: the Petites Pyrenees. It is an inverted depocentre consisting of several kilometers of Cretaceous turbiditic deposits, lying in kilometric SE-NW growth folds. Compressional deformation propagated northwards with time and strongly influenced by halokinesis of Keuper deposits that probably initiated in Jurassic time. We show the role of inherited crustal structures from Mesozoic extensional phases. The Petites Pyrenees Front is a reactivated fault active from Late Cretaceous to Oligocene and sealed by Miocene strata. In the North Pyrenean Zone, the North Pyrenean Thrust controlled the former border of an Albo-Cenomanian basin and its activity is sealed by Upper Cretaceous deposits.

In the North Pyrenean Zone, deformed Albo-Cenomanian deposits could be the result of a tectonic extension occurred before Iberia/Europe convergence.

This project is part of ANR PYRAMID and is founded by the BRGM (RGF-Pyrenees).

Key words: retro-foreland basin, Pyrenees, subsidence, lithostratigraphy

Remerciements

Je tiens tout d'abord à remercier Mary Ford pour m'avoir proposé ce passionnant sujet de deux ans et pour m'avoir fait confiance tout au long du projet. Ce stage a été pour moi une expérience très riche pendant laquelle j'ai énormément appris et me suis beaucoup investi. Merci pour m'avoir donné la possibilité de présenter mes travaux au congrès Pyramid en novembre dernier, et de m'avoir permis de participer à la formation PetroMod à Aachen. Merci pour votre patience, vos encouragements et votre expertise sur les bassins d'avant-pays et en géologie structurale, j'ai bien cru qu'on n'arriverait jamais à restaurer cette coupe (!!).

Un grand merci à Frédéric Christophoul d'avoir quitté durant quelques mois Toulouse pour venir aider toute l'équipe Pyramid du CRPG, et pour le nombre incalculable de fois que je l'ai dérangé ! Votre disponibilité et votre expertise sur la stratigraphie et sédimentologie du Bassin aquitain nous ont été très précieuses.

Je tiens également à remercier Anne-Gaëlle Bader pour son accueil à Orléans et pour nous avoir permis de collaborer avec le BRGM ; ainsi qu'à Thierry Baudin et son équipe qui ont choisi notre sujet de Master 2 pour le chantier RGF Pyrénées. De plus, je souhaite remercier Cédric Carpentier pour être venu plusieurs fois nous aider et pour tous ses bons conseils.

Merci à mes collègues de bureau, Louis Hemmer (« on va à l'inist ? »), Larissa NGomby et ses gâteaux, Arjan Grool (bon courage pour la poursuite de ta thèse) pour ses relectures et ses conseils. Merci aussi à mes amis François Turlin et Guillaume Barré de m'avoir supporté pendant ces deux années (à bientôt au Québec !), à mes parents et mon frère pour leur soutien.

Avant-propos

Ce projet de Master 2 s'est déroulé de février à juillet 2014 au Centre de Recherches Pétrographiques et Géochimiques (CRPG) (UMR 7358, Vandoeuvre-les-Nancy). Le CRPG est un laboratoire du CNRS, et fait partie de l'OSU OTELo qui est un des pôles de recherche de l'Université de Lorraine. Il a été créé par Marcel Roubault en 1953, et est actuellement dirigé par Christian France-Lanord.

Cette étude s'insère dans la thématique « Tectonique, Erosion et Evolution du relief » du laboratoire et s'inscrit dans le cadre de l'ANR PYRAMID¹, conduite par Mary Ford. Ce programme, débuté en Mai 2012, s'intéresse au système d'avant-pays associé à la chaîne pyrénéenne. Les quatre objectifs principaux de ce projet sont les suivants : il s'agit (1) de contraindre la structure et l'architecture du système d'avant-pays ; (2) de faire un lien entre les systèmes de transport des sédiments et les processus d'exhumation à l'évolution d'un bassin d'avant-pays ; (3) de quantifier les interactions fluides-roches-déformation ainsi que la migration et l'expulsion des fluides tout au long des phases d'extension et de compression ; (4) de modéliser les processus géodynamiques. Mon projet s'inscrit directement dans la première tache et une sous-partie de la deuxième tâche qui a pour objectif de contraindre la chronologie, l'ampleur et l'architecture de la déformation du Bassin aquitain.

Par ailleurs ce projet, financé par le BRGM, rentre dans le cadre du Référentiel Géologique de la France (RGF) dont le premier chantier régional est consacré aux Pyrénées. Il s'insère plus particulièrement dans la thématique « Sédimentologie des bassins tertiaires de la Zone Nord-Pyrénéenne » et a pour objectif d'harmoniser toutes les données géologiques relatives à ce domaine d'étude. Ma contribution se fait sous la forme de l'élaboration d'un lexique dans lequel un inventaire des différentes formations rencontrées à travers sept cartes géologiques dans le Bassin Aquitain central est réalisé.

Ce travail fait suite aux travaux de Master 1 qui ont conduit à réaliser une analyse préliminaire de la zone d'étude permettant de définir les grands axes d'approche pour la présente étude. Une étude structurale sur une centaine de kilomètres dans l'avant-pays pyrénéen ainsi qu'une analyse de subsidence et de diaglyphies de quelques puits au nord du bassin avaient été réalisées. Ce rapport présente une étude stratigraphique, structurale et de subsidence plus détaillée et plus approfondie afin de pouvoir répondre aux problématiques soulevées.

¹ Pyramid: North PYRenees: Integrated Assessment of fluid Migration history, rift Inversion, the role of surface processes and Deformation in the evolution of an orogenic retro-wedge and its foreland basin.

Table of contents

1. Introduction.....	1
2. Geological context.....	3
Main structures	3
Study area	5
Methodology	6
3. Chrono- & litho-stratigraphy in the Central Aquitaine basin	9
North-South Stratigraphy.....	9
West-East Stratigraphic correlation.....	10
Lithofacies associations.....	12
Groups and Formations.....	13
Main unconformities.....	18
4. Interpretation of seismic data.....	20
Construction of a velocity model	20
Seismic stratigraphy	20
5. Balanced cross-section	26
6. Subsidence analysis	32
7. Discussion.....	38
Interpretation of subsidence history	38
Paleogeographic evolution	40
Sequential restoration and evolution of Pyrenean retro-foreland basin.....	41
8. Conclusion	45
9. References	46
10. Appendices	50
List of Appendices	50

List of illustrations

FIGURE 1: SIMPLIFIED MAP OF THE PYRENEAN RETRO-FORELAND SYSTEM. STUDY AREA IS OUTLINED BY BOX. (MODIFIED FROM CHOUKROUNE 1976 AND BITEAU ET AL. 2006)	2
FIGURE 2: SCHEMATIC REPRESENTATION OF THE CONTRASTING CHARACTERISTICS OF PRO-FORELAND AND RETRO-FORELAND BASINS, MODIFIED FROM NAYLOR AND SINCLAIR (2008).....	3
FIGURE 3: GENERAL MAP OF THE PYRENEES SHOWING THE TWO PARTS OF THE DOUBLE VERGANT MOUNTAIN CHAIN: TO THE SOUTH THE PRO-FORELAND SYSTEM MADE OF THE PRO-WEDGE AND THE EBRO BASIN; AND TO THE NORTH THE RETRO-FORELAND SYSTEM COMPOSED OF THE RETRO-WEDGE AD THE AQUITAINE BASIN. THE PURPLE LINE CORRESPONDS TO THE STUDIED TRANSECT (FROM VERGES ET AL., 2012).....	4
FIGURE 4: ZOOM ON THE STUDY AREA SHOWING THE BOREHOLES USED IN THE CONSTRUCTION OF THE STRUCTURAL CROSS-SECTION; THE MAIN STRUCTURAL ZONES, AND THE POSITION OF THE SEISMIC PROFILE. FOR THE LEGEND, PLEASE REPORT TO FIGURE 1	6
FIGURE 5: STRUCTURAL MAP OF THE SOUTHERN PART OF THE STUDY AREA, INCLUDING THE NPZ AND THE PETITES PYRENEES, SHOWING THE MAIN STRUCTURAL AND LITHOLOGICAL UNITS (REPORT TO FIG.7 TO SEE THE AGE AND FACIES OF THE UNITS), LOCATIONS OF THE CROSS-SECTION AND THE SEISMIC PROFILE. IT HAS BEEN CONSTRUCTED USING GEOLOGICAL MAPS (1/50 000) (FEUILLES SAINT-GAUDENS AND FOUSSET). NPFT FOR NORTH PYRENEAN FRONTAL THRUST: PPF FOR PETITES PYRENEES FRONT. FOR THE RESPECTIVE AGES, PLEASE REPORT TO CHAPTER 3 "CHRONO- AND LITHO-STRATIGRAPHY IN THE CENTRAL AQUITAINE BASIN; FIG.9).....	7
FIGURE 6: GENERAL CHRONOSTRATIGRAPHY OF THE CENTRAL AND EASTERN PYRENEES. (CHRISTOPHOU & BERNARD (S1), FORD (S2), GROOL (S3), HEMMER (S4), ROUGIER (S5), NGOMBY MAVOUNGOU (S6), 2014). THE LOCATION OF THESE SECTIONS IS SHOWN IN APPENDIX 3. THE TOULOUSE FAULT IS LOCATED BETWEEN THE S4 AND S5.....	11
FIGURE 7: LITHOFACIES ASSOCIATIONS AND THE ASSOCIATED SHAPES USED IN THE CONSTRUCTION OF THE CHRONO-STRATIGRAPHY AND THE LITHO-STRATIGRAPHY.....	12
FIGURE 8: SCHEMATIC REPRESENTATION OF (A) A CARBONATE PLATFORM WITH A BARRIER REEF AND (B) A RAMP, SHOWING THE LITHOFACIES ASSOCIATIONS USED IN THIS STUDY FOR THE CONSTRUCTION OF THE CHRONO- AND LITHO-STRATIGRAPHY.....	14
FIGURE 9: CHRONOSTRATIGRAPHY OF THE STUDY AREA	15
FIGURE 10: LITHOSTRATIGRAPHY OF THE STUDY AREA	19
FIGURE 11: SEISMIC PROFILE AND INTERPRETATION IN THE STABLE PLATFORM AROUND THE BOREHOLE AG-1. IT SHOWS THE MAJOR REFLECTORS CORRESPONDING TO THE TOP OF STRATIGRAPHIC GROUPS: R1 (COUSTOUGE GROUP); R2 (RIEBACH GROUP), R3 (PETITES PYRENEES GROUP); R4 (DOGGER); R5 (KEUPER GROUP); R6 (BASEMENT); R7 (CARCASSONNE GROUP)	21
FIGURE 12: SEISMIC PROFILE AND INTERPRETATION IN THE STABLE PLATFORM AROUND THE BOREHOLE MTG1. IT SHOWS THE MAJOR REFLECTORS CORRESPONDING TO THE TOP OF STRATIGRAPHIC GROUPS: R1 (COUSTOUGE GROUP, FIRST EROSIONAL SURFACE); R2 (RIEBACH GROUP), R3 (PETITES PYRENEES GROUP); R4 (DOGGER); R5 (KEUPER GROUP); R6 (BASEMENT); R7 (CARCASSONNE GROUP; SECOND EROSIONAL SURFACE); R8 (THIRD EROSIONAL SURFACE)	23
FIGURE 13: SEISMIC PROFILE AND INTERPRETATION IN THE STABLE PLATFORM AROUND THE PETITES PYRENEES FRONT. IT SHOWS THE MAJOR REFLECTORS CORRESPONDING TO THE TOP OF STRATIGRAPHIC GROUPS: R1 (COUSTOUGE GROUP, FIRST EROSIONAL SURFACE); R2 (RIEBACH GROUP), R3 (PETITES PYRENEES GROUP); R4 (DOGGER); R5 (KEUPER GROUP); R6 (BASEMENT); R7 (CARCASSONNE GROUP). THIS FIGURE SHOWS THE OFFLAPS ABOVE THE THRUST FRONT REVEALING THE GROWTH OF THE THRUST, SEALED BY THE PASSIVE ONLAPS. THIS IS THE TRANSITION BETWEEN THE PETITES PYRENEES AND THE STABLE PLATFORM	24
FIGURE 14: SEISMIC PROFILE AND INTERPRETATION IN THE STABLE PLATFORM IN THE PETITES PYRENEES IT SHOWS THE MAJOR REFLECTORS CORRESPONDING TO THE TOP OF STRATIGRAPHIC GROUPS: R1 (COUSTOUGE GROUP); R2 (RIEBACH GROUP), R3 (PETITES PYRENEES GROUP); R7 (CARCASSONNE GROUP). IT SHOWS THE SUCCESSION OF ANTICLINES AND SYNCLINES AND THE TRANSITION WITH THE STABLE PLATFORM BY THE PETITES PYRENEES FRONT.	25
FIGURE 15: BALANCED CROSS-SECTION ALONG THE STUDIED TRANSECT.....	27
FIGURE 16: REPRESENTATION OF THE EVOLUTION OF A SALT DIAPIR: REACTIVE (ACTIVE) DIAPIRISM DURING EXTENSION, PASSIVE DIAPIRISM WHEN SEDIMENT LOAD IS IMPORTANT, THE SALT IS THUS FORCED TO MIGRATE (FROM FOSSEN, 2010)	29
FIGURE 17: REPRESENTATION OF AN INVERTED NORMAL FAULT. AT THE BASE OF THE FAULT THE DISPLACEMENT IS NORMAL, AT THE TOP IT IS INVERTED. THE NOD POINT CORRESPONDS TO ZERO DISPLACEMENT.	31

FIGURE 18: DECOMPACTION CURVES FOR THE BOREHOLE AV-101, REALIZED WITH PETROMOD.....	34
FIGURE 19: DECOMPACTION CURVES FOR THE BOREHOLE MTG-1, REALIZED WITH PETROMOD	35
FIGURE 20: DECOMPACTION CURVES FOR THE BOREHOLE SA-1, REALIZED WITH PETROMOD	36
FIGURE 21: DECOMPACTION CURVES FOR THE BOREHOLE PSI-1, REALIZED WITH PETROMOD	37
FIGURE 22: SUMMARIZING PLOT OF THE TOTAL SUBSIDENCE REALIZED FOR 4 BOREHOLES (AV-101, MTG-1, SA-1 AND PSI-1) WITH SUBSIDENCE.EXE.....	38
FIGURE 23: SEQUENTIAL RESTORATION OF THE BALANCED CROSS-SECTION (SEE FIG. 15) INTO FOUR STEPS. THE SHORTENING BETWEEN THE END OF APTO-LOWER ALBIAN AND THE PRESENT SECTION IS ESTIMATED AT 22%.....	42
FIGURE 24: SCHEMATIC REPRESENTATION OF THE RATIO USED (2:1) TO CONSTRUCT THE OVERHANGING BLOCK IN THE CONSTRUCTION OF THE RESTORATION (SECOND STEP), WHERE "X" IS THE LENGTH OF THE BASIN MARGIN.	43

List of tables

TABLE 1 : CHARACTERISTICS OF THE 21 WELLS USED IN THIS STUDY: NAME, LOCALITY, COORDINATES (LAMBERT 2 ÉTENDU), YEAR OF DRILLING, DEPTH AND ALTITUDE IN METRES (FROM INFO TERRE, BRGM WEBSITE)	8
---	---

1. Introduction

The Aquitaine basin is one of the most explored retro-foreland basins in the world. Regional exploration and exploitation of oil and gas resources have been intense over the last 60 years. This is the foreland basin associated with the north Pyrenean retro-wedge that was generated by the convergence of the Iberian and European plates. It developed on the overriding European plate, while the Ebro basin lying on the subducting Iberian plate constitutes the pro-foreland basin (Munoz, 1992; Roure et al., 1990). From Late Cretaceous to Miocene times, the Pyrenean orogeny generated a fold-and-thrust belt consisting of deformed Mesozoic and Cenozoic sub-basins.

From recent studies, retro-foreland basins are thought to preserve a complete syn-orogenic stratigraphic history. They display a condensed record of sedimentation as the basin does not migrate (or to a very limited degree) towards the foreland (Naylor & Sinclair, 2008). In contrast, in the pro-foreland basin these authors show onlaps onto the pro-foreland forebulge indicating a series of disconnected successive depocentres due to relatively important migration. Furthermore, these authors suggest that retro-foreland basins are narrower than pro-basins. Their model subdivides orogenesis into two periods: (i) growth due to orogenic-wedge accretion and (ii) stabilization of the mountain chain after convergence has stopped; subsidence is then only due to sedimentation. Subsidence rate is considered to be constant during the growth phase in the retro-foreland basin; it decreases with time and is null during the quiescence phase (Sinclair & Naylor, 2012).

In the case of the north Pyrenean foreland, early propagation of the retro-wedge thrust front occurred from Late Campanian until Early Eocene (Sinclair et al., 2005), associated with the inversion of extensional structures and the growth of the pro-wedge. Using thermochronology, magnetostratigraphic data and sediment rates in the two foreland basins, these authors create sand-box experiments representing a flux-based evolutionary model. They demonstrate that the ending of pro-wedge frontal accretion led to accretion in the retro-wedge resulting in internal thickening. This may have been developed between Middle Eocene and Upper Eocene. In contrast to the pro-side, the retro-wedge thrust front activity ceased in the Priabonian according to Sinclair et al. (2005).

The aim of this work is to use the Central Aquitaine basin as a detailed case study to address the following questions: what are the controlling factors on a retro-foreland system and what are the structural characteristics? What is the influence/control of the Pyrenean orogeny on the sedimentation? What was its chronology? What role did salt play in deformation of the foreland area? What role did crustal structures inherited from the pre-convergence tectonic history play? How did they influence the actual basinal and structural geometries? What is the amount of shortening? What is the evolution of the subsidence history and what is its driving force? What is the part of tectonic subsidence

inferred from the total subsidence? How can we interpret the subsidence curves in terms of regional tectonic events?

Although this basin has been well-studied, the stratigraphy of syn-orogenic deposits and their deformation history are poorly documented in literature as they are not of interest to petroleum industry. The first objective of our work was to provide a new litho- and chrono-stratigraphy along a 120 km-long transect, from Saint-Gaudens to Montauban (fig.1). The second objective was to study the foreland deformation style along this section based on the examination on geological maps, borehole data and seismic lines, most of poor-quality. Three zones with different deformation styles are identified: the North Pyrenean Zone (ZNP), the Petites Pyrenees, and the northern platform. In each zone structures are defined including thrust faults, fold, growth folds and salt diapirs.

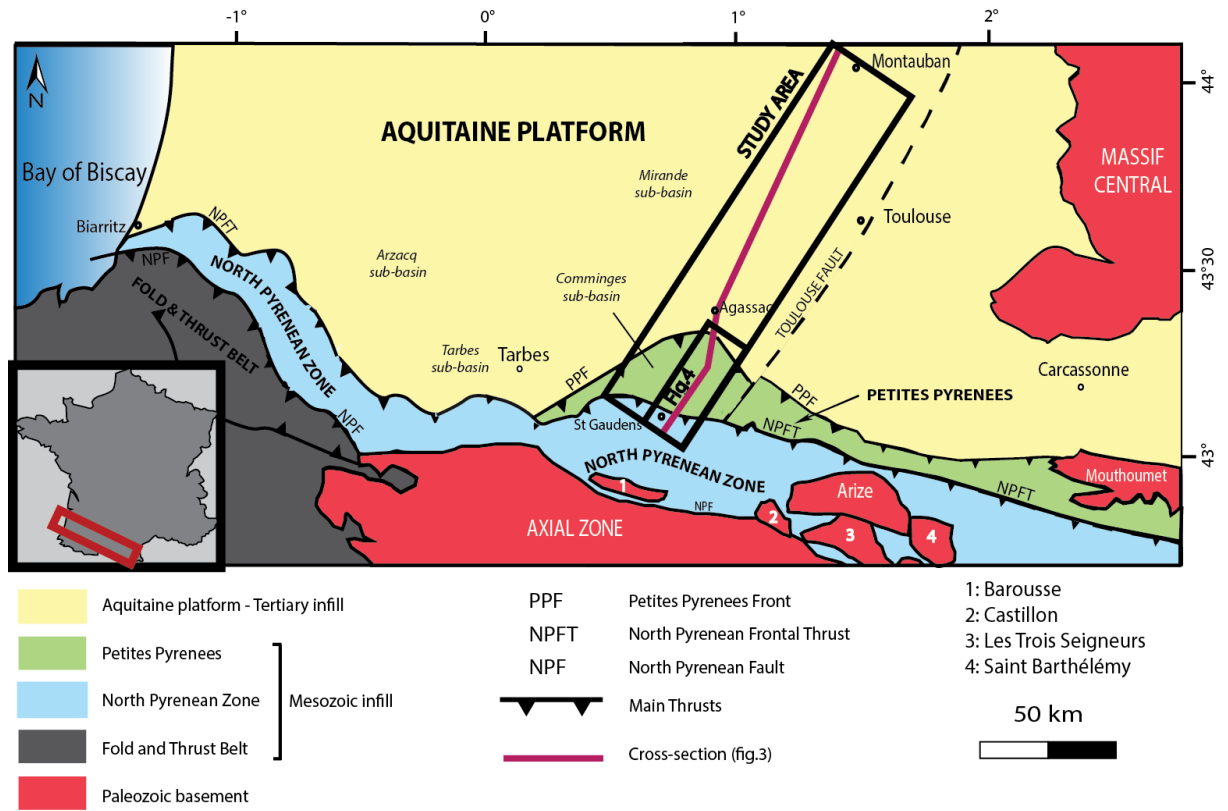


Figure 1: Simplified map of the Pyrenean retro-foreland system. Study area is outlined by box. (modified from Choukroune 1976 and Biteau et al. 2006)

These structures are sequentially restored constrained by detailed stratigraphic geometries. The amount, timing and distribution of shortening due to Pyrenean compression within the retro-foreland basin can thus be estimated. We discuss the role of palaeo-relief on the Paleozoic substratum (Choukroune, 1974), inherited crustal structures from Mesozoic extensional phases (Debroas, 1990; Baby et al., 1988) as well as Keuper evaporite diapirism (Jammes et al., 2010; Ferrer et al., 2012) these features may have a crucial control on the mechanics and the distribution of the deformation. Since the Late Cretaceous, series thicknesses and facies migrations were controlled by

subsidence variations linked to Pyrenean orogenesis and salt tectonics. Consequently, the final objective of the present study is the construction of subsidence curves along the whole transect. Results from these analyses enable us to define and constrain the timing of alpine deformation, its distribution in time and space, and the subsidence history in the Central Aquitaine basin. Finally, we comment on published models for the retro-foreland basins of Naylor & Sinclair (2008), Sinclair & Naylor (2012), and Sinclair et al (2005).

2. Geological context

Main structures

The Pyrenean orogen has two foreland systems, the Aquitaine foreland system composed of the retro-wedge and retro-basin (French side) and the Ebro foreland system composed of its pro-wedge and pro-basin (Spanish side)(fig.2). These two sides are separated by the Axial Zone (fig.3). This zone is an antiformal stack that comprises crystalline basement rocks and locally preserved Permian, Triassic, and Cretaceous cover (Verges et al., 2012). After several episodes of crustal thinning and rifting from Early Trias until Early Cretaceous, the convergence between these two plates is thought to have begun during Late Cretaceous (Santonian times) and completed in Miocene times. N-S convergence between Iberia and Europe led to a N100°-110° oriented mountain range with double vergence (Sinclair et al., 2005). The shortening accommodated by upper crustal thickening is estimated as about 165 km (Munoz, 1992; Beaumont et al., 2000).

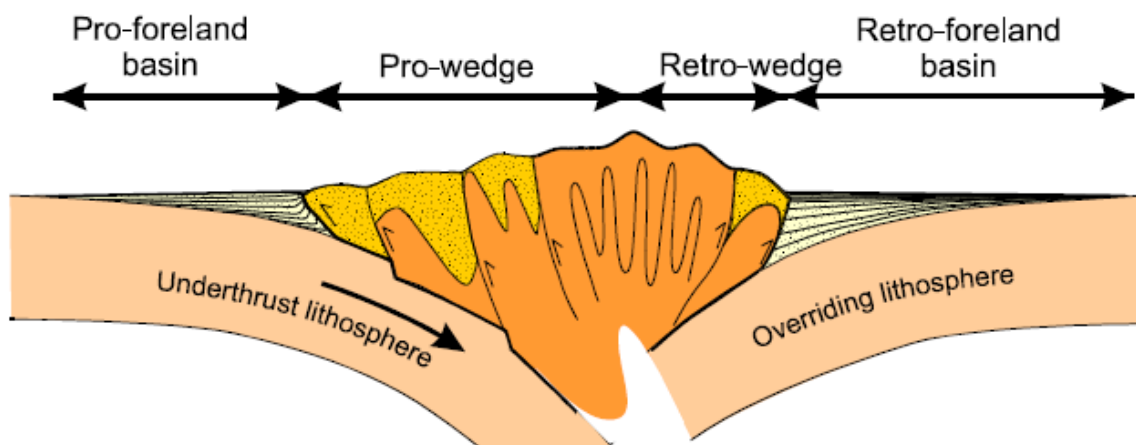


Figure 2: Schematic representation of the contrasting characteristics of pro-foreland and retro-foreland basins, modified from Naylor and Sinclair (2008)

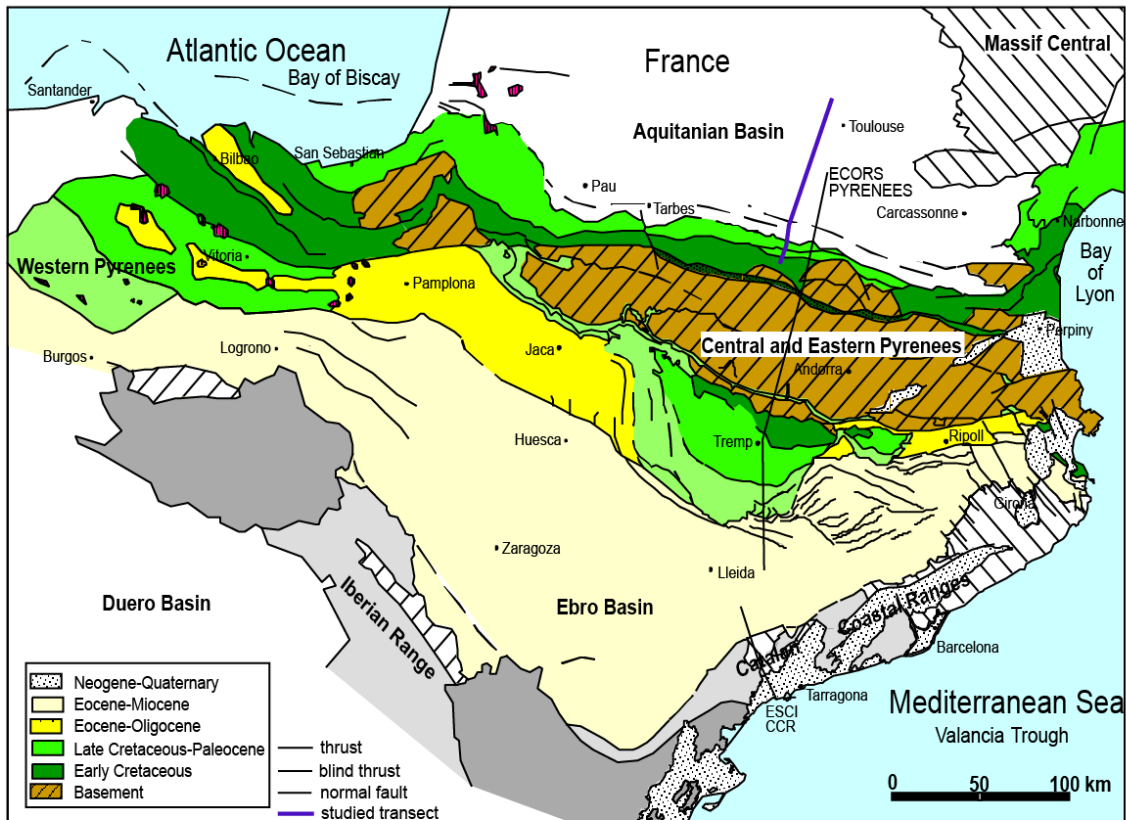


Figure 3: General map of the Pyrenees showing the two parts of the double vergent mountain chain: to the south the pro-foreland system made of the pro-wedge and the Ebro basin; and to the north the retro-foreland system composed of the retro-wedge ad the Aquitaine basin. The purple line corresponds to the studied transect (from Verges et al., 2012)

In the present study we focus on the northern foreland system, and more particularly on the central eastern Aquitaine foreland basin, within which three tectonostratigraphic units are defined. From north to south these are (fig.1):

- (i) The slightly deformed Aquitaine platform integrating Mesozoic and Tertiary deposits over a Paleozoic basement; it extends to the north towards the Variscan French Massif Central.

- (ii) The Sub-Pyrenean Zone (SPZ) or Petites Pyrenees, is overthrust by the NPZ along the North Pyrenean Frontal Thrust (NPFT) to the south and delimited to the north by the Petites Pyrenees Front (PPF). The PPF is also a major south-dipping thrust sealed by post-orogenic sediments, which has been recognized thanks to geophysical prospection (fig. 13). The SPZ is composed of folded pre- and syn-orogenic sediments lying in several sub-basins, such as Comminges, Arzacq, Mirande or Tarbes for instance. These folds are sealed by Miocene and younger post-orogenic strata.

- (iii) The North Pyrenean Zone (NPZ), delimited to the south by the E-W steeply dipping North Pyrenean Fault (NPF), is characterized by extremely deformed Mesozoic deposits in thrust sheets, Paleozoic sediments and metasediments and crystalline basement forming the external crystalline massifs. Many known Albo-Cenomanian

basins (Bigorre basin, Debroas 1990; Camarade basin, Baby 1988) lie in the immediate hanging wall of the south-dipping North Pyrenean Frontal Thrust (NPTF).

Study area

The study area is located in the central foreland basin, from south of Saint-Gaudens to the north of Montauban (fig. 4). This 120 km-long transect has a SSW-NNE trend from Estabens to Aurignac; a N-S trend from Aurignac to Agassac; a SSW-NNE trend from Agassac to the northern end of the section.

From south to north it cuts through several structures (fig.4):

(1) the NPZ extending towards Castillon (fig. 5) where the Albo-Cenomanian basin constitutes a 10 km-wide north-dipping monocline. The NPFT is a salt-injected structure and is partly hidden by post-orogenic deposits in this area, while it outcrops in the eastern part of the Saint-Gaudens map (Paris et al. 1971).

(2) The SPZ, also termed in this area “Petites Pyrenees” from Castillon to Saint-André (fig.5). First order folds are identified in the NPZ and the SPZ: (i) the Cabanes syncline and (ii) the Lôo anticline in the NZP showing a WSW-ENE axis; (iii) the Latoue syncline, (iv) the Proupiary anticline, (v) the Frechet syncline, (vi) the Aurignac anticline and (vii) Saint-André anticline in the SPZ that all display a NW-SE axial trend. This part of the Petites Pyrenees zone is called the Comminges sub-basin. This zone has been intensely drilled especially in the Aurignac and Proupiary anticlines as it is very rich in natural oil and gas resources (Biteau et al., 2006). The Saint-Marcel field (the western extension of the Proupiary anticline) is the best-known gas field in the Comminges sub-basin that was exploited for more than 50 years since 1949.

(3) The stable northern platform constitutes the northern part of the transect. The Aquitaine platform is covered by Miocene detrital deposits and Quaternary alluvium. In the study area, this part of the platform is termed the Mirande sub-basin. Less rich in natural resources, the density of wells is much lower in this zone than in the Petites Pyrenees.

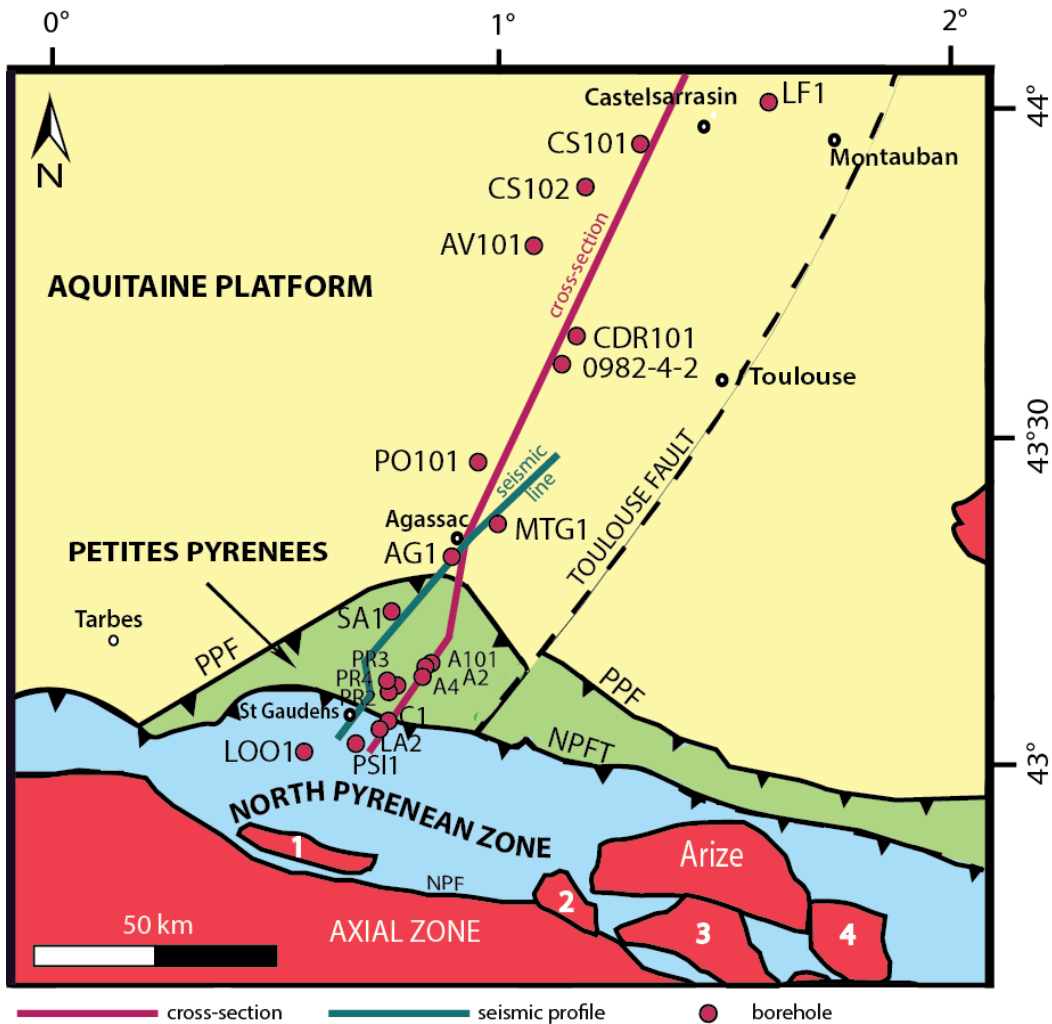


Figure 4: Zoom on the study area showing the boreholes used in the construction of the structural cross-section; the main structural zones, and the position of the seismic profile. For the legend, please report to figure 1

Methodology

In order to provide a detailed analysis of the study area, 21 wells (fig.4) are used in addition to the following eight geological maps (1/50 000) published by the BRGM (Appendix 1):

Montréjeau (n°1054)	Gimont (n°982)
Saint-Gaudens (n°1055)	Beaumont-de-Lomagne (n°955)
Le Fousseret (n°1033)	Saint-Nicolas de la Grave (n°929)
Lombez (n°1008)	Montauban (n°930)

The maps constrain lithostratigraphic boundaries at surface as well as providing dips and information on thicknesses of layers.

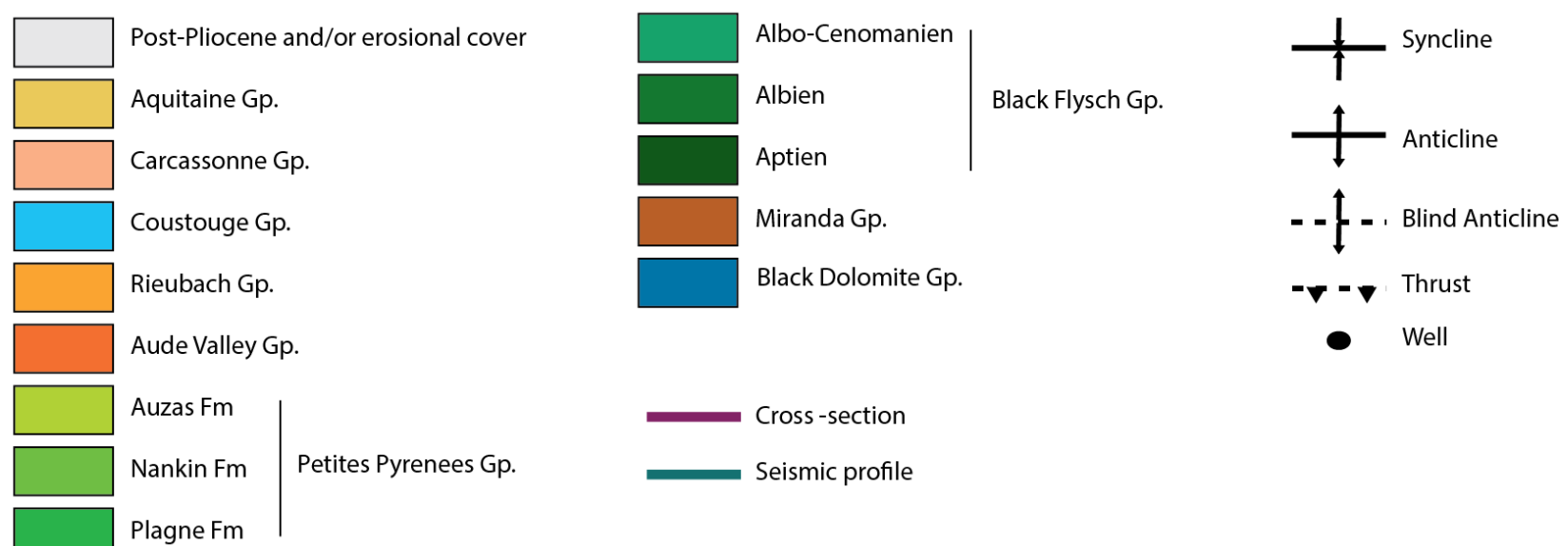
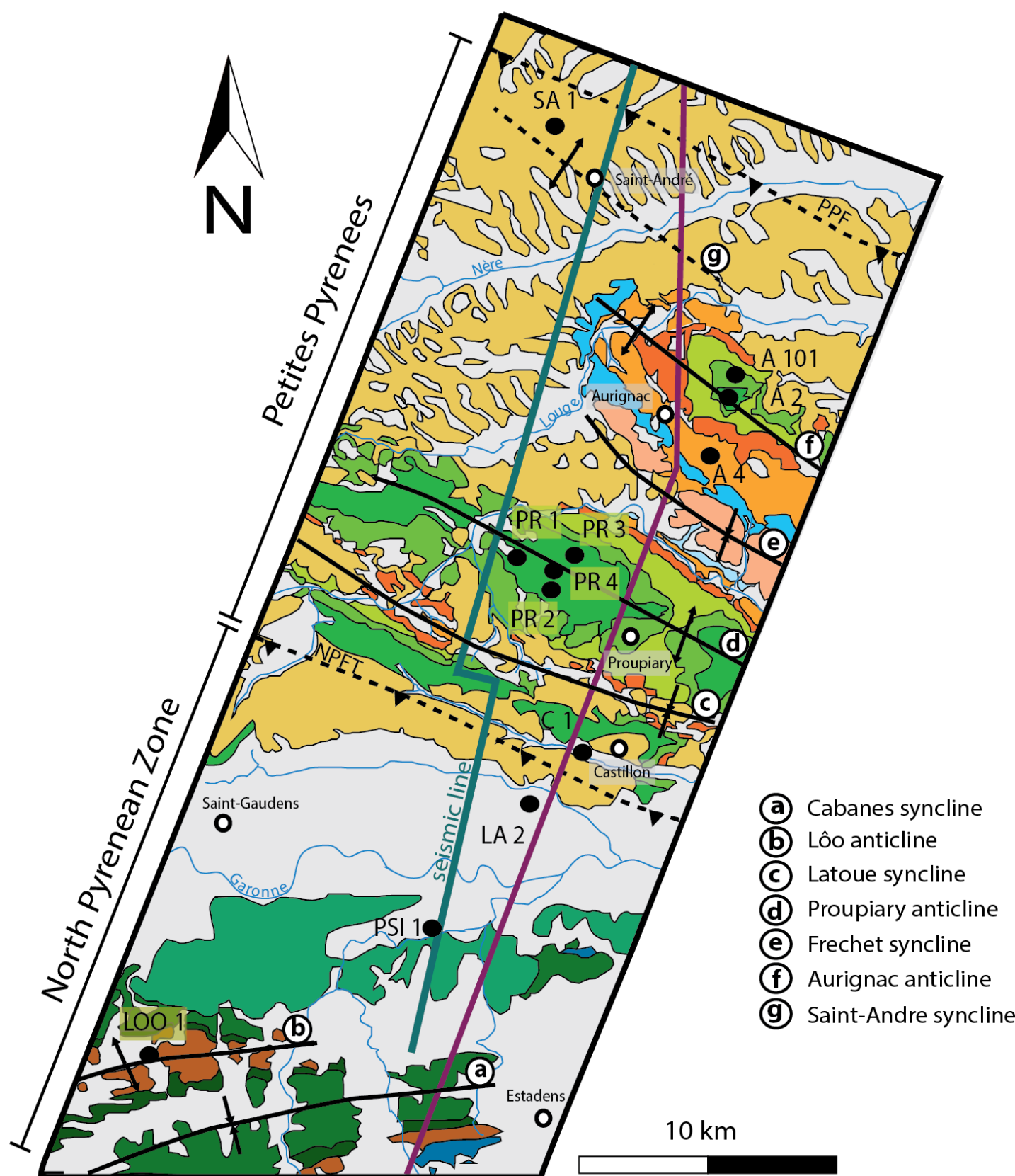


Figure 5: Structural map of the southern part of the study area, including the NPZ and the Petites Pyrenees, showing the main structural and lithological units (report to fig. 7 to see the age and facies of the units), locations of the cross-section and the seismic profile. It has been constructed using geological maps (1/50 000) (Feuilles Saint-Gaudens and Fousseret). NPFT for North Pyrenean Frontal Thrust; PPF for Petites Pyrenees Front. For the respective ages, please report to Chapter 3 "Chrono-and litho-stratigraphy in the Central Aquitaine basin; fig.9)

Well data are available on InfoTerre (BRGM website, Table 1, Fig. 4, and Appendices 4 to 24). They all lie within 10 km of the section line. Six wells reach the crystalline basement (LF-1; CS-101, CS-102, AV-101, CDR-101 in the platform and LA-2 in the NPZ). An orthogonal projection onto the cross-section is required, except for 4 wells (Lôo-1, A-101, A-4, A-2) that are projected parallel to the relevant anticlinal axial plane. For each well, the depth, the year of drilling and the altitude are listed in Table 1. The location of the wells is shown in figure 4.

Well name	Locality	Coordinates Lambert 2 étendu (m)		Year of drilling	Depth (m)	Altitude (m)
		X	Y			
LF1	La Française	516110,0	1899999	1958	547,0	77,2
CS101		494604,4	1892452	1957	609,5	84,2
CS102	Castelsarrasin	487073,2	1882936	1958	1685,0	149,2
AV101	Avensac	480666,0	1871988	1957	2329,2	176,1
CDR101	Cadours	493513,0	1860252	1959	1913,7	162,6
0982-4-2	Saint-Cricq	491837,0	1855226	1967	1035,0	153,0
PO101	Polastron	481797,0	1836597	1958	2748,2	214,9
MTG1	Montaigut	488411,0	1827958	1978	4283,0	196,0
AG1	Agassac	482804,0	1818637	1959	3440,0	215,0
SA1	Saint-André	478214,0	1810777	1957	4202,4	305,0
A101		483873,0	1803720	1969	4405,5	386,9
A2	Aurignac	483702,0	1803139	1947	2419,7	391,0
A4		483120,0	1801387	1955	3960,6	397,6
PR3		478910,0	1798565	1948	2782,0	360,0
PR1	Proupiary	477057,0	1798547	1945	2299,5	405,0
PR4		478229,0	1798105	1949	2042,2	381,8
PR2		478118,0	1797634	1947	2725,4	425,0
C1	Castillon	479096,0	1793075	1949	2786,9	334,4
LA2	Labarthe	477472,0	1791584	1952	2393,2	363,4
PSI1	Pointis-Inard	474433,0	1788080	1970	3301,5	337,5
LOO1	Lôo	465503,0	1784501	1954	3052,7	435,0

Table 1 : Characteristics of the 21 wells used in this study: name, locality, coordinates (Lambert 2 étendu), year of drilling, depth and altitude in metres (from InfoTerre, BRGM website)

Lithological descriptions, biostratigraphic data and well logs are available in the survey reports of each well provided by the BRGM (InfoTerre) and via the Bureau Exploration-Production des Hydrocarbures (BEPH) database. This very large database lists all the documents available for every well drilled in the Aquitaine basin (seismic profiles, stratigraphic logs, well logs, survey reports). The stratigraphy and the lithologies are most of time better detailed in theses survey reports than on the InfoTerre site.

We used the software Move™ 2014.1 to build a 3D database. All the wells were represented as lithostratigraphic columns below the georeferenced geological maps that are themselves projected onto the regional digital elevation model (DEM; ASTER). Dipmeter measurements and well deviations (Appendices 4 to 24) are added on these columns and are useful to have a quick overview of the structures at depth.

We also used a seismic profile to guide us in subsurface structural interpretations. This line starts at the northwest of Estabens (fig.5) and is sub-parallel to the cross-section to the southern part of the Petites Pyrenees (NE trend). Then the seismic line marks a sudden divergence to the west, and it finally has a continuous NE trend to the east of Polastron (fig.4). Thus, it crosses through the NPZ, the Petites Pyrenees and the south of the northern platform. It is not parallel to the cross-section, so boreholes, which have been converted into time, also need to be projected on it. Sometimes, the location from where the well is projected has a different altitude from the point of projection on the seismic line. In order to minimize the risk of variations of the altitudes, a vertical shift is made manually so that the wells and the seismic profile match. The vertical scale of this profile reaches 5seconds.

Finally, comparisons are made between our structural cross-section and previous interpreted work (Paris et al., 1971; Héritier et al., 1972; Debroas, 1990; Bourrouilh et al., 1995; Total database, 1998; Serrano et al., 2006).

3. Chrono- & litho-stratigraphy in the Central Aquitaine basin

In this section we present a chrono-stratigraphy and a litho-stratigraphy of the central foreland basin along a NNE-SSW transect. In order to apprehend the spatial distribution and thus the basin fill architecture, we adopt a harmonized approach along the whole transect so data can be more easily compared. To this end, we carried out an inventory of all stratigraphic units in boreholes along the segment, we defined a series of lithofacies associations and we created lithostratigraphic groups. This work was carried out along cross-sections to the east and west to present section in order to establish a harmonized stratigraphic scheme along the proximal Aquitaine foreland basin and covers a 200 km-long area, from the Corbières to Lourdes for the PYRAMID project (fig.6).

North-South Stratigraphy

An inventory of all stratigraphic units (formations) outcropping and identified in boreholes in the study area has been established (Appendix 2). For each main structural zone (NPZ, Petites Pyrenees, platform), all lithostratigraphic units are identified by formation names and/or age (often only defined by their age) and by a stratigraphic code. These codes are frequently in-consistent between BRGM maps due to the year of publication. On well logs, assignment of age and formation names to stratigraphic units is very heterogeneous in precision and certainty both along the borehole and between boreholes. Lots of time was spent on this essential task because of the lack of detailed descriptions and lack of precision in age assignment in the logs provided by InfoTerre and the BEPH database. In some cases, ages were referenced only as series name such as

“Upper Cretaceous” or Malm” for instance, with detailed lithological descriptions or biostratigraphic markers to confirm age assignment. The goal was to assign the most reasonable age to each layer (e.g. Maastrichtian, Campanian, Santonian and so on). The first step was to check in the explanatory notes (in InfoTerre and BEPH) in order to see if dating details were provided and with what uncertainty. Then, the log descriptions are compared to palaeogeographic maps (BRGM, 1974; and Barnolas et al., unpublished) to check that they corresponded to the proposed spatial and temporal extension of assigned lithological formations.

The construction of this stratigraphic lexicon harmonizes for the first time the stratigraphic nomenclature and age estimates of all the geological maps and borehole data in the proximal Aquitaine basin. This detailed work was essential to allow the N-S correlation of stratigraphy. It constitutes the basis for the construction of the chronostratigraphy, the lithostratigraphy and structural history leading to foreland basin reconstruction.

West-East Stratigraphic correlation

The same kind of inventories have been synchronously established for 5 others N-S sections (Appendix 3): one to the west (n°6, near Boulogne-sur-Gesse,) and 4 at the east (n°1 and n°2 crossing the Mouthoumet massif, n°3 near Lavelanet, n°4 near Mas d'Azil) of the studied section. For each cross-section, a chronostratigraphic column is realized (fig.6) summarizing all the formations present (in outcrop and/or in boreholes) in the Petites Pyrenees. Juxtaposed side by side, regional E-W correlation is possible.

Sediment distribution across the central and eastern foreland basin presents some discontinuities. The Toulouse Fault separates two main zones: the western part displays an almost complete stratigraphic sequence from Trias to Miocene, whereas the eastern part includes a 110 km-long zone (W-E trend, from Toulouse Fault through the Carcassonne Strait to Mouthoumet Massif) where Trias to Upper Cretaceous strata are absent. These strata reappear along the eastern side of the Mouthoumet massif in the “Nappe des Corbières”. Moreover, it must be noticed that the sedimentation at the East of the Toulouse Fault is more continental than the sedimentation at the West.

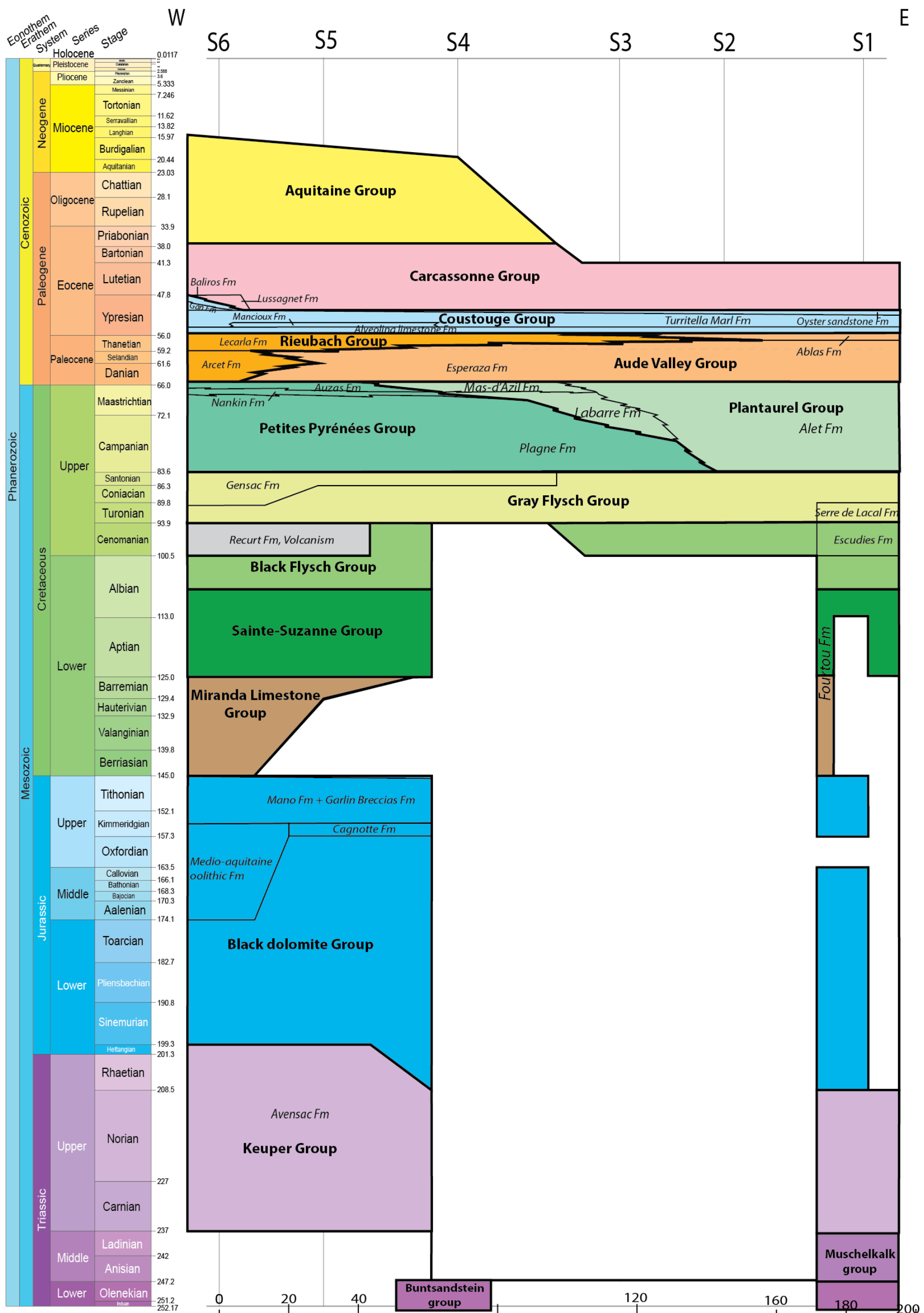


Figure 6: General chronostratigraphy of the Central and Eastern Pyrenees. (Christophoul & Bernard (S1), Ford (S2), Grool (S3), Hemmer (S4), Rougier (S5), Ngomby Mavounou (S6), 2014). The location of these sections is shown in Appendix 3. The Toulouse fault is located between the S4 and S5.

Lithofacies associations

We distinguish several lithofacies associations (LFA), classified according to their depositional environment. Four main categories are differentiated (fig.7), and their respective bathymetries are indicated in figure 8.

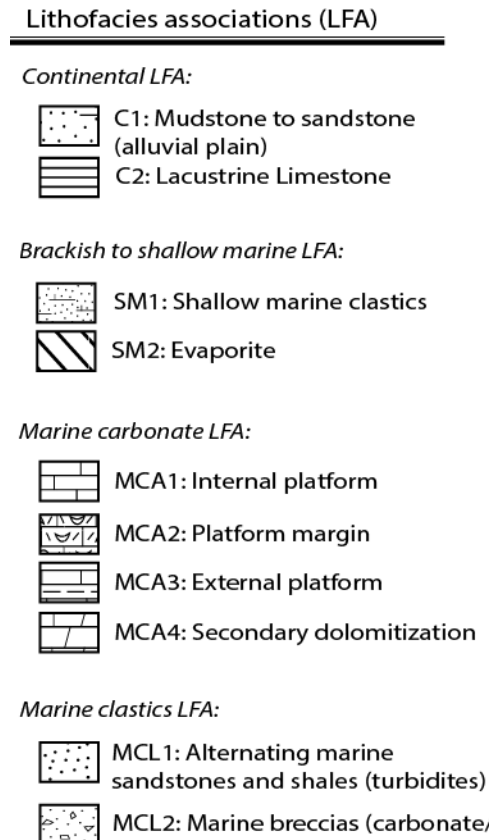


Figure 7: Lithofacies associations and the associated shapes used in the construction of the chrono-stratigraphy and the litho-stratigraphy.

-1] *Continental LFA* including fluvial and alluvial plain deposits, backswamps and oxbow lakes with mudstones and sandstones. It comprises mainly brown and red marls, variegated shales, shaly sand and sandstones with quartz pebbles and organic matter (C1); lacustrine limestone (C2);

-2] *Brackish to shallow marine clastic LFA* including shallow marine clastic deposits (SM1) and evaporite (SM2). This LFA comprises confined coastal environments, but also continental-marine transitional environments. It is mainly represented by variegated marls interbedded with gypsum and sand. Fossils such as Alveolina and Nummulites are often described.

-3] *Marine carbonate LFA* (fig. 8a) including low energy internal platform (lagoons, embayments) deposits (MCA1); high-energy sediments of platform margin (MCA2) and low-energy settings of external platform (MCA3); secondary dolomitized carbonates are grouped into a fourth sub-group (MCA4). MCA1 is represented by white limestone, oolithic limestone, slightly marly. Echinoderms, molluscs, brachiopods,

Turitella, Alveolina and algae are the fossils often described. MCA2 is fossil-rich (rudists, ooliths, reef).

-4] *Marine clastics LFA* (fig.8b) including marine sandstones interbedded with shales, corresponding to offshore deposits or turbiditic deposits (MCL1); marine polygenic breccias (MCL2). The respective bathymetries are indicated on the figure 8. They are deduced from the depositional environments and the presence of specific fossils. For instance Turitella, Nummulites and Alveolina are fossils found into the internal platform. When the environments are not easily deduced, we need to refer to palaeogeographic synthesis (BRGM, 1974; Barnolas et al., unpublished).

Groups and Formations

From the NPZ to the northern part of the Aquitaine platform, deposits can be divided into eleven informal stratigraphic groups which in turn can be subdivided into formations (fig. 9). This is a first proposal or working model of stratigraphic nomenclature and it is clear that in places the definition of formations in particular is incomplete. Established names of formations are respected as much as possible. However, many group names are newly assigned. From these subdivisions and borehole information, a lithostratigraphy is also constructed (Fig. 10).

Buntsandstein Group (Lower Trias) It is found only in one borehole (AV-101) in the platform. It is constituted by shaly and fine-grained sandstone with rare black shale. It is 300 metres thick. For this group, there is no formation name assigned.

Keuper Group This group is found everywhere along the transect and corresponds to Upper Triassic and Lower Liassic evaporites (halite, anhydrite and gypsum) interbedded with variegated marls, dolomite and polygenic breccias. It comprises three formations: the Avensac Formation (Carnian, Norian and Rhaetian), Gypsiferous and saline shale Formation (Carnian and Norian) and the Anhydrite Formation (Hettangian/Sinemurian). These evaporites deposits are found deep in boreholes but also in outcrops along thrust faults at the border between the NPZ and the Petites Pyrenees.

Black Dolomite Group This unit comprises all Jurassic strata except the Lower Liassic Anhydrite Formation. The description is subdivided into three parts:

- a] Liassic unit is found all along the transect. It is made of marls, marly limestones and black shaly marls. Dolomite and limestones are also present at the base of the Lias. Thickness can vary widely, between 40 and 300m in the platform and about 400 m thick in the NPZ and the Petites Pyrenees zone. Toarcian marls are the source rock of the Saint-Marcet gas field (Biteau et al., 2006). There is no specific formation name assigned for this group.

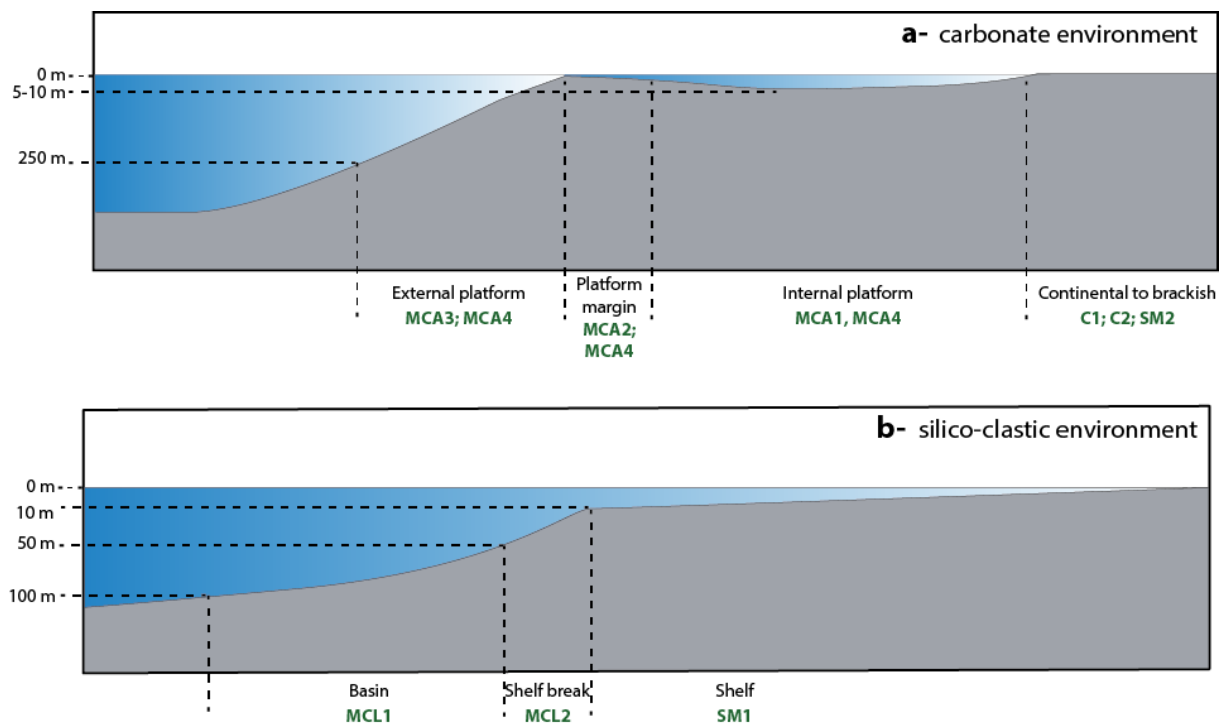


Figure 8: Schematic representation of (a) a carbonate platform with a barrier reef and (b) a ramp, showing the lithofacies associations used in this study for the construction of the chrono- and litho-stratigraphy

- b] Middle Jurassic: this unit is found along the whole segment except in the northern part of the platform. It consists of dolomites and dolomitic breccias. The thickness varies between about 130 m (NPZ) and 280 m in the southern part of the platform. This is the equivalent of the *Ossun Formation* described by Biteau et al. (2006), in the northeast of the Aquitaine basin.

- c] Upper Jurassic: strata of this age are found everywhere except in the northern part of the platform. It consists of limestones, calcareous dolomite, and gray dolomitic breccias in the Petites Pyrenees. Several formations are recognized : (i) *Cagnotte Formation* (Lower Kimmeridgian) is made of fossil-rich dolomitic limestones (*Pseudoclammina jaccardi*); (ii) *Lons Formation* (Upper Kimmeridgian) comprises dolomitic limestones containing lots of fragments of shells; (iii) *Mano Formation* (Tithonian), known as “Mano Dolomite”, is a grainstone dolomitic limestone; (iv) “*Breche de Garlin Formation*” (top of Tithonian) consists of brecciated limestone (Biteau et al., 2006). This Upper Jurassic unit is 830 m thick in the south of the platform and about 400 m thick in the northern part. These deposits constitute the main reservoirs of the Saint-Marcet gas field (Biteau et al., 2006). The fractured dolomites and limestones are directly in contact with Toarcian source rock giving them an important role in the Comminges petroleum system as a reservoir.

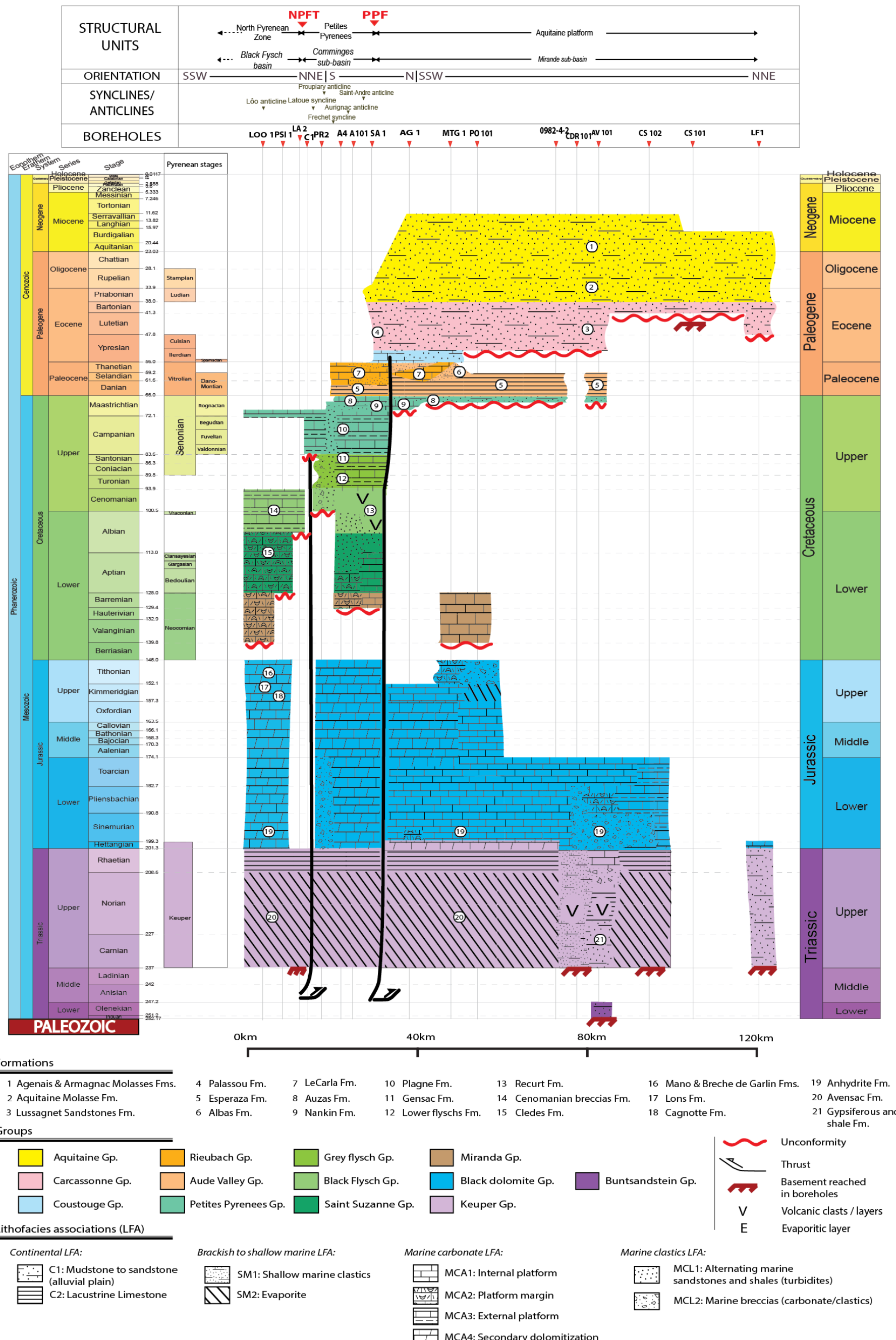


Figure 9: Chronostratigraphy of the study area

Miranda Limestone Group This group represents Neocomian ages (Berriasiian to Hauterivian). It is found in the NPZ where the Berriasiian stage is missing; the whole group is completely absent in the Petites Pyrenees, and is found again in the southern part of the northern platform in two wells (MTG-1 and PO-101). This group consists of fossil-rich limestones (*characea*, *choffatella* and annelids) with intercalations of dolomitic limestone.

Sainte Suzanne Group is situated in the NPZ and the Petites Pyrenees but it is not present on the platform. This group comprises Aptian and Lower Albian black marls and shaly limestones, reef limestone (Upper Aptian, *Cledes Fm*) and fossil-rich limestone (Lower Albian) (*Toucasia*, *Florideae*, *Melobesia*).

Black Flysch Group The ZNP contains undifferentiated Albo-Cenomanian marine clastic deposits (marls alternating with breccias and sandstones). They are approximately two kilometers thick. At the same time in the Aurignac region volcanism was very important and widespread (*Recurt Formation*). Its thickness increases northwards, from about 300 meters in the anticline hinge to 700 meters in its northern flank, and can reach more than 1 km near Saint-André (Fig.15). This magmatic episode ranges from Upper Albian to Turonian, and can be divided into two phases (Tchimichkian, 1971): (i) a volcanic phase is distinguished from Late Albian to Early Cenomanian and (ii) an intrusive phase during Late Cenomanian and Turonian. The *Recurt Formation* consists of many different black to purple rocks. They are described as syenites through to theralites, such as ankaramites, diabases and picrites (Cavaillé & Paris, 1975). This important volcanic body is probably responsible for the positive magnetic anomaly in Aurignac area (Cavaillé & Paris, 1975).

Gray Flysch Group (Turonian-Santonian) This group is found in the Petites Pyrenees only. It consists of marly limestone, muddy sandstone and breccias. Thickness of this group is about a hundred metres excluding volcanism whose thickness can vary widely. *The Gensac Formation* (Santonian) is made of coastal sandstones. This formation is the equivalent of a formation described in the explanatory note of the Saint-Gaudens geological map: the dark-coloured “*Lower Flyschs Formation*”.

Petites Pyrenees Group (Campanian to Maastrichtian) consists of the light-coloured “*Upper Flysch Formation*” called in this area the *Plagne Formation* (Campanian to Lower Maastrichtian) made of marls alternating with sandstones, rich in a variety of planktonic foraminifera (*globotruncana*). This formation is present everywhere except in the northern platform and its thickness varies from a few meters above the Black Flysch Group between LA-2 and C-1 (Fig. 15) to more than 2400 metres in the Petites Pyrenees (in the borehole A-4, fig.4) The top of the *Plagne Formation* comprises limestones and forms the transition with the overlying *Nankin Formation* (Upper Maastrichtian) which is made of massive slightly sandy limestone deposits, associated with fossil-rich marls up to 150 m of thickness. This formation is mainly present in the Petites Pyrenees and in

the southern part of the northern platform. The *Auzas Formation* (Upper Maastrichtian) is the youngest formation of the Upper Cretaceous and is mainly present in the northern platform. It consists of 250 metres thick marine shaly marls associated with local occurrences of continental facies.

Rieubach and Aude Valley groups (Paleocene) These groups are present both in the Petites Pyrenees and the northern platform. Aude Valley Group (Danian & Selandian) comprises the *Esperaza Formation* which is a continental formation, composed of lacustrine limestone and dolomite (lacustrine gastropods), interbedded with variegated marls. It is 130 m thick in the south and only 20 m thick in the north. Thanetian times are represented by *LeCarla Formation* belonging to the Rieubach Group. Contrary to the Aude Valley Group, this is a marine unit, particularly present in the south of the northern platform (60 m thick) and in the Petites Pyrenees (from 100 to 250 m thick). It consists of internal platform organism-rich sandy limestones and shaly sandstones (*Miliolina*, *Operculina*). The top of Thanetian stage has a marine-continental transitional sedimentation (*Albas Formation*), constituted of variegated marls with lignite intercalations.

Coustouge Group (Lower Ilerdian) corresponds to an important marine transgression and is widespread both in the north of the Petites Pyrenees and the south of the northern platform. Its thickness rapidly decreases northward from 50 m to a few meters. This group is subdivided into 3 formations. At the base lies *Alveolina Limestone Formation*, composed of shaly limestones and sandy shales; it is characterized by the *Alveolina cucumiformis* zone (Plaziat, 1981; Tambareau et al., 1995), *Alveolina ellipsoidalis* (Serra-Kiel et al., 1998) and *Operculina granulosa* (Tambareau et al., 1995). The *Mancioux limestone Formation* is located above and is composed of massive white limestone with sand-rich intercalations; it is rich in various species such as *Operculina*, *Assilina*, nummulites and algae. The *Turitella Marls Formation* constitutes the uppermost formation but is rarely found along the section.

Carcassonne group (Upper Ypresian to Bartonian). Its base corresponds to the appearance of detrital continental sediments recording the westward marine regression (Cahuzac et al., 2005). It is found from the north of the Petites Pyrenees to Avensac. It is made of two formations: (i) the *Palassou Formation* is mainly made of continental and coarse detrital deposits such as red shale and conglomerates with calcareous pebbles interbedded with yellowish sandstone layers. This formation passes laterally northwards into (ii) the *Lussagnet Sandstone Formation* composed of azoic fine- to coarse-grained sandstone, interbedded with variegated marls, and pebbles (Sztrakov, 1998). The *Lussagnet Sandstone Formation* is the coastal equivalent of the *Palassou Formation*, which is considered to be the first significant contribution of the destruction of the orogen to the foreland basin sedimentation (Cavaillé & Paris, 1975). The thickness of this group does not exceed 70 metres and progressively decreases northwards.

Aquitaine group (Priabonian–Serravallian) This group comprises detrital continental sediments extending from the northern part of the Petites Pyrenees to the northern part of the platform. It includes also littoral to lagoon environment deposits (Sztrakov, 1998) due to several Oligo-Miocene marine transgressions from the western Aquitaine basin (Cahuzac et al., 2005). Thickness decreases northward from 900 m to a hundred metres. It is mainly composed of variegated marls and shales, becoming sandy toward the north. This group comprises several formations (*Campagne Formation* (Sztrakov, 1998), *Agenais Formation*, *Armagnac Formation*...). Serravallian sedimentation seals the syn-orogenic structures.

Main unconformities

- a] In the northern platform, four main unconformities are recognized: one at the base of Bartonian in the area of Castelsarrasin (fig.4) where fluvial sediments directly lie on the basement in the borehole CS-101; one at the base of Carcassonne Group in the south of the platform where the Coustouge Group (Thanetian) is absent; the third main unconformity is seen in 5 wells at the base of the Auzas Formation, and at the base of the Nankin Formation in AG-1. The unconformity at the base of the Miranda Group (Valanginian) is found near MTG-1 and PO-101 (fig.4).
- b] In the southern part of the Petites Pyrenees, sediments representing the stages between Cenomanian and Tithonian are absent, thus a major unconformity appears in the borehole C-1 where the *Plagne Formation* lies directly above the Keuper Group; near Aurignac, sediments representing the Hauterivian, Valanginian and Berriasiian stages are missing.
- c] A progressive unconformity appears in the NPZ, near the NPFT where Albo-Cenomanian deposits lie directly on Keuper Group and southwards at the base of Aptian and Valanginian where Berriasiian stage is not represented (Miranda Limestone Group).

The lithostratigraphy (fig. 10) allows a quick overview of the thicknesses of the Groups in boreholes. The reference level chosen is the base of Cenomanian in order to see the evolution of thicknesses in the retro-foreland basin. In the NPZ and the Petites Pyrenees, groups and lithologies represented are those described in boreholes. The complex structure at depth will be represented further in the structural cross-section.

From this lithostratigraphy, we can see a migration of sedimentation northwards, toward the foreland basin. We can also see that the major faults control the sedimentation (NPFT and FPP and the normal fault to the south of the 0982-4-2 borehole). These lithostratigraphy and chronostratigraphy constitute the base for the construction of the structural cross-section.

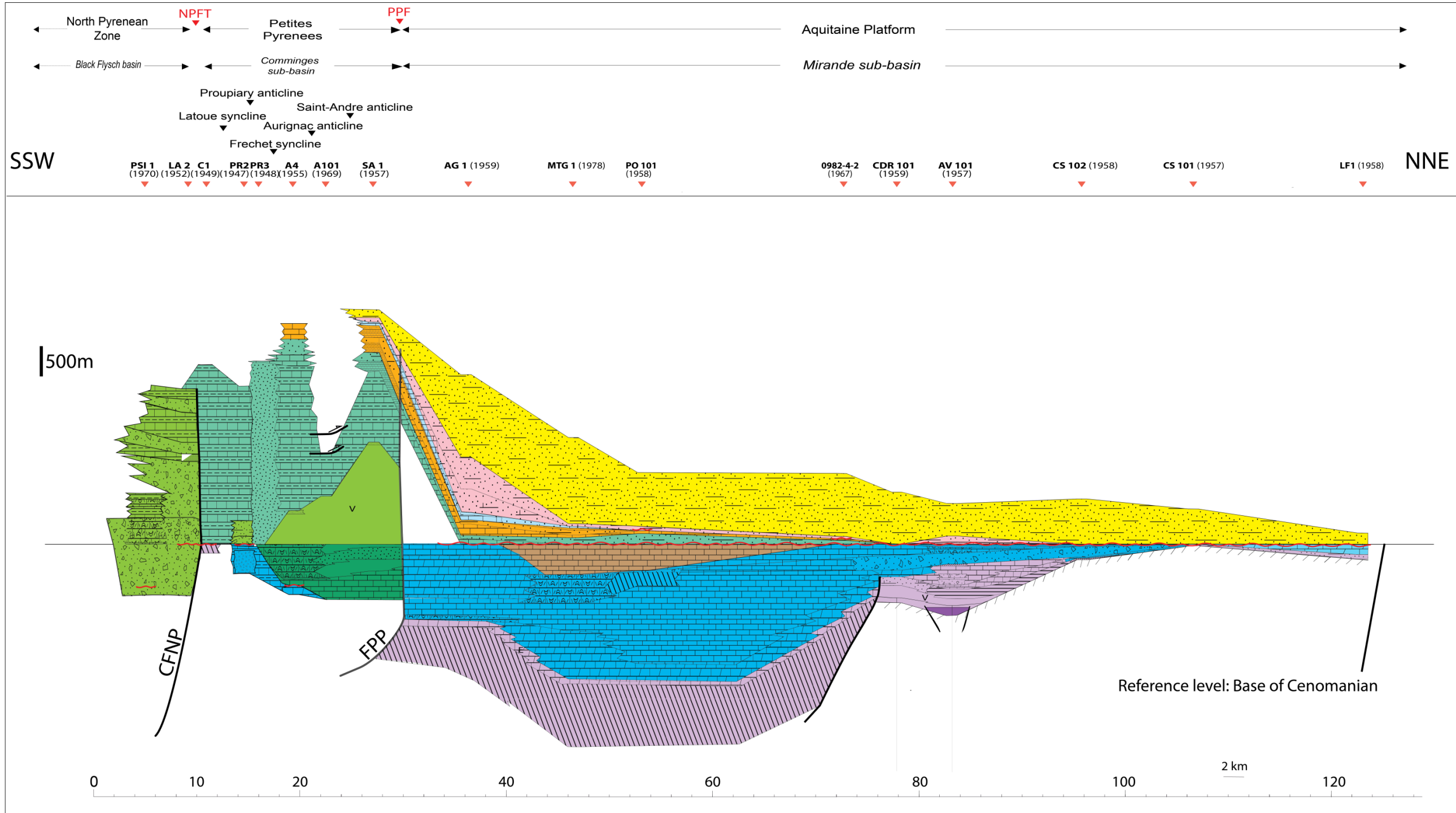


Figure 10: Lithostratigraphy of the study area

4. Interpretation of seismic data

Construction of a velocity model

This task has been realized by three engineering students from the Ecole Nationale Supérieure de Géologie (ENSG, Nancy, May 214). The first objective was to convert scanned seismic lines provided by the BRGM into SEG-Y files, thanks to a MATLAB program developed by the GOCAD team (ENSG). The second objective was to import SEG-Y files into the geomodeling software GOCAD. It constitutes the basis of our work. After importing these files in the software, they appeared georeferenced in space (UTM coordinates). We also provided the students all the well data we had on our sections. They used them to create vertical wells and deviated wells on GOCAD.

VSP (Vertical Seismic profile) data, sonic data and well logging constitutes very useful data for the construction of the velocity model. Unfortunately in this case, well logs data were not available, but the BRGM provided us VSP data. These velocities correspond to well data and were integrated to calculate time-to-depth curves for all the wells. Then, they interpolated all the vertical wells that allowed the creation of a 3D cube, which constitutes the velocity model. This model is thus used to convert wells in depth into wells in time.

Then they reported the top of all the groups (as defined previously) on each well as horizon markers. This task is essential in order to interpret the seismic profile.

Seismic stratigraphy

-A- (Fig. 11)

In the platform, the well AG-1 is the only well that is perfectly at the meeting point between the cross-section and the seismic profile (Fig. 4). For that reason, we consider the major horizons recognized cutting through this well are reliable. After projecting the wells MTG-1 and PO-101 on the section too, the different horizons are followed from AG-1 northwards. The first well-marked reflector (R1) corresponds to the top of the Coustouge Group, as the sedimentation changes from continental to marine it may imprint high velocities contrasts. Below R1, another well-defined reflector appear (R2) and seem to coincide with marine sedimentation of Rieubach Group, since there are alternating layers of limestones, shaly sandstones and variegated marls (*Albas Formation*). Upper Cretaceous (*Auzas Formation*) is correlated to the third less-marked reflector (R3). The Dogger and Keuper Group seem to be the last ones (respectively R4 and R5): they cross MTG-1 and we can follow those southwards to AG-1. In the absence of boreholes reaching deeper layers, the top of the basement is guessed (R6). All the horizons seem to dip slightly toward the southwest.

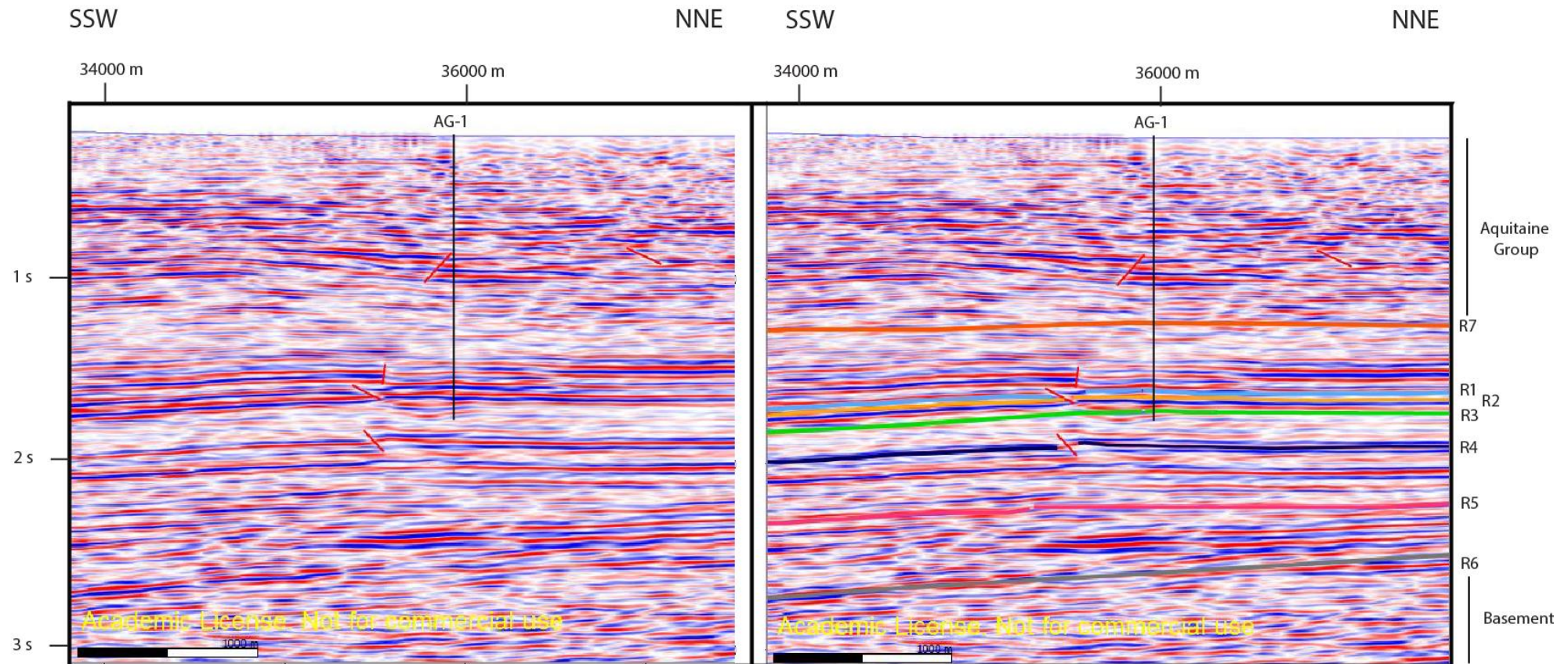


Figure 11: Seismic profile and interpretation in the stable platform around the borehole AG-1. It shows the major reflectors corresponding to the top of stratigraphic groups: R1 (Coustouge Group); R2 (Rieubach Group), R3 (Petites Pyrenees Group); R4 (Dogger); R5 (Keuper Group); R6 (Basement); R7 (Carcassonne Group)

-B- (Fig. 12)

The borehole MTG-1 is very close to the cross-section (Fig.4). The last group that is reached is the Keuper Group at 3482 metres, equivalent to ~2.1 seconds. This area is particular because of the presence of many erosional surfaces, extending on 7 kms around MTG-1. The first one corresponds to the Carcassonne Group. This horizon is not visible in AG-1 probably because the facies in this well are represented by marls. In MTG-1, this group becomes sandier and thus makes contrast between the above shales and marls (Aquitaine Group). This horizon (R7) dips towards the southwest with a larger angle than the ones below and it cuts across small reflectors between the 47.5th km and the 48th km. Between AG-1 and MTG-1, above R7 (Carcassonne Group) and below the flat reflectors at ~1 second, the reflectors are curved on the edges and seem to represent a sediment infill.

The second erosional surface is R1 (Coustouge Group) and cuts across many horizons such as Rieubach and Aude Valley Groups, Petites Pyrenees Group and Miranda Limestone Group between the 44.5th and the 47th km. Further towards the 49th km, the flat horizons noticed previously dip towards the northeast and cut across small reflectors. This is the third incision surface, extending over 1.5 km (R8). It becomes a reflector lying conformably on the underlying horizons at ~50.5th km.

The northern part of the seismic profile reveals no major deformation. The different horizons recognized are continuous and dip slightly towards the southwest. The Keuper Group thickens near MTG-1. It must be noticed that the borehole PO-101 is situated 10 kms far from the profile. For that reason, the major reflectors marked on the section are not necessarily found in the borehole. This is the case with the Coustouge and the Rieubach Groups, visible on the seismic profile but not in the well. The spatial extension of this marine transgression probably stopped between them.

-C- (Fig. 13)

The southern part of the platform and the relationship between the platform and the Petites Pyrenees is recorded on the seismic profile. Indeed, each side of the thrust zone is recognizable; the south-dipping PPF can be deduced from the blurred area. R1, R2, R3 and R4 define packages showing a thickening towards the thrust front. The same reflectors are marked on the southern side of the front. The Carcassonne reflector (R7) on the southern side of the PPF is the highest reflector which dips northwards and ends on the thrust. Above it, remarkable reflectors are outlined. Packages of inclined lines represent offlaps, revealing the growth of the thrust front, pushing northwards the Aquitaine Group sedimentation. At 0.75 s, flat reflectors appear and make the transition to a passive sedimentation: progressive onlaps cover the top of the Carcassonne Group. They sealed the front activity.

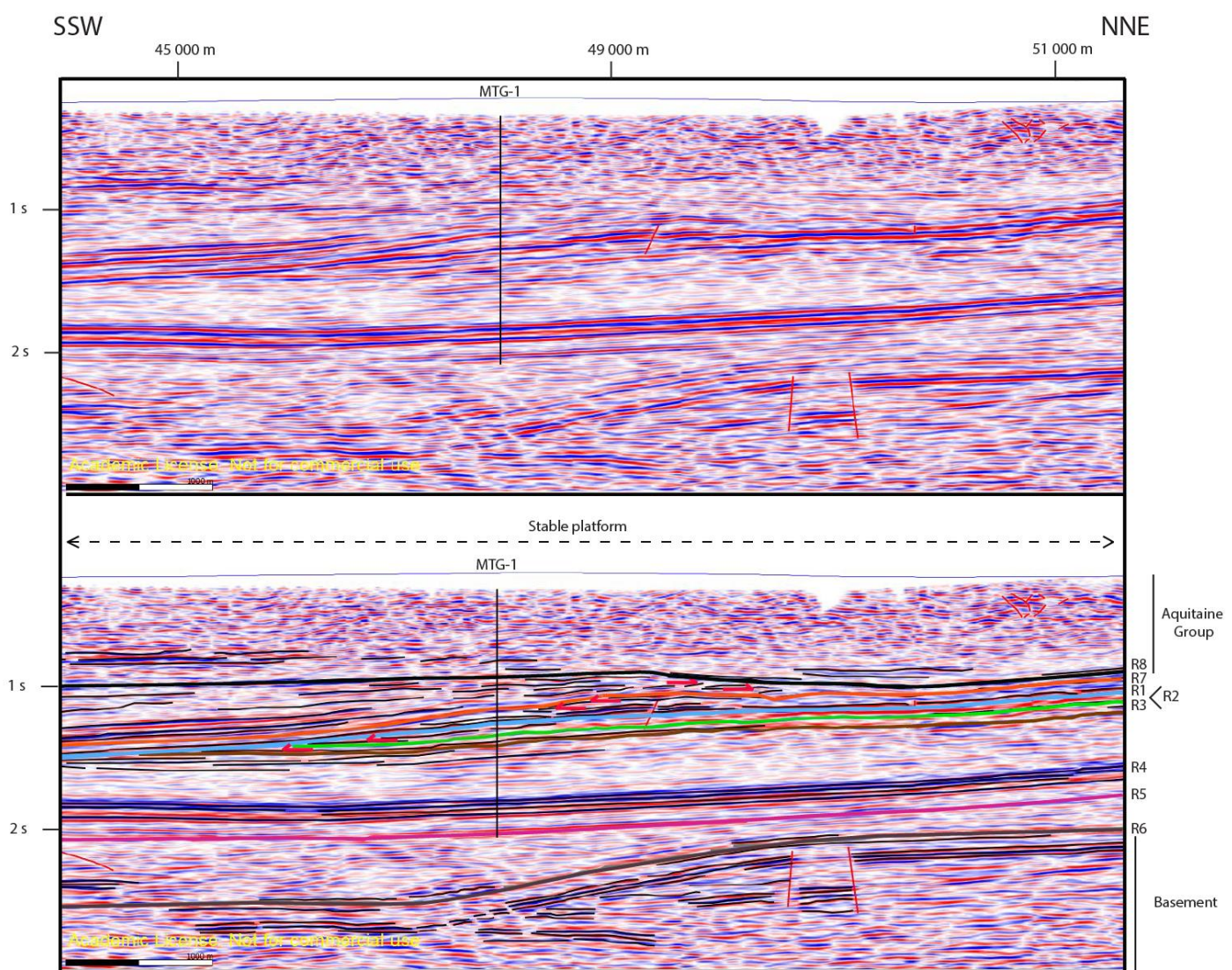


Figure 12: Seismic profile and interpretation in the stable platform around the borehole MTG1. It shows the major reflectors corresponding to the top of stratigraphic groups: R1 (Coustouge Group, first erosional surface); R2 (Rieubach Group), R3 (Petites Pyrenees Group); R4 (Dogger); R5 (Keuper Group); R6 (Basement); R7 (Carcassonne Group; second erosional surface); R8 (third erosional surface)

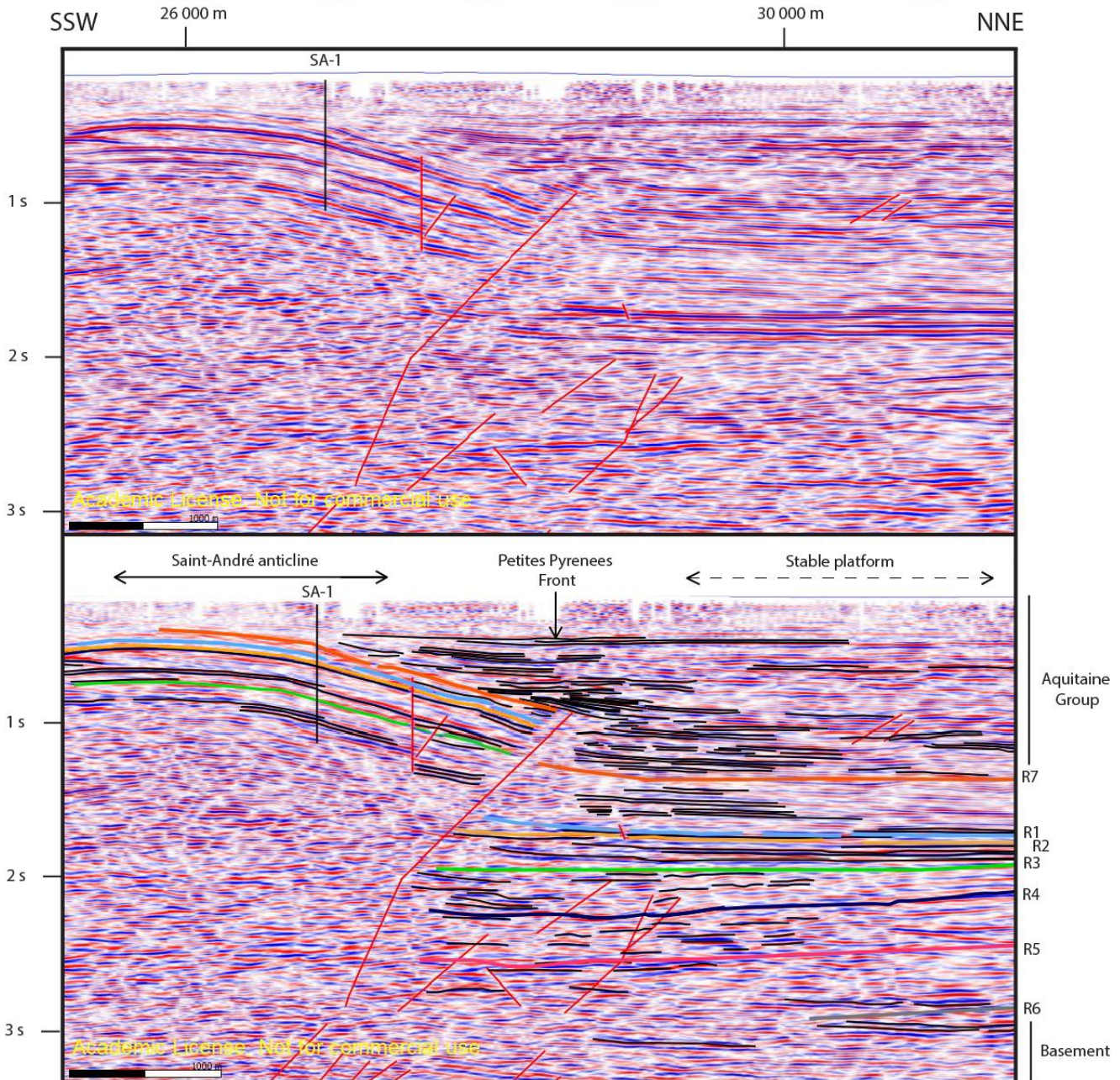
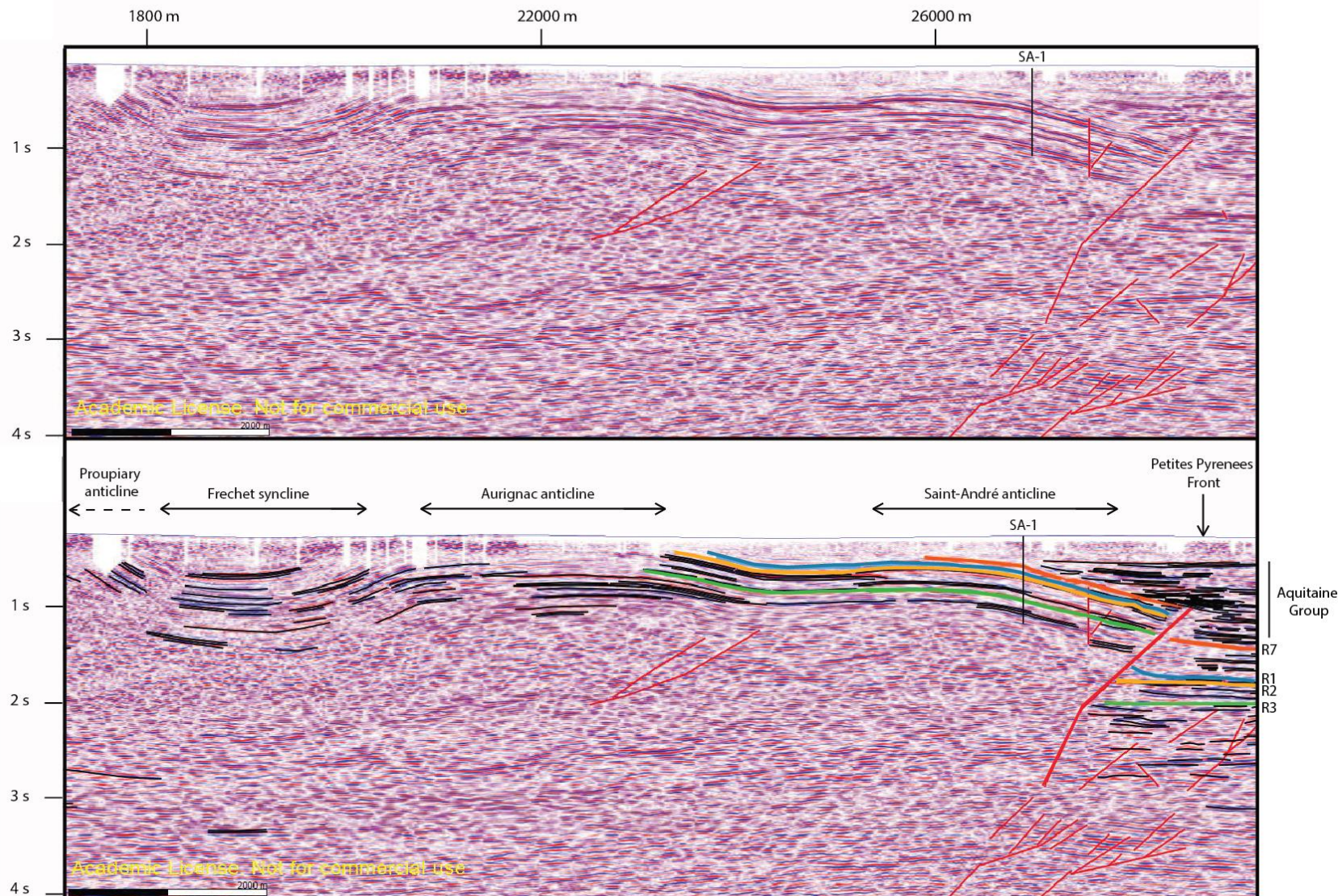


Figure 13: Seismic profile and interpretation in the stable platform around the Petites Pyrenees Front. It shows the major reflectors corresponding to the top of stratigraphic groups: R1 (Coustouge Group, first erosional surface); R2 (Rieubach Group), R3 (Petites Pyrenees Group); R4 (Dogger); R5 (Keuper Group); R6 (Basement); R7 (Carcassonne Group). This figure shows the offlaps above the thrust front revealing the growth of the thrust, sealed by the passive onlaps. This is the transition between the Petites Pyrenees and the stable platform.

The first second (in vertical scale) on the seismic profile is of good quality. The Saint-André, Aurignac and Proupiary anticlines are recognized, as well as the Frechet syncline. Structures at depth are blurred because of the deformation. Because of the lack of visibility, this part of the section will be interpreted with borehole and surface data.

SSW

NNE



25

Figure 14: Seismic profile and interpretation in the stable platform in the Petites Pyrenees. It shows the major reflectors corresponding to the top of stratigraphic groups: R1 (Coustouge Group); R2 (Rieubach Group), R3 (Petites Pyrenees Group); R7 (Carcassonne Group). It shows the succession of anticlines and synclines and the transition with the stable platform by the Petites Pyrenees Front.

5. Balanced cross-section

A balanced cross-section was realized using surface data, seismic data and well information. From the structural section, three zones showing different deformation styles are identified. From south to north these are:

1] The NPZ (Fig. 15)

To the south, the Synclinal des Cabanes is a north-verging fold (Fig.5) showing steep Black Dolomite and Saint-Suzanne Groups strata (up to 70°) revealing a complex structure at depth, folded and faulted along a salt layer. Pre-Albian folding does not correspond to the timing of deformation that is commonly accepted. Indeed, compression is thought to have begun during Late Cretaceous. The folding could thus be explained by salt diapirism that pushed the strata upwards. This is the explanation chosen here; although it could also result from an extensional context (sliding tectonics) as described by Lagabrielle et al. (2010).

The structure at depth of the Lôo anticline is constrained by the borehole LOO-1. It successively crosses the Saint-Suzanne Group (200 m thick), the Black Dolomite Group (Upper and the Middle Jurassic, 1200 m thick), Keuper Group (*Avensac Formation*, 240 m thick), and the Black Dolomite Group (Dogger and Oxfordian, about 350 m thick). The first 150 m of the Liassic unit belong to a normal series, the fold axial plane is recognized at 2478 m deep and the series below are described reversed (Paris et al., 1971). Regarding these observations and the dips at depth, we draw below the salt a north-verging anticline. In this zone, it is impossible to evaluate the thickness of the salt as the well does not reach the basement.

Further to the north, the Albo-Cenomanian turbiditic deposits (Black Flysch Group) are restricted into a 5.5 km-large sub-basin bordered to the North by the NPFT. The borehole PSI-1 crosses through this sub-basin the Black Dolomite Group and ends in the Keuper Group. It is about 3.3 km thick. The Black Flysch Group sedimentation is unconformably deposited above the south-dipping older series (Appendix 25, Paris et al., 1971). This depocentre forms a north-verging monocline and contains lots of steeply north-dipping (40 to 70°) tectonic breccias, composed of Paleozoic, Black Dolomite and Saint Suzanne clasts (Paris et al., 1971). The well LA-2, which mainly encounters tectonic breccias, reaches the basement at 2 km deep. This suggests that the basement is probably involved in the deformation, thus the structural style is characterized by thick-skinned structures. The top of LA-2 comprises a few meters of the *Plagne Formation* that sealed the NPFT activity.

It must be noticed that the uppermost part of the Black Flysch sub-basin is hidden by Quaternary alluvium so its northern boundary was initially placed arbitrarily. The borehole C-1 cuts through 940 m of the Petites Pyrenees Group (*Plagne Formation*) and

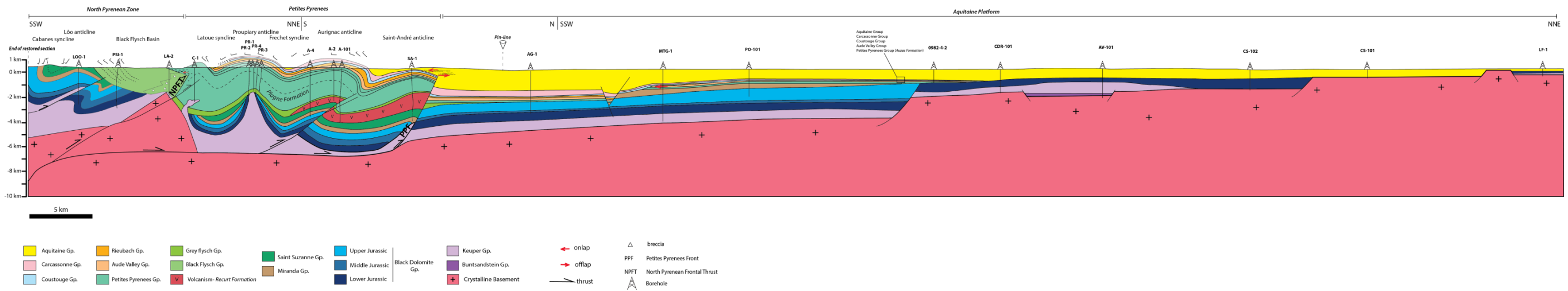


Figure 15: Balanced cross-section along the studied transect

ends in the Keuper Group. There is no Black Flysch Group deposit in this borehole. Consequently, this allows a little area to put the northern boundary of the sub-basin between the wells LA-2 and C-1. Tectonic breccias are described at the base of the *Plagne Formation*; this is why a fault probably crosses it.

Debroas (1990) describes the Albo-Cenomanian Bigorre (Appendix 26) sub-basin that is equivalent to this Black Flysch sub-basin. The author outlines the presence of the north-dipping tectonic breccias and the monocline. The author does not show the underlying strata and the connection with the Petites Pyrenees.

2] *The Petites Pyrenees* (Fig.15)

The Petites Pyrenees represent the deepest depocentre along the studied transect and extend for about 30 km in the NNE-SSW direction. Bounded by the NPFT to the south and by the PPF to the north, it accumulated several thousand metres of Petites Pyrenees, Rieubach and Aude Valley, Coustouge and Carcassonne Groups deposits lying in kilometric SE-NW growth folds. The depocentre is affected by salt tectonics where salt forms a diapir in Proupiary region and acts as a detachment level for the major thrust faults. The northern part of this zone, near the borehole SA-1 and the PPF, is better constrained by the seismic line (Fig. 13).

a- The synclinal de Latoue is visible in outcrop but disappears quickly under the Miocene cover (Paris et al, 1971). On the geological map (Paris et al., 1971) several triple points reveal the unconformity between the Aquitaine Group and Paleocene (both the Rieubach and the Aude Valley Group) and the Petites Pyrenees Group (*Auzas and Nankin Formations*). This is an asymmetrical fold; the southern limb dips at 40-45° to the north and the northern limb dips at 30° to the south. Its wavelength is 600 m and is 300 m in amplitude. This is consistent with the interpretation of Paris et al. (1971).

b- The Proupiary anticline is described here by 4 boreholes (PR-1, PR-2, PR-3, PR-4 (Fig.4, Appendices 17-20). It is a straight fold (Paris et al., 1971) with an amplitude of 1.5 km and a half wavelength of 5.5 km. The dips at surface (10-15°) are much shallower than those at depth (Paris et al., 1971). This is a growth fold where lie the Petites Pyrenees, the Rieubach, the Aude Valley, the Coustouge and the Carcassonne Groups. We observe variations of thickness: layers are thicker in the synclines (more than 3000m in the Latoue & Frechet synclines) and thinner in the Proupiary anticline (about 2300 m in PR-2). This means that the sedimentation was syn-deformation.

Its structure has been well studied as it was the major gas field of the Comminges basin. At depth it appears as a diapir. This part of our seismic profile is of bad-quality. Our interpretation was only based on the 4 wells cited previously. PR-2 crosses the *Plagne Formation*, the Grey Flysch Group and the Lower Jurassic, and this is the only borehole that reaches the Keuper Group. PR-4 crosses the *Plagne Formation*, the Grey Flysch Group and ends in the Upper Jurassic. PR-3 starts and ends in the *Plagne Formation*. Some breccias are found at the base of the boreholes PR-2 and PR-4. According to Fossen (2010), fractures at the top of a diapir are the consequence of passive salt diapirism. The author presents the ideal evolution of a salt diapir (Fig. 16):

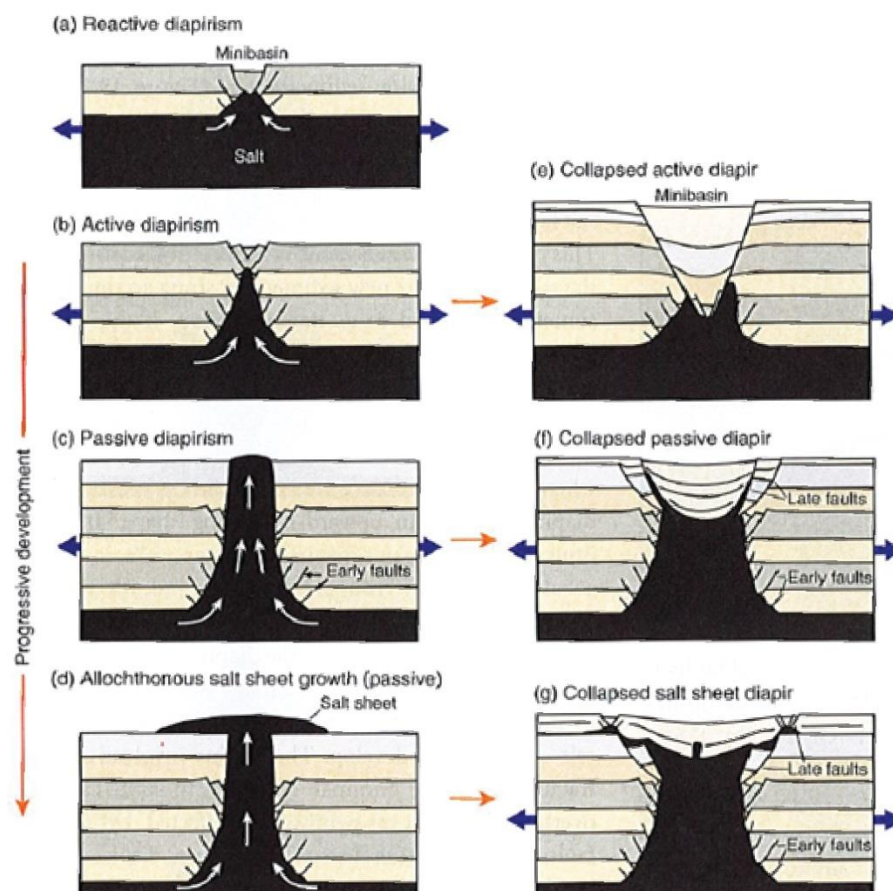


Figure 16: Representation of the evolution of a salt diapir: reactive (active) diapirism during extension, passive diapirism when sediment load is important, the salt is thus forced to migrate (from Fossen, 2010)

- (i) Active (or reactive) diapirism starts during an extensional event; the thinning of the crust allows the salt to migrate upwards;
- (ii) As the sedimentation continues, the load applied on the salt becomes important and the salt is *forced* to migrate. The diapirism is thus passive. During this step, the top of the diapir is stretched and can break, leading to fractures. At that moment, the flanks of the diapir are very steep.

Published cross-sections propose different interpretations of this area (Serrano et al., 2006 (Appendix 27); Total, 1998 (Appendices 28-29), Bourrouilh et al., 1995 (Appendix 30)). The interpretation of Serrano et al. (2006) was based on seismic data and an only well (PR-1). The interpretation of Total (1998) presents a squeezed diapir with many fractures at the top and is very close to our interpretation. Bourrouilh et al. (1995) studied the Saint-Marcet anticline constrained by 6 wells. It is the western continuation of the Proupiary anticline. Their interpretation is very close to ours: it is a squeezed diapir with many faults and breccias at its top, revealing the breakup of its roof.

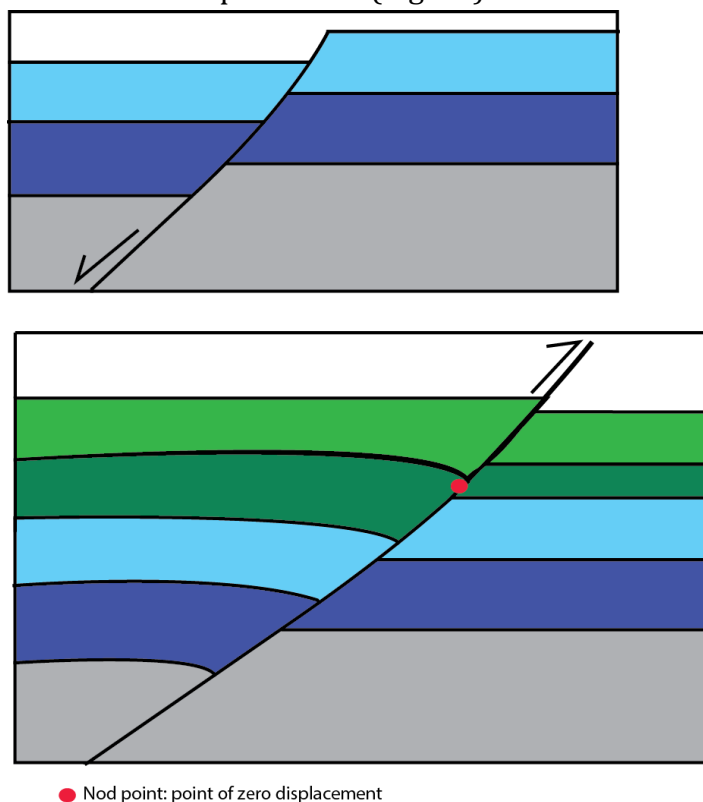
Jammes et al. (2010) study the interactions between salt and detachment faults in a hyper-extensional context in the Parentis sub-basin (NW of the Aquitaine basin). According to them, thick evaporite layer has a major control on the evolution of the basin geometry. In our case study, we are aware of the importance of the salt tectonics, it is very probable to have had huge amount of evaporite deposits (probably more than 2 km). Indeed, the salt diapir is sealed by the Grey Flysch Group. If we consider that the active diapirism began during Early Jurassic until the Late Albian, the salt was reworked during ~100 Ma and its thickness is apparently still important. This point will be discussed in the chapter "7. Discussion-Restoration"

C- Further to the north, the Aurignac anticline seems to be slightly north-verging. Three boreholes are available (A-4, A-2, A-101). The borehole A-4 crosses the Rieubach and the Aude Valley Groups (230 m), the Petites Pyrenees Group (2490 m), the Grey Flysch Group (60 m), the Cenomanian volcanic deposits (460 m), the Sainte-Suzanne Group and the Miranda Limestone Group (575 m) and ends in the Upper Jurassic. The borehole A-2 crosses the Petites Pyrenees Group (2255 m) and ends in the Grey Flysch Group. The borehole A-101 presents stratigraphic repetitions: Petites Pyrenees Group and Grey Flysch Group from the top of the well to 2815 m deep; the Plagne Formation between 2815 m and 3026 m deep, and the succession Petites Pyrenees-Grey Flysch Groups until the base (4405 m deep). These repetitions are interpreted as thrusts, as shown on the cross-section (Fig.15).

Heritier et al. (1998) (Appendix 31) present a structural cross-section of the Aurignac anticline, based on the same three wells as us (A-4, A-2 and A-101). They place a thrust between the wells A-4 and A-2 but they do not have any constrain. They want to justify the fact that they do not find any Grey Flysch deposits at the base of A-2. In the well description available on InfoTerre (Appendices 14-16), it is said that A-2 crosses more than 500 m of Grey Flysch Group, including lots of volcanic deposits. Plus, we consider that the thickness of volcanic deposits can vary widely so no thrust is needed. They interpret the repetition of stratigraphic units in A-101 as a recumbent fold. In the lithological descriptions, there is no evidence for the presence of reverse series; this is why we interpret this as a second thrust crossing through A-101. Also, they continue the thrust up to the Montian (Paleocene). In our cross-section we decide to seal it by the

Plagne Formation, according to the timing of the deformation described in Chapter “7. Discussion- Sequential restoration and evolution of Pyrenean retro-foreland”.

- According to the dips at surface, there is a syncline between the Aurignac and the Saint-Andre anticlines. This has not been represented on the cross-sections from Total (1998) (Appendices 28-29), where the Aurignac anticline is continuous with the Saint-André anticline. In our representation, this south-verging syncline is 2 km deep, consisting of the Petites Pyrenees Group, as well as the Paleocene (both the Rieubach and the Aude Valley Groups), the Coustouge, the Carcassonne and the Aquitaine Groups. It must be noticed that the thickness of the Carcassonne Group increased a lot in the syncline axial plane. This means that the sedimentation of this group occurred during the growth of the fold.
- The Saint-Andre anticline is located at the northern border of the Petites Pyrenees. It crosses all the groups from the Aquitaine Group to the Miranda Limestone Group. The volcanic deposits are very important (1440 m thick).
- The PPF presents a normal displacement at the base of the fault, and an inverse displacement at the top. This sort of configuration is often seen in compressional contexts where extensional faults are reactivated and inverted. The nod point is the point where there is no displacement (Fig. 17):



● Nod point: point of zero displacement

Figure 17: Representation of an inverted normal fault. At the base of the fault the displacement is normal, at the top it is inverted. The nod point corresponds to zero displacement.

3] The platform (Fig. 15)

As the cross-section shows, the major features recognizable in this part of the transect are the following:

-It is slightly deformed; the thickness of Carcassonne strata increased beyond the Petites Pyrenees Front as well as the Aquitaine Group.

-As described with the interpretation of seismic data, there is a major unconformity situated at the base of the Coustouge Group and two other erosional surfaces. There is no evidence of this unconformity in literature. At first sight, it looks like an incisional surface at the base of Ilerdian times, but this does not make sense as this was the onset of a major transgression, recorded along the whole Aquitaine basin (Cahuzac et al., 1995). Indeed, if we consider that this is an incision, it means that there was a forced regression, the fall of the sea level led to the creation of an incised valley. Thus, this is not consistent with a transgression. We propose that this geometry is a consequence of the normal faults situated between MTG-1 and AG-1: this is confirmed by the sequences found in the mini-graben.

-Plus, there is an important thickness variation of the Black Dolomite Group that is due to the presence of a normal fault between PO-101 and 0982-4-2 that makes the Upper Jurassic absent in the northern part of the platform.

6. Subsidence analysis

Sediment deposits record the variations of subsidence through time. A sedimentological log is thus an essential tool to study the history of the subsidence.

The representation in time of the subsidence can be visualized on a geohistory plot. This plot presents the vertical movements of a point of the basement as a function of time in a fixed point of reference (Brunet, 1991). In order to calculate this depth, we need to know the thicknesses, the ages and the lithologies of the sediments, as well as their palaeobathymetry and the eustatic variations. Some parameters has a huge influence on the subsidence, such as the palaeobathymetry which is directly related to the type of sedimentation, and the eustatic variations that lead to variations of the isostatic compensation.

A geohistory plot allows to quickly see the variations of subsidence rate. In this study we calculate decompression curves, the total subsidence and the tectonic subsidence (e.g. without the effect of sediment load, eustasy and palaeobathymetry). Tectonic subsidence represents the subsidence caused by deep tectonic events (Brunet, 1991).

For subsidence analysis, two softwares programs are used: PetroMod and *subsidence.exe*. They use the “backstripping” method: they iteratively calculate the accommodation by time increment. Every layer is decompacted and the initial thickness is found. Several parameters are needed: (1) the age of the top of all the layers, (2) the altitude of the top and the base of each layer, (3) the bathymetry, evaluated according to facies and/or fossils, (4) the eustatism, determined thanks to a eustatic chart (Hardenbol et al., 1998 (Appendix 32), (5) the compaction coefficient, the bulk density and the initial porosity of each facies defined by Allen & Allen (2009) and completed with those from Verges (1998) (Appendix 33)

Two formulas are used. The first one calculates the decompaction:

$$y'_1 - y'_2 = y_2 - y_1 - \frac{\Phi_0}{c} (\exp(-cy_1) - \exp(-cy_2)) + \frac{\Phi_0}{c} (\exp(-cy'_1) - \exp(-cy'_2))$$

where Φ_0 is the initial porosity of the rock, c is the compaction coefficient, y_n is the depth of every strata limit giving the thickness of every layer.

The tectonic subsidence formula is (modified from Allen & Allen, 2009):

$$y_{tecto} = \phi \left(S \frac{\rho_m - \bar{\rho}_s}{\rho_m - \rho_w} - \Delta_{sl} \frac{\rho_w}{\rho_m - \rho_w} \right) + (W_d - \Delta_{sl})$$

where ϕ is for Airy isostasy (another value can also be used if we want to quantify the influence of lithospheric flexure); S is the total thickness of the sedimentary pile; ρ_m , ρ_w and $\bar{\rho}_s$ are respectively the bulk density of the mantle (3300 km/m^3), of water (1030 km/m^3) and the bulk density of the sedimentary pile (depending on the facies, see Appendix 33); Δ_{sl} is the difference between the palaeo- and the present-day sea level; W_d is the palaeobathymetry.

PetroMod is a petroleum geomodeling software. We used it in order to calculate the decompaction curves and the total subsidence. *Subsidence.exe* is based on the code given by Allen & Allen (2009). It gives us the total subsidence and the tectonic subsidence.

In this study, we present subsidence curves for 4 wells: two in the northern platform (AV-101 and MTG-1, one in the Petites Pyrenees (SA-1) and the last one in the NPZ (PSI-1), see fig. 4 for location and Appendices 7, 11, 13, 23);. They were chosen because they are the most complete wells in terms of stratigraphic units, and AV-101 reaches the basement so it possibly records the complete history of the northern platform. As shown in Appendices 11 & 13, the boreholes MTG-1 and SA-1 do not reach the basement. According to our cross-section, we completed the wells with the missing units. Thus, the Keuper Group is added to MTG-1 that is 600 m thick (BRGM, 1974) and also to SA-1 that is 1000 m thick (BRGM, 1974). The decompaction curves are presented in Fig. 18 to 21. It must be noticed that the lowest curve represents the Total subsidence curve. The

calculation tables are presented in Appendices 34 to 37, and the respective subsidence curves (total and tectonic) in Appendices 39 &40.

- AV-101 (fig. 18)

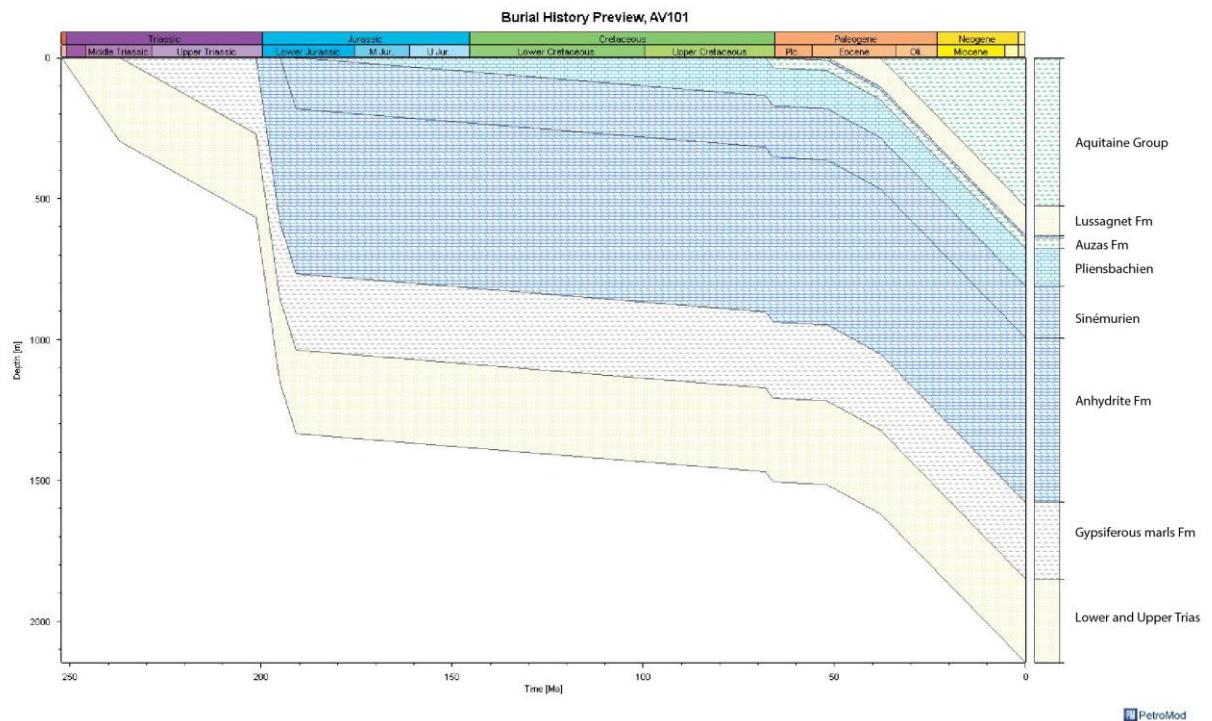


Figure 18: Decompression curves for the borehole AV-101, realized with PetroMod

This plot presents the decompression curves for the borehole AV-101 situated in the northern part of the platform. It shows four periods of rapid subsidence:

- Lower and Middle Trias: 300 m of subsidence (0.05 mm/yr) followed by a decrease of subsidence until the Late Trias (0.006 mm/yr)
- Upper Trias to Lower Lias (*Anhydrite Formation*): this is the most rapid phase of subsidence in this borehole. The subsidence rate is 0.07 mm/yr. From that time to Upper Cretaceous, the subsidence rate is very low (0.001 mm/yr), it is not zero even though this is a period of non-deposition.
- An acceleration of subsidence (0.1 mm/yr) is recorded in the *Auzas Formation* (Upper Maastrichtian), and is followed by a quiescence phase in the Paleocene (*Esperaza Formation*).
- The last phase of subsidence is recorded from Paleocene to Early Miocene times (0.06 mm/yr), during the sedimentation of the Carcassonne Group and the Aquitaine Group.

- MTG-1 (fig. 19)

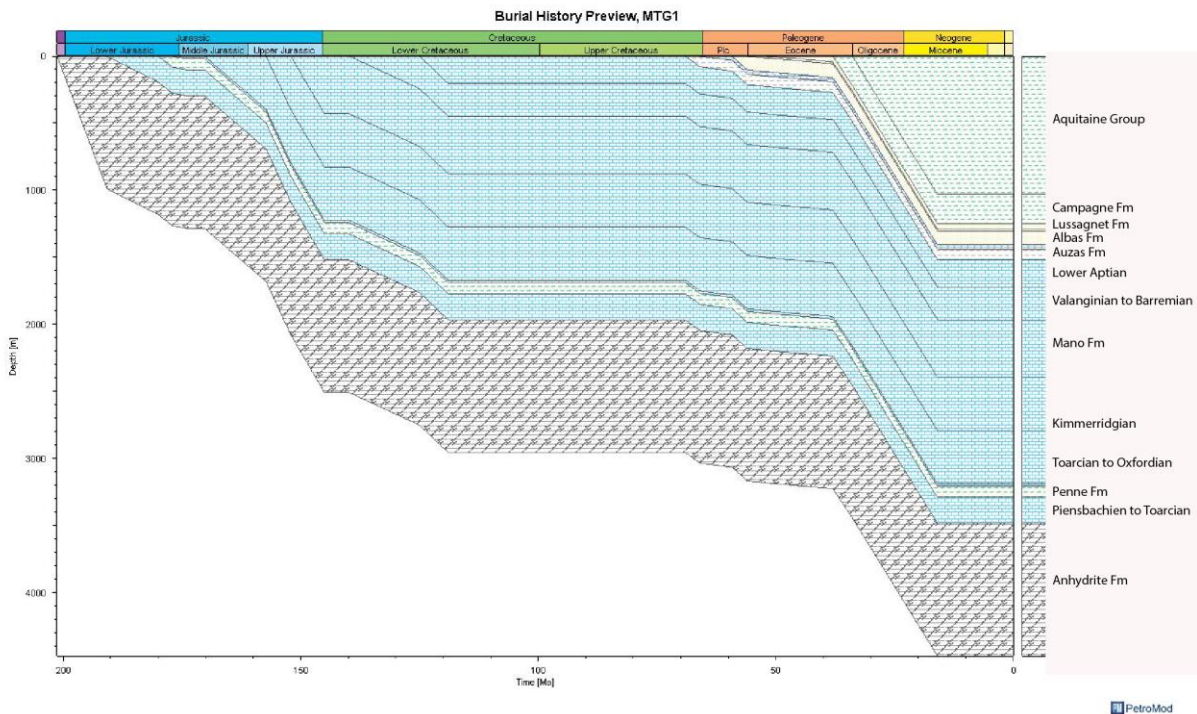


Figure 19: Decompression curves for the borehole MTG-1, realized with PetroMod

This borehole, situated in the south of the platform, records 3 three phases of rapid subsidence:

- a very rapid subsidence rate is recorded in the *Anhydrite Formation* (0.2 mm/yr). Subsidence is also very rapid at the end of Jurassic (0.07 mm/yr). This is the most rapid phase of subsidence recorded in this borehole.
- a second rapid subsidence rate is recorded in Lower Aptian time (0.02 mm/yr), which is followed by a period of quiescence due to a non-deposition phase until the Upper Maastrichtian (*Auzas Formation*).
- the end of the Paleocene (*Albas Formation*) records a subsidence rate of 0.03 mm/yr.
- a major subsidence phase occurred during the deposition of the Carcassonne Group (*Lussagnet Sandstones Formation*) and the deposition of the Aquitaine Group (0.05 mm/yr).

- SA-1 (fig. 20)

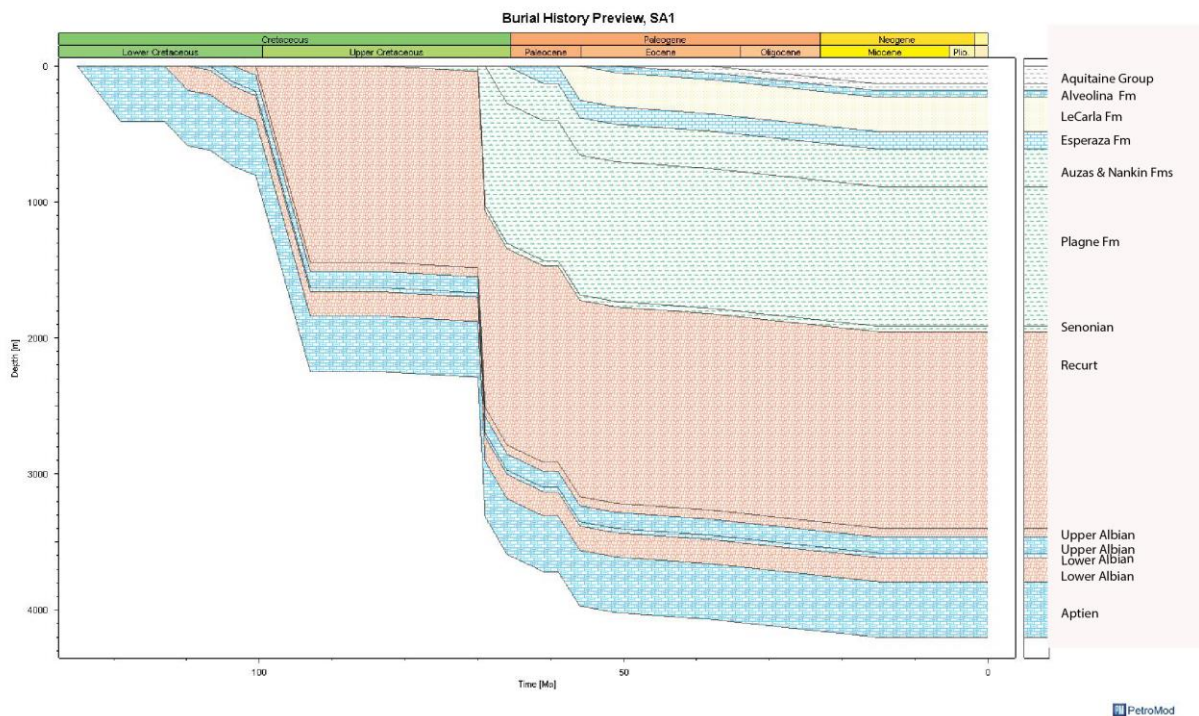


Figure 20: Decompression curves for the borehole SA-1, realized with PetroMod

This borehole is located near the PPF in the Petites Pyrenees. It records four major subsidence phases:

- the Lower Cretaceous (Aptian to Albian) reveals a subsidence rate of 0.03 mm/yr.
- a very rapid subsidence phase occurred during the appearance of the *Recurt Formation* (volcanism) during Late Albian to Turonian (0.3 mm/yr);
- a major subsidence rate occurred during the deposition of the Grey Flysch Group (0.6 mm/yr).
- the last acceleration of the subsidence rate (0.06 mm/yr) occurred during Late Paleocene (*LeCarla Formation*) following a short quiescence phase (Middle Eocene). The end of the graph shows a relatively quiet subsidence until Early Miocene (Aquitaine Group).

- PSI-1 (fig.21)

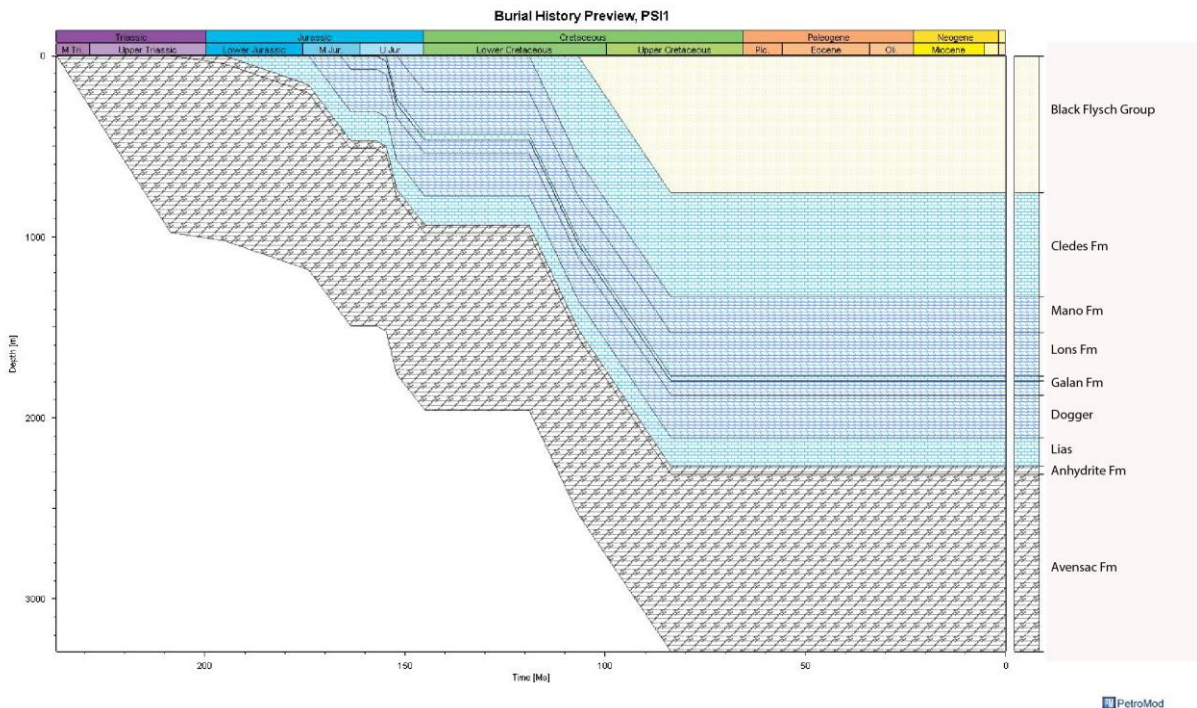


Figure 21: Decompression curves for the borehole PSI-1, realized with PetroMod

We did a last subsidence analysis on the borehole PSI-1 that is situated in the NPZ. It records three main subsidence phases:

- the first phase occurred during Middle to Late Trias (0.06 mm/yr);
- the second acceleration of subsidence rate occurred during Early and Late Jurassic (0.4 mm/yr).
- the last major acceleration of subsidence occurred during the Late Cretaceous, at the rate 0.04 mm/yr.

To summarize, in the platform there is an acceleration of subsidence during Trias and Jurassic and Aptian, then another acceleration during the end of Maastrichtian (*Auzas Formation*), and the final one occurred during the Late Eocene (Carcassonne Group and Aquitaine Group). In the Petites Pyrenees, the major subsidence is related to the volcanic episode, whereas in the NPZ major subsidence rates are recorded from Trias to the Black Flysch deposition. The interpretation of these phases is discussed in the following "Chapter 7: Discussion-*Interpretation of subsidence history*"

7. Discussion

Interpretation of subsidence history

In order to easily compare the subsidence curves (fig. 18 to 21) and to evaluate the differences of subsidence rates between the stratigraphic zones, we constructed two graphs summarizing the total subsidence for the four wells (fig.22) and the tectonic subsidence (Appendix 38). It must be noticed that the curves show a typical trend of foreland basins, they are concave upwards (Sinclair & Naylor, 2008).

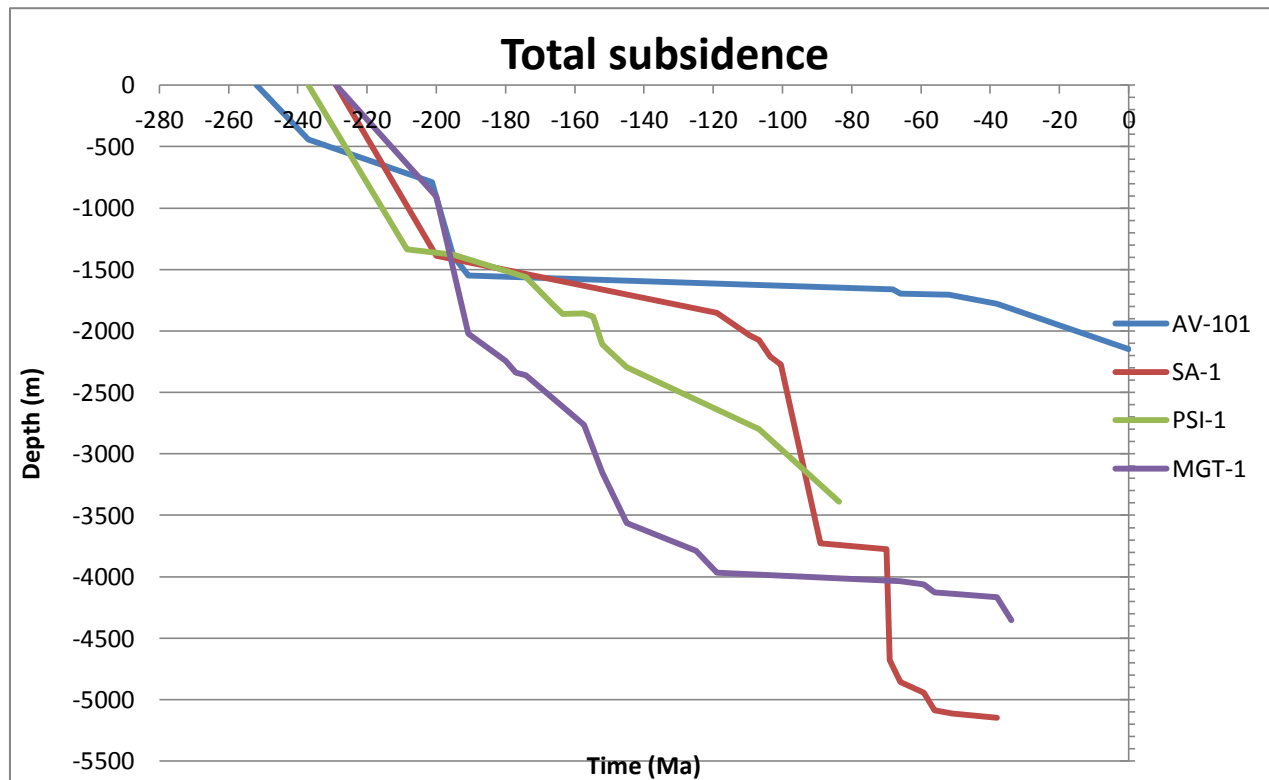


Figure 22: Summarizing plot of the total subsidence realized for 4 boreholes (AV-101, MTG-1, SA-1 and PSI-1) with *subsidence.exe*

The several accelerations of subsidence from Early to Late Trias are recorded in the four wells. They mainly occurred during the deposition of the *Avensac Formation* and the *Anhydrite Formation*. This is linked to the formation of several extensional basins, due to movements between the Iberian and the European plates (Brunet, 1991). A second acceleration of subsidence rate is seen during the Late Jurassic (Oxfordian to Kimmeridgian) revealing the formation of the Aquitaine sub-basins with a N110 trend (Brunet, 1991). These sub-basins are thought to have been created in a transpressional context; this is also linked to the rotation between the two plates (Serrano et al., 2006).

A third acceleration of subsidence is seen in SA-1 and PSI-1 (in the Petites Pyrenees and in the NPZ) from Aptian to Cenomanian. This is a major phase of distension recorded along the whole basin and all the sub-basins underwent crustal thinning (Desegaulx &

Brunet, 1990). During that time, the wells in the platform do not show acceleration of subsidence as there is a major unconformity at the base of the *Auzas Formation*. It shows these basins were restricted to the southern part of the Aquitaine basin. The borehole SA-1 is the only well that records the important extensional event during the Albo-Cenomanian. It is also visible in PSI-I but at a smaller scale. This phase is well-known in the Aquitaine basin because it led to the formation of Albo-Cenomanian basins in the NPZ, infilled with turbiditic deposits and breccias (Debroas, 1990). Also, the volcanism seen in the Comminges basin (Proupiary anticline) is considered to have appeared during this time increment. This is due to an extreme crustal thinning (Jammes et al., 2010; Lagabrielle et al., 2010).

The tectonic regime changed during Late Cretaceous, from an extension to compression. In SA-1, only few subsidence is recorded. This can be correlated to the pre-orogenic thermal subsidence period (Sinclair & Naylor, 2008). In this well, the total subsidence sharply increased (0.6 mm/yr) at ~70Ma (Campanian). It is also recorded in the borehole AV-101 with less intensity. This phase can be interpreted as either a thermic subsidence or a flexural subsidence, as it corresponds to the onset of the convergence between the Iberian and European plates. Moreover, the extreme crustal thinning occurring during Albo-Cenomanian times may have heated the crust northwards and led to a thermal re-adjustment during the Late Cretaceous. According to Sinclair et al. (2005), Pyrenean compression began during the Campanian (~75Ma). This episode is not seen on the subsidence curves, but the acceleration of the subsidence rates during the Paleocene (Late Danian) seems to be related. A relatively low subsidence rate (not null) occurred between Late Cretaceous and Early Paleocene. This is interpreted in literature as a quiescence phase (Sinclair et al., 2005; Whitchurch et al., 2011). Indeed, two wells (MTG-1 and SA-1) record this increasing rate of subsidence during Late Paleocene. This can be interpreted as the formation of flexural basins and the inversion of extensional faults (Sinclair et al., 2005).

MTG-1 records a last acceleration of subsidence rate the Priabonian (Late Eocene). In our case study, this corresponds to the deposition of the upper part of the Carcassonne Group, constituted of coarse detrital deposits. Moreover, we saw on the cross-section between the Aurignac and the Saint-Andre anticlines an increasing of the thickness of these sediments in a growth fold (Fig. 15). Thus, this acceleration of subsidence can be the consequence of the major phase of compression that led to the formation of the succession of anticlines and synclines in the Petites Pyrenees, concomitant with a phase of flexural subsidence in the platform. The subsidence curve for SA-1 does not show such a trend because it is situated in the Petites Pyrenees and the flexural subsidence was mainly occurring in the Aquitaine platform. By these times, the Petites Pyrenees were part of the thrust wedge.

According to Sinclair et al. (2005), the subsidence is considered to stop since the Priabonian, as the retro-wedge thrust front activity ceased. In the case of AV-101 which

records sedimentation until Miocene, we can see that the subsidence rate is 0.06 mm/yr so it is not null as predicted by authors.

Moreover, Naylor & Sinclair (2008) predict the non-migration of the sedimentation in the retro-foreland basin, in contrast with the pro-foreland basin where stratigraphic onlaps on the cratonic margin are described. They show a progressive onlap cratonward at a rate of 5 mm/yr. In order to comment this proposition, we evaluate the migration of sedimentation in the retro-foreland basin along the studied transect. In our cross-section, there is no onlap on the cratonic margin, but there is slight onlaps on pre-orogenic sequences: to the south of the well CDR-101, we can see the Petites Pyrenees, the Rieubach and the Coustouge Group deposits making progressive onlaps on the Jurassic substratum. Between the Petites Pyrenees and the Rieubach Group we calculate a onlap propagation of 0.088mm/yr, and between the Rieubach and Coustouge Group sediments a rate of 0.36 mm/yr. Thus, the onlap propagation rate increased with time, as described by Sinclair et al. (2005). Although they are 1 or 2 order of magnitude less, the propagation is not null and this contradicts their prediction. The authors interpreted this increasing rate by a flexural component: they assume that as the flexure is very important during the growth phase, the propagation of the cratonic onlap is low. On the contrary, as soon as the flexure decreases, the stratigraphic onlaps become more and more important and so the rate increases. The evolution we have along the studied transect is similar but it is much smaller in scale.

Paleogeographic evolution

Triassic and Liassic times were characterized by evaporitic to shallow marine deposits where shallow carbonate platforms predominate. The thicknesses of these deposits are homogeneous in the southern part of the Petites Pyrenees, and are thicker in the platform. This shallow marine sedimentation is related to an extensional tectonics leading to the opening to the West of the Atlantic Ocean (Brunet, 1991).

Variations in facies occurred during Early Cretaceous near the thrust front showing a relative shallowing, as testified by fossil-rich reef facies (Aptian Urgonian limestones for instance). The transition between Albian and Cenomanian is marked by marine clastic sedimentation (Albo-Cenomanian sedimentation). At the same time, the considerable thickness of volcanism (*Recurt Formation*) deposited in the north of the Petites Pyrenees must be noted. This is probably related to an extreme crustal extension event (Choukroune, 1976; Jammes et al., 2010; Lagabrielle et al., 2010). Late Cretaceous sedimentation is predominantly present south to the PPF and shows a progressive shallowing, from the turbidites deposits (*Plagne Formation*) to shallow marine (*Nankin Formation*) and marine-continental transitional sedimentation (*Auzas Formation*). As the Pyrenean chain grew during the Cenozoic, conditions became continental except for Late Paleocene and Ilerdian marine transgressions. Variations in thicknesses, facies and spatial distribution of deposits are related to an increase in tectonic activity which is

marked by the first contribution of the chain's uplift and erosion during Middle Eocene (*Palassou Formation* and *Lussagnet Sandstone Formation*), and extends to Miocene. Syn-growth folds are sealed by the post-orogenic Aquitaine Group.

Sequential restoration and evolution of Pyrenean retro-foreland basin

The studied transect has been sequentially restored into four steps in order to estimate the amount, timing and distribution of shortening due to Pyrenean compression within the retro-foreland basin. It also allows to understand the current structural geometries, their relationship with sedimentation and their inheritance from Mesozoic extensional phases. The major role of Keuper evaporite diapirism and its crucial control on the distribution of deformation will also be discussed. Constrained by detailed stratigraphic geometries, the method used consists in restoring step by step the structures and evaluate the timing of their activity and their influence on the basins; from a pin-line situated in the south of the non-deformed platform (see Fig.15 for the location of the pin-line). As salt diapirism is present in the studied zone, the strain can be concentrated over a large area. The thicknesses of the units near the salt structures can thus vary along the transect as well as the thickness of the salt, which is very ductile. The restoration of the pre-orogenic state is shown by two stages, the third one is an intermediate stage and the last one represents the first state of orogeny (fig. 23 a-e).

The pre-orogenic stage corresponds to Apto-Lower Albian times (fig. 23e). Three mini-basins are distinguished along ~45 km from south to north. They are separated by three diapirs. The southernmost diapir was very thick and evolved along a south-dipping normal fault that was the precursor of the northern margin of the Black Flysch basin. This fault took its origin in the basement. On both sides of this diapir, thicknesses of the Black Dolomite Group varied; they were thicker on the southern side. This indicates that diapirism was active from Early Jurassic, and as the salt moved upwards, the strata were tilted and slightly folded. At that time, the crystalline basement was 3 km deep. The southernmost mini-basin comprised a very thick Apto-Lower Albian sequence (probably more than 4 km thick), overlying the Miranda Limestone and Black Dolomite deposits. The central mini-basin comprised thinner layers pinching out along the flanks of the diapirs. The third mini-basin had a similar shape, with longer strata. The down-dipping strata along the northernmost diapir are typical of a turtle-back structure, revealing the collapse of the diapir. The growth of this diapir was facilitated thanks to a south-dipping normal fault, taking its origin in the Keuper Group. This fault was the precursor of the Petites Pyrenees Front. To the north, strata were straight and there was no sedimentation of the Miranda Limestone and Sainte-Suzanne Groups. The top of Apto-Lower Albian represents a major erosional stage.

The second stage (fig. 23d) shows the architecture at the end of Upper Albian-Cenomanian. It is characterized by the development of a 15 km-wide Black Flysch basin. This step corresponds to a major extensional stage. To the south, the normal fault led to the sliding of the underlying strata. As the extension continued, the basement was

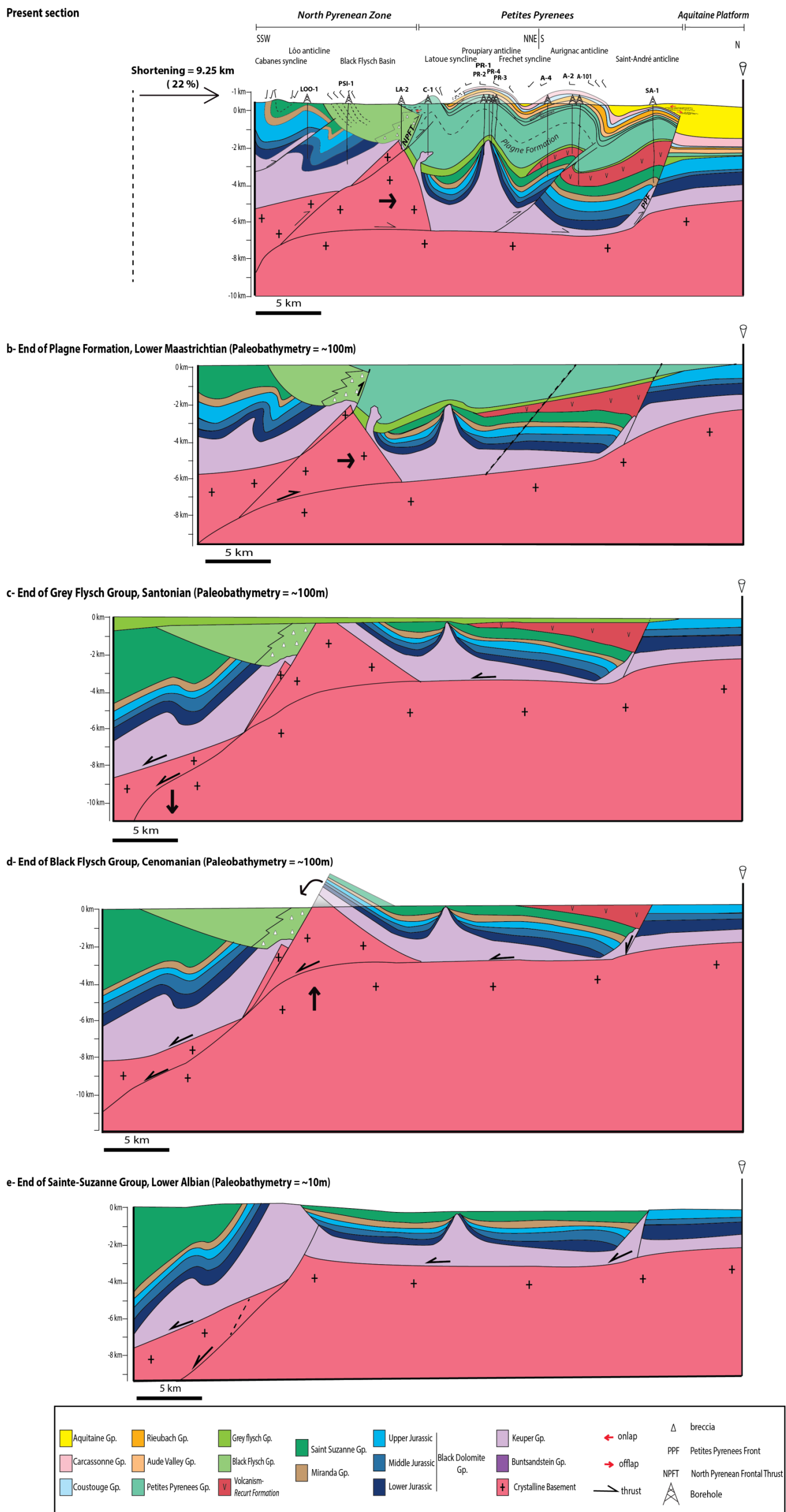


Figure 23: Sequential restoration of the balanced cross-section (see Fig. 15) into four steps. The shortening between the end of Apto-Lower Albian and the present section is estimated at 22%.

pushed upwards and reached the surface as well as the overlying deposits. It was drawn considering a ratio of 2 to 1 (the length of the basin margin is twice as big as the overhanging block length, fig. 24).

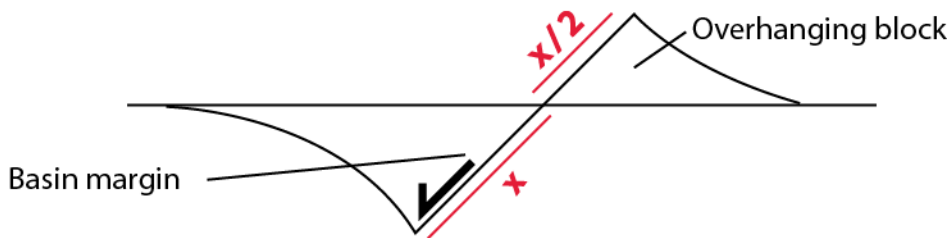


Figure 24: Schematic representation of the ratio used (2:1) to construct the overhanging block in the construction of the restoration (second step), where "x" is the length of the basin margin.

Consequently, the erosion of the overhanging block filled the northern margin of the newly-formed basin in breccias made of Paleozoic to Lower Albian clasts. They are thus south-dipping. Also, the sliding caused the decrease in thickness of the salt; the dips of the strata below this basin were less steep than in the previous stage and their folding increased. A second smaller normal fault was formed to the south of the major normal fault and it appeared at the base of the Albo-Cenomanian basin. To the north along the second major normal fault, extension led to the sliding of the strata above the salt diapir. It must be noticed that this step is marked by the onset of extrusive volcanism (*Recurt Formation*, Cenomanian time). The hyper-extensional context caused the extreme thinning of the crust and promoted magmatic ascents along normal faults.

Figure 23c shows the transition between the extension and the onset of the compression. After the erosion of the overhanging block, the Grey Flysch sediments deposited over the whole area. They lied unconformably on the underlying strata. Constrained by well descriptions, the thickness of this Group is thicker to the south than in the north. We interpreted this as a thermal subsidence stage, leading to a slight flexure of the southern part of the transect. To the north, the Grey Flysch sedimentation made a progressive unconformity upon the Upper Jurassic strata. At this time, the volcanism at the north of the restored cross-section became intrusive (Turonian time), and thickened the overall *Recurt Formation*.

The fourth stage corresponds to the onset of the convergence (fig. 23b). This stage represents the top of the *Plagne Formation* (Campanian-Lower Maastrichtian time). To the south, the major normal faults were inverted and are at this stage the NPFT and the PPF. In the southern part of the transect, the strata above the NPFT (from Black Dolomite to Grey Flysch sediments) were tilted, and their folding is accentuated. Consequently, the Apto-Lower Albian basin, the Black Flysch basin and the Grey Flysch deposits were eroded (1.5 km), as none of these sediments are found at present-day in this area. The convergence caused also the tilting of the basement, which from that time is pushed by the NPFT and it started to push the mini-basin sedimentation northwards, acting as bulldozer. The major diapir (in the future Proupiary anticline) started to be squeezed. On the both sides of the NPFT, the salt migrated downwards and its thickness

decreased. This stage shows the beginning of the formation of the flexural basin, filled by the *Plagne Formation*. The blind thrust fault is sealed by these sediments that deposited onlapping onto the Black Flysch basin. The newly-formed flexural basin was well-delimited to the south (NPFT) and the north (PPF), and the biggest flexure occurred in its southern part. Thus, the *Plagne Formation* is thicker to south of the main diapir (~ 3.5 km) and thinner northwards (~ 2.5 km). To the north, the sedimentation prograded progressively upon the Grey Flysch deposits and extends 5 km further to the north than these sediments.

This sequential restoration shows that the deposits are slightly folded at the end of the Maastrichtian, but the main folding episode occurred after this phase. The main compressional phase seems to have occurred during Early Eocene until Late Eocene revealed by the thickening of the Carcassonne Group between the Aurignac and the Saint-Andre anticlines. Also, the stratigraphic repetitions seen in the borehole A-101 (fig. 15) are caused by a reverse fault appeared after the *Plagne Formation* sedimentation. The Quaternary erosion is estimated between 700 and 750 m (calculated from fig. 15).

By comparison between the first stage (Apto-Lower Albian, Fig. 23e) and the present day section (Fig. 23a), the shortening is calculated to be ~ 9.25 km, which represents 22% of the undeformed length. The major part of the shortening is attributed to the NPFT (~ 5.65 km), the displacement due to the PPF is much lower (1.8 km) and 1.8 km can be ascribed to the thrust between them affecting A-101. It is important to remember that these values do not represent the total shortening of the Pyrenean chain; it only concerns the retro-foreland basin from the northern part of the NPZ.

8. Conclusion

The aim of this work was to use the Central Aquitaine basin as a detailed case study, in order to estimate the amount, timing and distribution of shortening due to Pyrenean compression within the retro-foreland basin. We show along the studied transect that there are three zones with different deformation style. To the south, the NPZ records the pre-orogenic history, from Trias to Lower Albian. It presents a pre-orogenic folding and a major discordance at the base of the Upper Albian. The Petites Pyrenees are bordered to the north by the PPF which controlled its sedimentation. They contain the whole stratigraphic series, from Trias to the Aquitaine Group. The northern platform is slightly deformed.

Thanks to the sequentially restoration, we outline several points: (i) inherited structures from Mesozoic extensional phases have a major role on the mechanics of deformation; (ii) the major faults (extensional and then inverted NPFT and PPF) controlled the sedimentation since the Early Mesozoic; (iii) the salt has a major role in the deformation: active salt diapirism from Jurassic separated several min-basins and several faults, such as the PPF, took their origin in the Keuper group.

The shortening is estimated at 22%, equivalent to 9.25 km, from the northern part of the NPZ to the south of the stable platform.

The chronology of the deformation was constrained thanks to the sequential restoration and the subsidence curves: the Trias and the Jurassic corresponded to extensional phases as the west of the Atlantic ocean opened. A major extensional phase is recorded since the Aptian until the Cenomanian, leading to the deposition of deep basins and to extrusive volcanism. From the Turonian until the Santonian, this is probably a thermal subsidence phase, the south of the studied transect sagged slightly downwards. This phase has also probably a flexural component, but the major onset of flexural phase occurred during the Upper Cretaceous and more particularly during the Petites Pyrenees Group (*Plagne Formation*). This is the beginning of the creation of the flexural basin. The subsidence rate, which is not important during this stage, increased during the Late Paleocene, revealing the creation of the flexural basin (Petites Pyrenees). The Late Eocene is also marked by a high subsidence rate, which has been interpreted as a major deformation stage, during which the folding seen in the Petites Pyrenees occurred. We also outlined the timing of the main faults: the NPFT activity is sealed by the *Plagne Formation* whereas the PPF activity is sealed by the Aquitaine Group. This shows that the deformation propagated northwards with time. Moreover, we were able to calculate onlap propagation rate in the northern platform showing a slight migration of the sediments northwards over pre-orogenic sequences. Thus the retro-foreland basin is not static, by contrast with the proposition of Sinclair & Naylor (2008).

9. References

- Allen PA, Allen JR (2009) Basin Analysis. Principles and Applications. Blackwell Publishing. London, 549p
- Baby P, Crouzet G, Specht M, Deramond J, Bilotte M, Debroas EJ (1988) Rôle des paléo-structures albo-cénomanianes dans la géométrie des chevauchements frontaux nord-pyrénéens. C.R Acad. Sci. Paris, 306(II) 307-313
- Barnolas A, Guérangé B, Chiron JC, Courbouleix S, coord. (unpublished) Synthèse Géologique et Géophysique des Pyrénées. Cycle alpin. Volume 2, 946p
- Beaumont C, Munoz JA, Hamilton J, Fullsack P (2000) Factors controlling the Alpine evolution of the central Pyrenees inferred from a comparison of observations and geodynamical models. Journal of Geophysical Research. 105:8121-8145
- Biteau JJ, Le Marrec A, Le Vot M, Masset JM (2006) The Aquitaine Basin. Petroleum Geosciences, Vol. 12, pp 247–273
- Bourrouilh R, Richert JP, Zolnai G (1995) The North Pyrenean Aquitaine Basin, France. American Association of Petroleum Geologists Bulletin. 79 (6), pp 831-853
- BRGM, Elf-Re, ESSO-REP, SNPA (1974) Géologie du Bassin d'Aquitaine. Atlas, 27 pl. Editions du Bureau de Recherches Géologiques et Minières, Orléans
- Brunet MF (1991) Subsidence et géodynamique du Bassin d'Aquitaine ; relations avec l'ouverture de l'Atlantique. Thèse de doctorat d'état, Université Pierre et Marie Curie, Paris, 91-8 :288p
- Cahuzac B, Janin MC, Steurbaut E (1995) Biostratigraphie de l'Oligo-Miocène du bassin d'Aquitaine fondée sur les nannofossiles calcaires. Implications paléogéographiques. Géologie de la France, 2 :57-82
- Cavaillé A (1968) Notice explicative. Carte géologique de la France (1/50 000). Feuille Beaumont-de-Lomagne (955), 8p
- Cavaillé A (1969) Notice explicative. Carte géologique de la France (1/50 000). Feuille Gimont (982), 7p
- Cavaillé A (1970) Notice explicative. Carte géologique de la France (1/50 000). Feuille Lombez (1008), 7p
- Cavaillé A, Paris JP (1975) Notice explicative. Carte géologique de la France (1/50 000). Feuille Fousseret (1033), 25 p

Choukroune P (1976) Structure et évolution tectonique de la zone nord-pyrénéenne. Analyse de la déformation dans une portion de chaîne à schistosité sub-verticale. Mém. Soc. Géol. Fr, 127:116 p

Debroas EJ (1990) Le flysch noir albo-cénomanien témoin de la structuration albienne à sénonienne de la Zone nord-pyrénéenne en Bigorre (Hautes-Pyrénées, France). Bull. Soc. Géol. France, (8), VI, n°2, pp 273-285

Desegaulx P, Brunet MF (1990) Tectonic subsidence of the Aquitaine basin since Cretaceous times. Bull. Soc. Géol. France, (8), VI, 2:295-306

Ferrer O, Jackson MPA, Roca E, Rubinat M (2012) Evolution of salt structures during extension and inversion of the Offshore Parentis Basin (Easter Bay of Biscay). Salt Tectonics, Sediments and Prospectivity. Ed. ALSOP. Geological Society, London Special Publications, 363:361–379. doi: 10.1144/SP363.16

Fossen H (2010) Structural geology. Cambridge University Press, United Kingdom, p463

Haq BU, Hardenbol J, Vail PR (1987) Chronology of fluctuating sea levels since the Triassic (250 million years ago to present). Science, 235:1156-1167

Hardenbol J, Thierry J, Farley MB, Jacquin T, de Graciansky PC, Vail PR (1998) Mesozoic and Cenozoic Sequence Chronostratigraphic Framework of European Basins. Mesozoic and Cenozoic Sequence Stratigraphy of European Basins, SEPM Special Publication 6

Heritier F, Nicolai R, Ricateau R, Villemin J (1972) Les chevauchements frontaux nord-pyrénéens entre l'Ariège et l'Adour (Pyrénées centrales). C. R. Ac. Sc. Paris. Série D, t.275, pp1533-1736

Jammes S, Manatschal G, Lavier L (2010) Interaction between prerift salt and detachment faulting in hyperextended rift systems: the example of the Parentis and Mauléon basins (Bay of Biscay and western Pyrenees). AAPG Bulletin, 94, n°7, pp 957-975. doi :10.1306/12090909116

Lagabrielle Y, Labaume P, de Saint Blanquat M (2010) Mantle exhumation, crustal denudation, and gravity tectonics during Cretaceous rifting in the Pyrenean realm (SW Europe): Insights from the geological setting of the lherzolite bodies. Tectonics, 29, tc4012, doi:10.1029/2009tc002588

Munoz JA (1992) Evolution of a continental collision belt: ECORS-Pyrenees crustal balanced cross-section. In McClay K: Thrust tectonics. London. Chapman and Hall, pp 235-246

Naylor M, Sinclair HD (2008) Pro- vs. retro-foreland basin. Basin Research 20:285–303. doi: 10.1111/j.1365-2117.2008.00366.x

Paris JP, Appert G, Bugnicourt D, Carbonnier A, Dumon E, Gorce P, de Jekhowski B, Michel P, Nougarède G, Ricateau R, Saint-Martin L, Thibaut P, Thyssen B (1971) Notice explicative. Carte géologique de la France (1/50 000). Feuille Saint-Gaudens (1055) 23p

Paris JP, Icole M, Tegyey A, Monciardini C, Andreieff P (1976) Notice explicative. Carte géologique de la France (1/50 000). Feuille Montréjeau (1056). Ed. BRGM, 25 p

Plaziat JC (1981) Late Cretaceous to Late Eocene Paleogeographic evolution of Southwest Europe. *Palaeoclimatol., Palaeoecol.*, 36:263-320

Serra-Kiel J, Hottinger L, Caus E, Drobne K, Ferrandez C, Jauhri AK, Less G, Pavlovec R, Pignatti J, Samso JM, Schaub H, Sirel E, Strougo A, Tambareau Y, Tosquella J, Zakrevskaya E (1998) Larger foraminiferal biostratigraphy of the Tethyan Paleocene and Eocene. *Bull. Soc. Géol. France*. 169(2) :281-299

Serrano O, Delmas J, Hanot F, Vially R, Herbin JP, Houel P, Tourliere B (2006) Le Bassin d'Aquitaine : valorisation des données sismiques, cartographie structurale et potentiel pétrolier. Ed. BRGM, 245 p

Sinclair HD, Gibson M, Naylor M, Morris RG (2005) Asymmetric growth of the Pyrenees revealed through measurement and modeling of orogenic fluxes. *American Journal of Science*, 305:369–406

Sinclair HD, Naylor M (2012) Foreland basin subsidence driven by topographic growth versus plate subduction. *Geological Society of America Bulletin* 124(3-4):368-379. doi: 10.1130/B30383.1

Sztrakos K, Gély JP, Blondeau A, Muller C (1998) L'Eocène du Bassin sud-aquitain : lithostratigraphie, biostratigraphie et analyse séquentielle. *Géologie de la France*, 4 :57-105

Tambareau Y, Crochet B, Villatte J, Deramond J (1995) Evolution tectono-sédimentaire du versant nord des Pyrenees centre-orientales au Paléocène et à l'Eocène inférieur. *Bull. Soc. Géol. France*, 166(4):375-387.

Tchimichkian G (1974) L'activité magmatique dans le Crétacé traversé en sondages au Nord de Saint-Gaudens. *C. R. Congrès National des Sociétés Savantes. Section des Sciences. Géologie, minéralogie* 96(2):171-178

Verges J (1998) Quantified vertical motions and tectonic volution of th SE Pyrenean foreland basin. *Geological Society Special Publications* 134:107-134

Verges J, Fernandez M (2012) Tethys-Atlantic interaction along the Iberia-Africa plate boundary: The Betic-Rif orogenic system. *Tectonophysics* 579:144-172

Whitchurch AL, Carter A, Sinclair HD, Duller RA, Whittaker AC, Allen PA (2011)
Sediment routing system evolution within a diachronously uplifting orogen : Insights
from detrital zircon thermochronological analyses from the south-central Pyrenees.
American Journal of Earth Science 311:442-442

10. Appendices

List of Appendices

1- Boreholes listed according to their locality (number and name of the geological maps (1/50 000)

2- Lexicon

3- Location of the 6 cross-sections of the PYRAMID team

4- Legend & Lithostratigraphic log and detailed summary table for the borehole LF-1

5- Lithostratigraphic log and detailed summary table for the borehole CS-101

6- Lithostratigraphic log and detailed summary table for the borehole CS-102

7- Lithostratigraphic log and detailed summary table for the borehole AV-101

8- Lithostratigraphic log and detailed summary table for the borehole CDR-101

9- Lithostratigraphic log and detailed summary table for the borehole 0982-4-2

10- Lithostratigraphic log and detailed summary table for the borehole PO-101

11- Lithostratigraphic log and detailed summary table for the borehole MTG-1

12- Lithostratigraphic log and detailed summary table for the borehole AG-1

13- Lithostratigraphic log and detailed summary table for the borehole SA-1

14- Lithostratigraphic log and detailed summary table for the borehole A-101

15- Lithostratigraphic log and detailed summary table for the borehole A-2

16- Lithostratigraphic log and detailed summary table for the borehole A-4

17- Lithostratigraphic log and detailed summary table for the borehole PR-3

18- Lithostratigraphic log and detailed summary table for the borehole PR-4

19- Lithostratigraphic log and detailed summary table for the borehole PR-1

20- Lithostratigraphic log and detailed summary table for the borehole PR-2

21- Lithostratigraphic log and detailed summary table for the borehole C-1

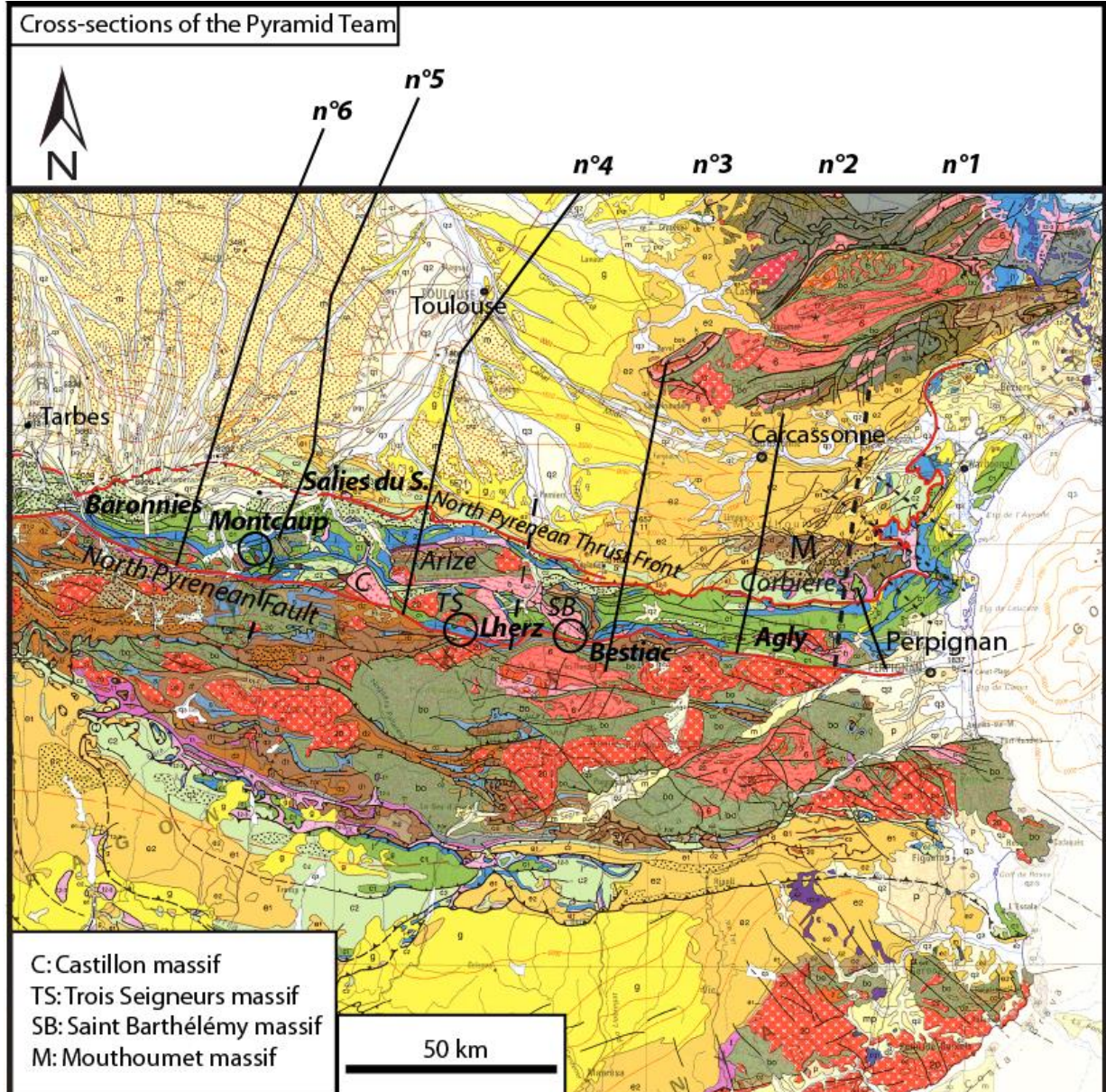
22- Lithostratigraphic log and detailed summary table for the borehole LA-2

23- Lithostratigraphic log and detailed summary table for the borehole PSI-1

- 24- Lithostratigraphic log and detailed summary table for the borehole LOO-1
- 25- Structural cross-section of the south of the Petites Pyrenees and the northern part of the NPZ (Paris et al., 1971)
- 26- Structural cross-section of the NPZ (Debroas 1990)
- 27- Interpreted seismic cross-section (Serrano et al. 2006)
- 28- Structural cross-section of the NPZ, the Petites Pyrenees and the south of the platform (Total, 1998, n°13)
- 29- Structural cross-section of the NPZ, the Petites Pyrenees and the south of the platform (Total, 1998, n°14)
- 30- Structural cross-section of the Petites Pyrenees (Bourrouilh 1995)
- 31- Structural cross-section of the Aurignac anticline (Heritier et al. 1972)
- 32- Eustatic chart used for the calculation of subsidence (Hardenbol et al., 1998)
- 33- Coefficients used for the calculation of subsidence (from Vergès (1998) and Allen & Allen (2009))
- 34- Calculation table used for the construction of the subsidence curves for the borehole AV-101
- 35- Calculation table used for the construction of the subsidence curves for the borehole MTG-1
- 36- Calculation table used for the construction of the subsidence curves for the borehole SA-1
- 37- Calculation table used for the construction of the subsidence curves for the borehole PSI-1
- 38- Summarizing plot of the tectonic subsidence realized for the boreholes AV-101, MTG-1, SA-1 and PSI-1 with the software *subsidence.exe*
- 39- Subsidence curves pour the boreholes AV-101 and SA-1
- 40- Subsidence curves pour the boreholes PSI-1 and MTG-1

Zones	Maps numbers	Maps names	Wells
Northern platform	930	Montauban	LF 1
	929	Saint-Nicolas de la Grave	CS 101 CS 102
	955	Beaumont-de-Lomagne	AV 101
	982	Gimont	CDR 101 0982-4-2
	1008	Lombez	PO 101 MTG 1
	1033 - North of the PPF	Le Fousseret	AG 1
Petites Pyrenees Front			
Petites Pyrenees	1033 - South of the PPF	Le Fousseret	SA 1
			A 101
			A 2
			A 1
			A 4
	1055 - North of the NPTF	Saint-Gaudens	PR 3
			PR 1
			PR 4
			PR 2
			C 1
North Pyrenean Thrust Front			
North Pyrenean Zone	1055 - Sud du CFNP	Saint-Gaudens	LA 2 PSI 1 LOO 1

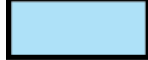
1- Boreholes listed according to their locality (number and name of the geological maps (1/50 000)



3- Location of the 6 cross-sections of the PYRAMID team

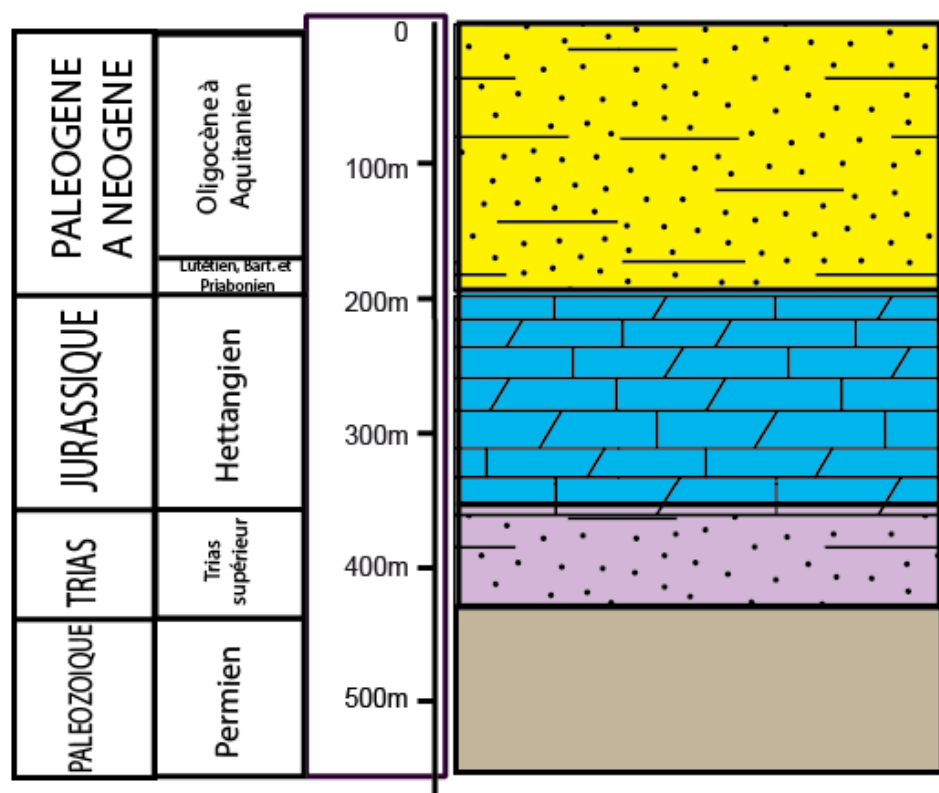
4- Legend & Lithostratigraphic log and detailed summary table for the borehole LF-1

LEGENDE

	Aquitaine Group
	Carcassonne Group
	Coustouge Group
	Rieubach & Aude Valley Groups
	Petites Pyrenees Group
	Grey flysch Group
	Black Flysch Group
	Sainte-Suzanne Group
	Miranda Limestone Group
	Black dolomite Group
	Keuper Group
	Basement

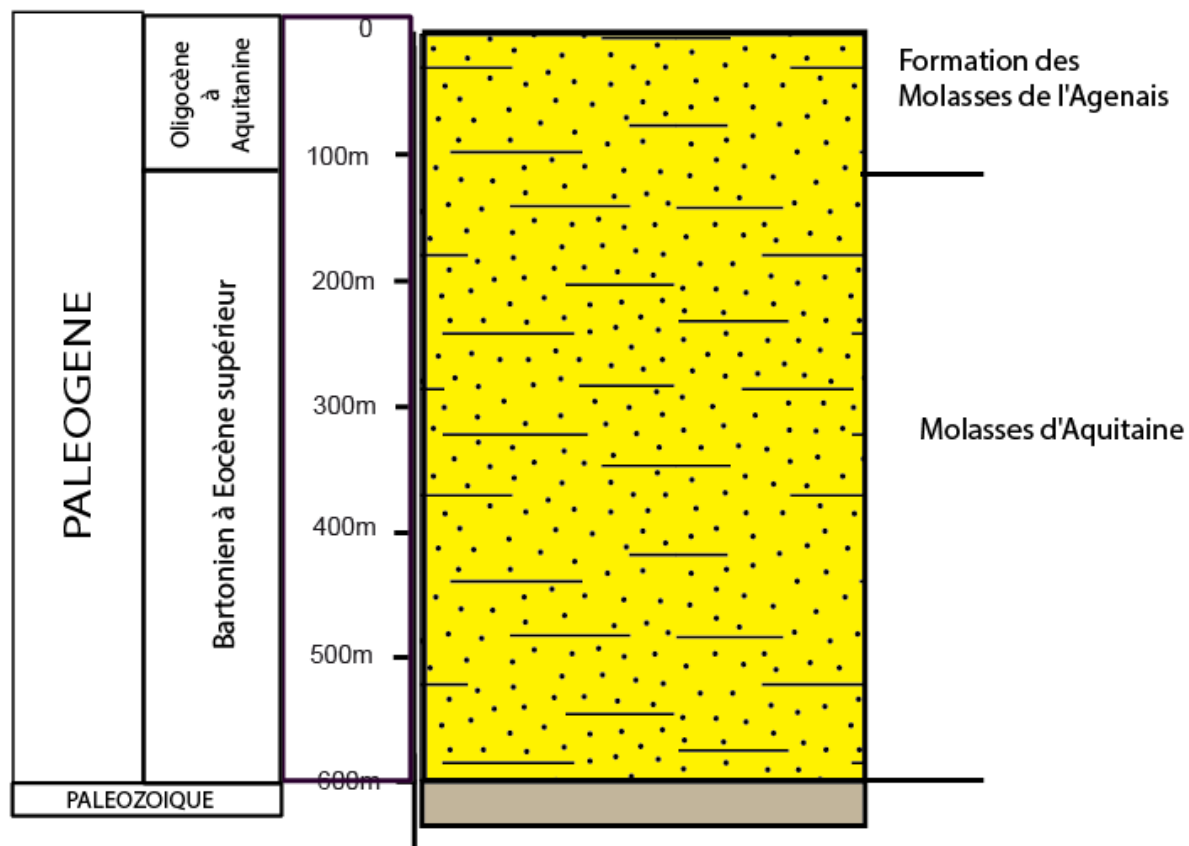
4- Legend & Lithostratigraphic log and detailed summary table for the borehole LF-1

LF 1

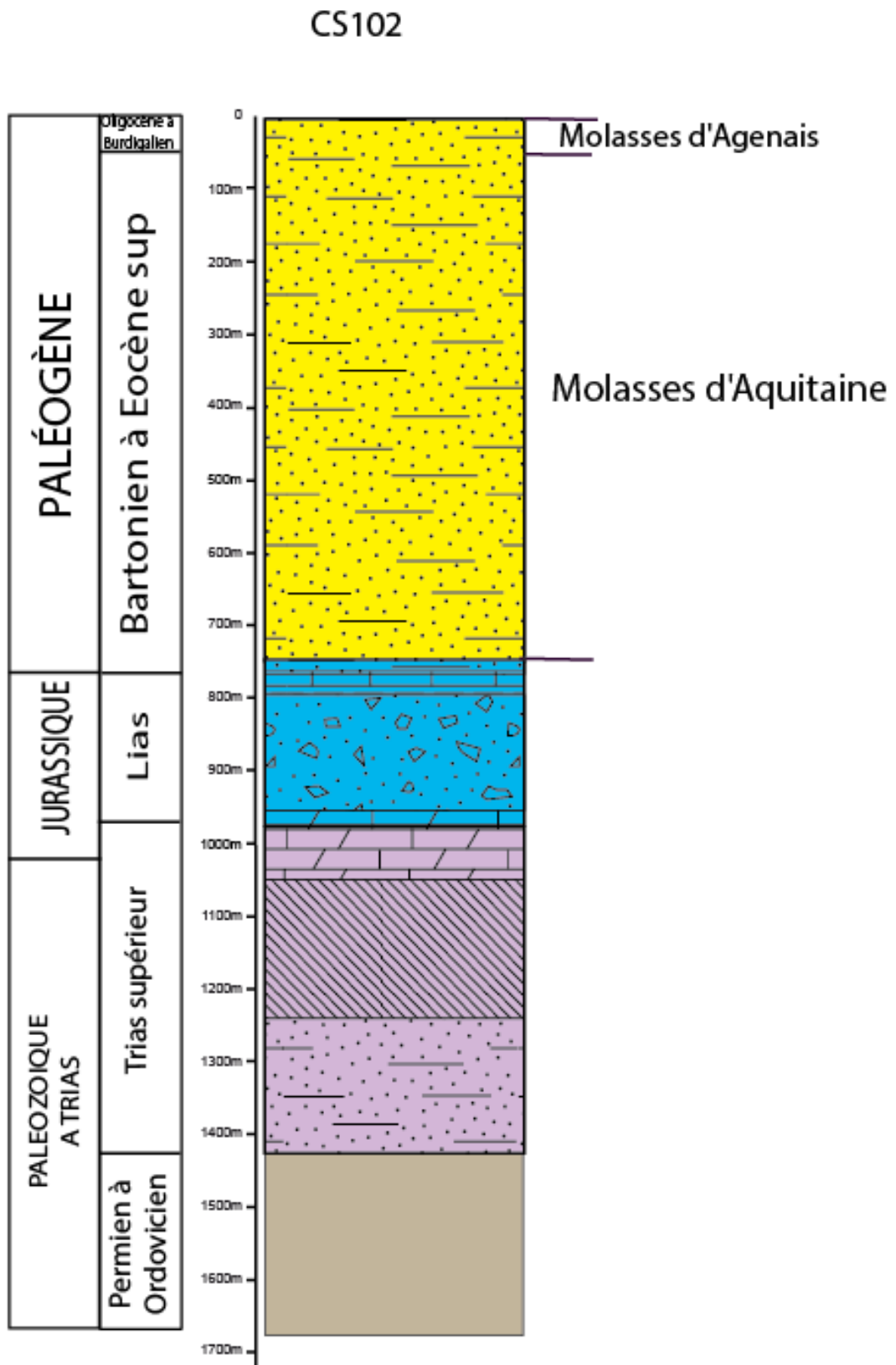


5- Lithostratigraphic log and detailed summary table for the borehole CS-101

CS101

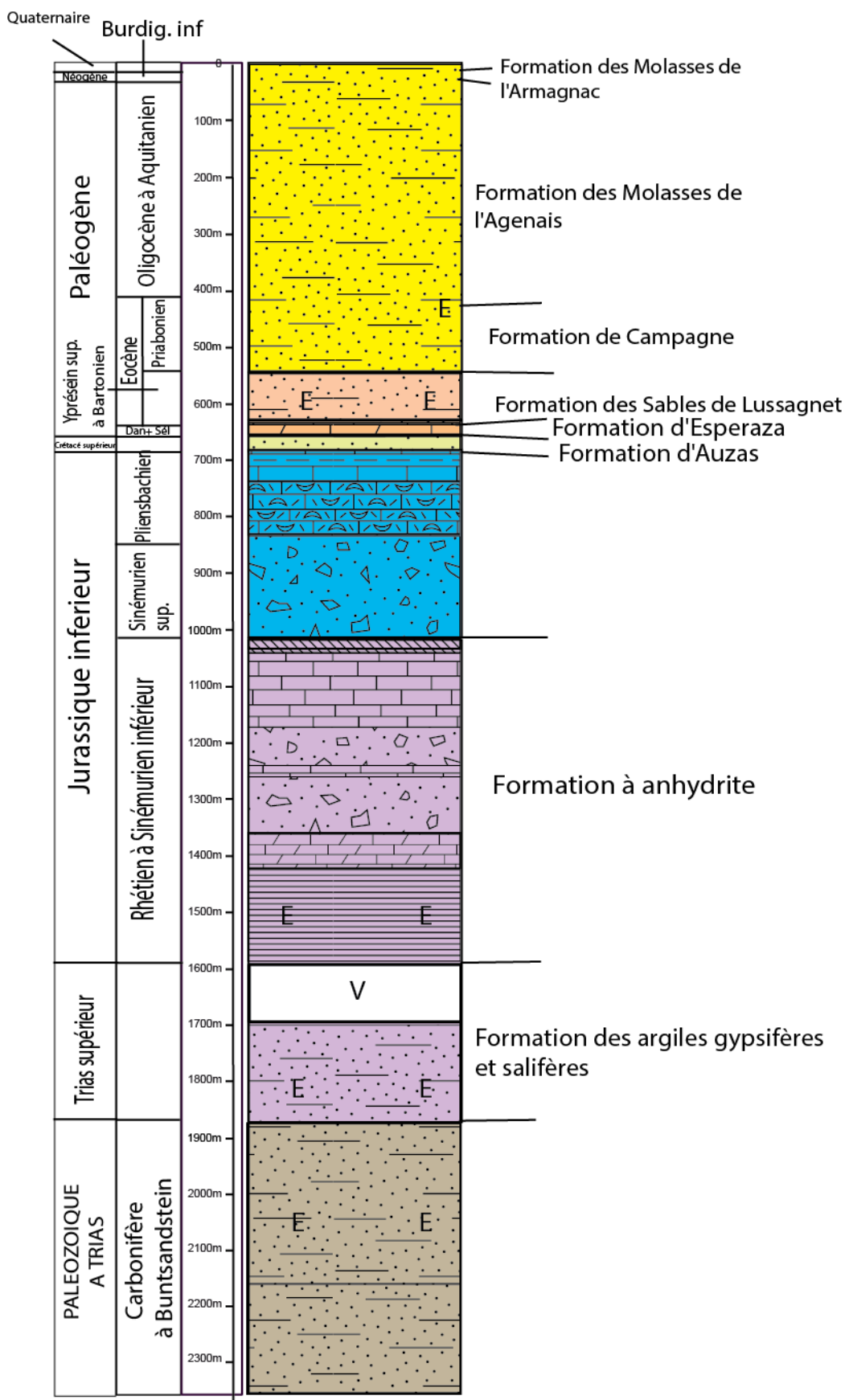


6- Lithostratigraphic log and detailed summary table for the borehole CS-102



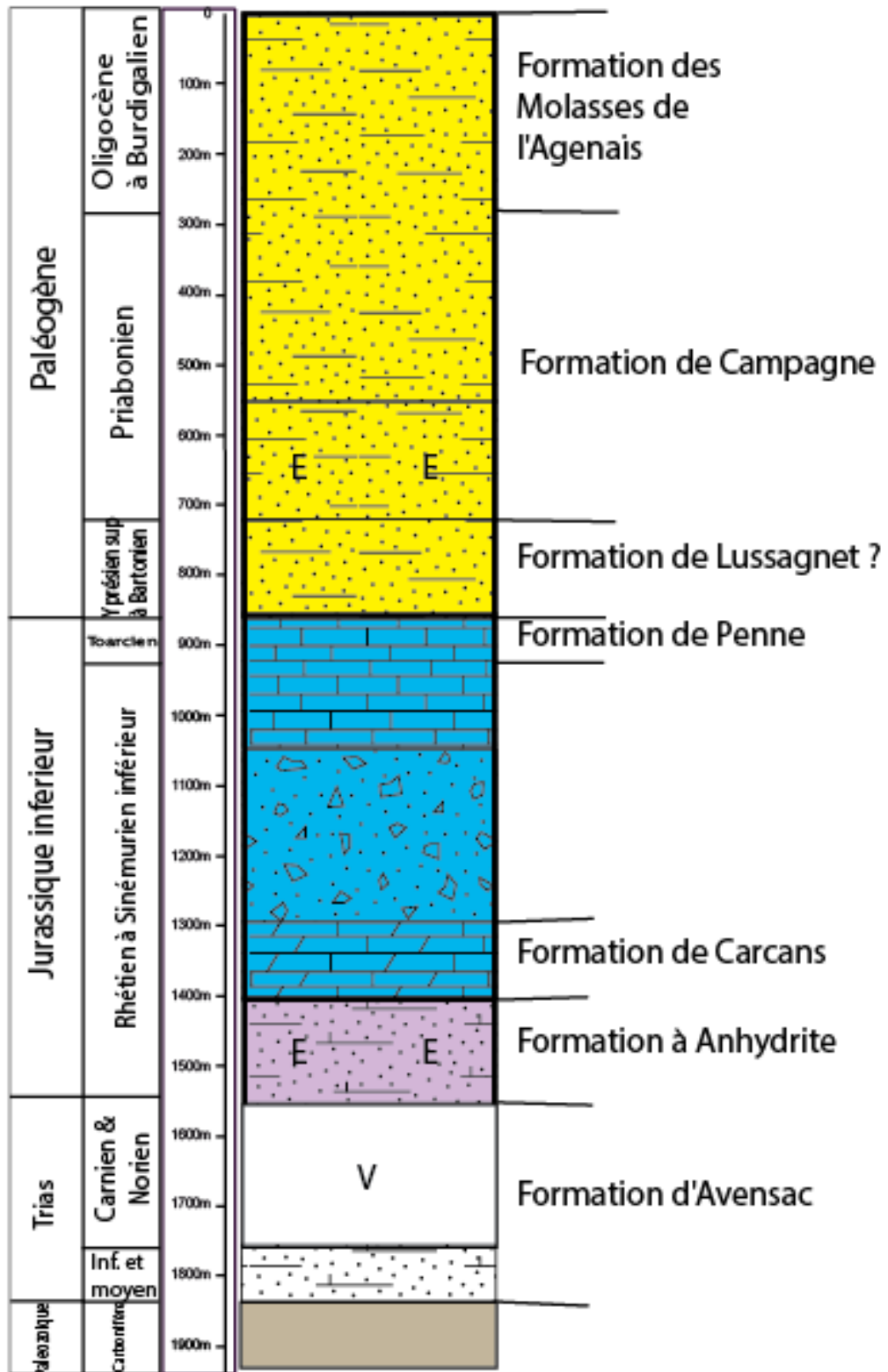
7- Lithostratigraphic log and detailed summary table for the borehole AV-101

AV 101



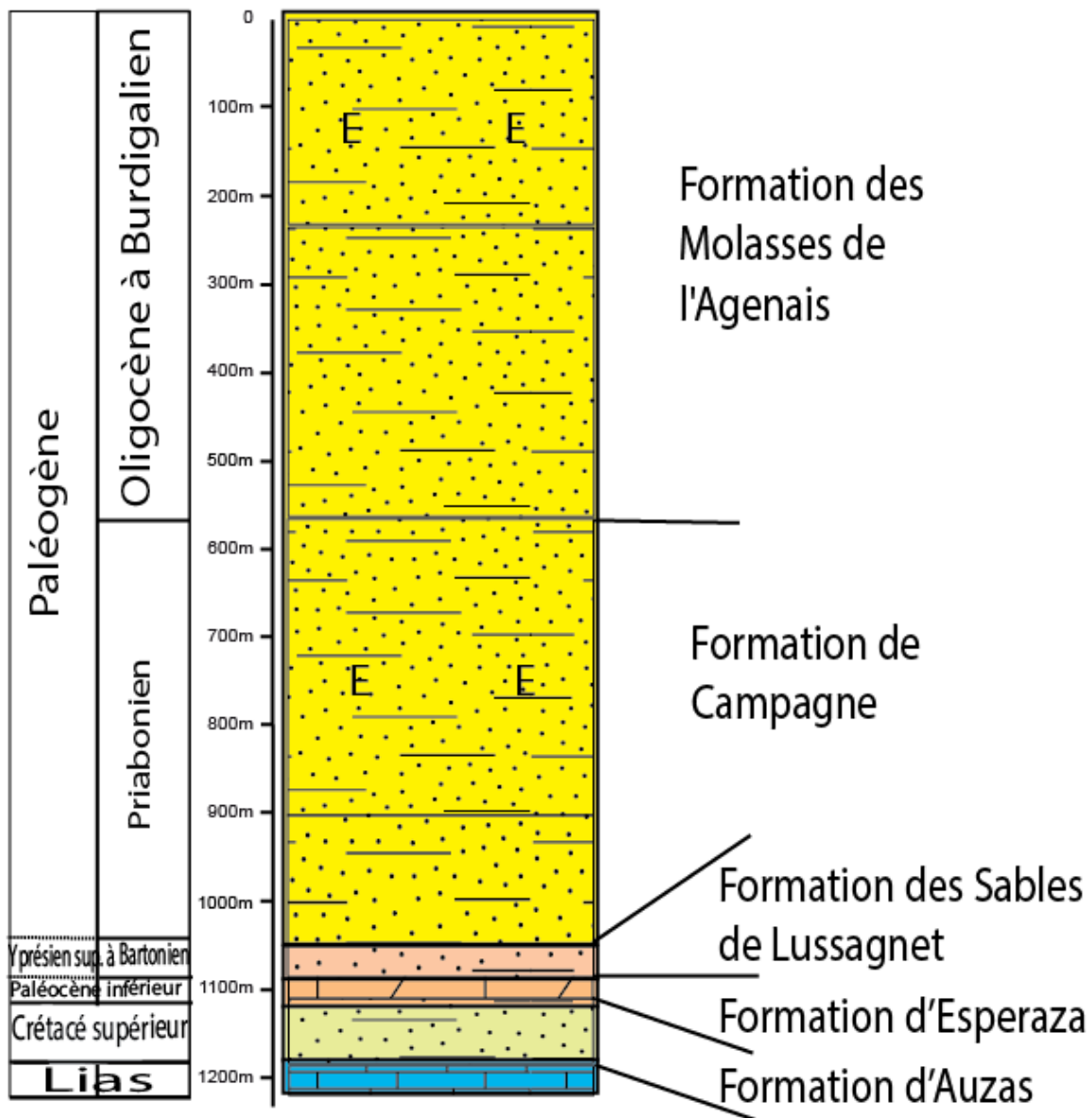
8- Lithostratigraphic log and detailed summary table for the borehole CDR-101

CDR 101



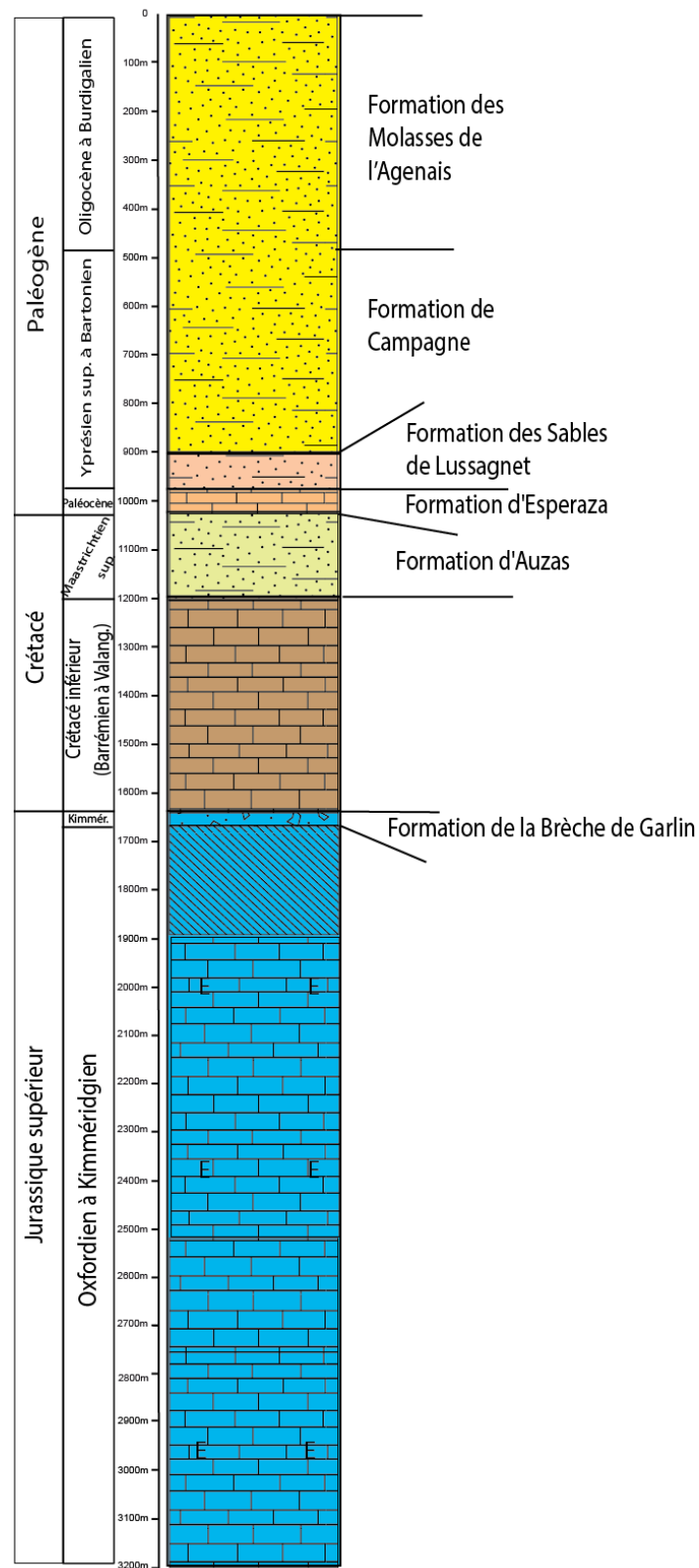
9- Lithostratigraphic log and detailed summary table for the borehole 0982-4-2

0982-4-2



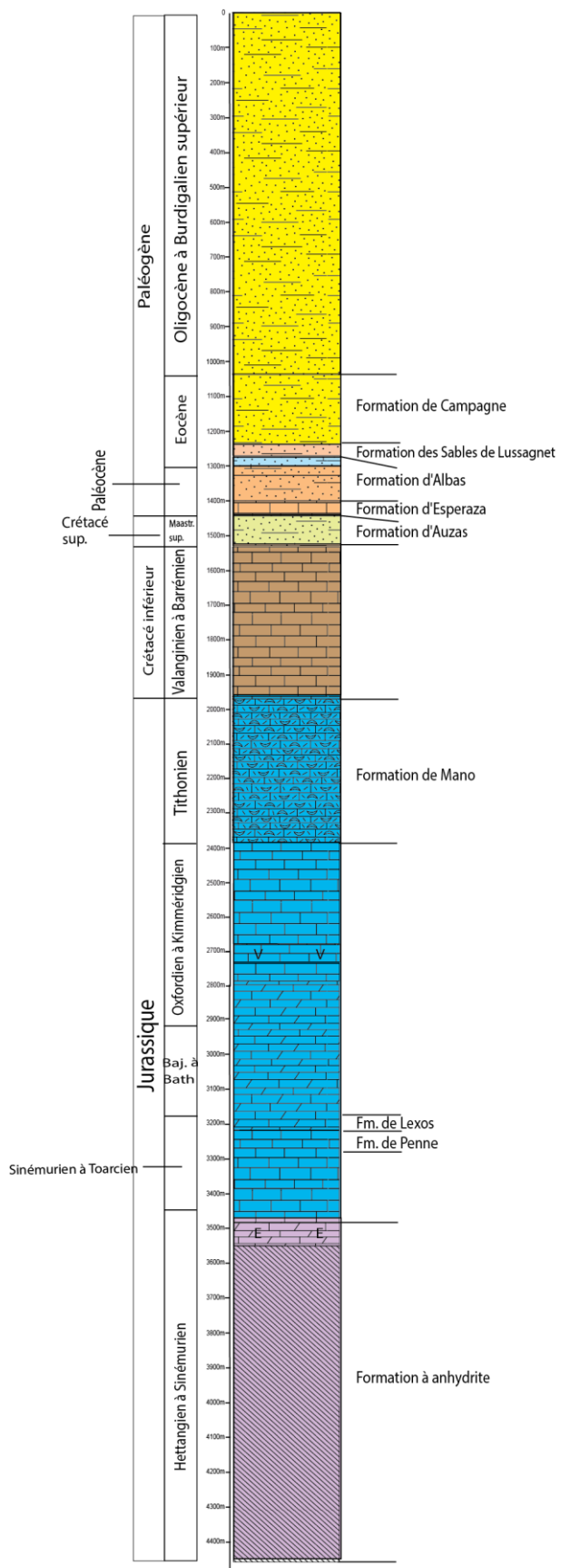
10- Lithostratigraphic log and detailed summary table for the borehole PO-101

PO 101



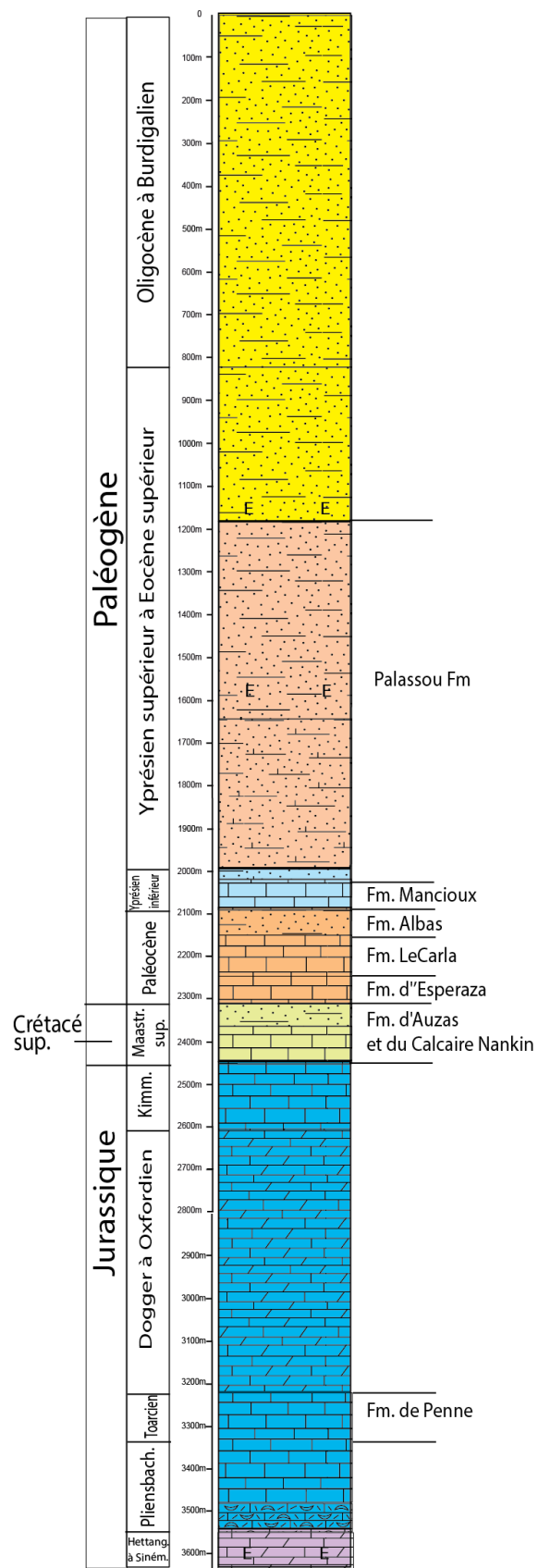
11- Lithostratigraphic log and detailed summary table for the borehole MTG-1

MTG 1



12- Lithostratigraphic log and detailed summary table for the borehole AG-1

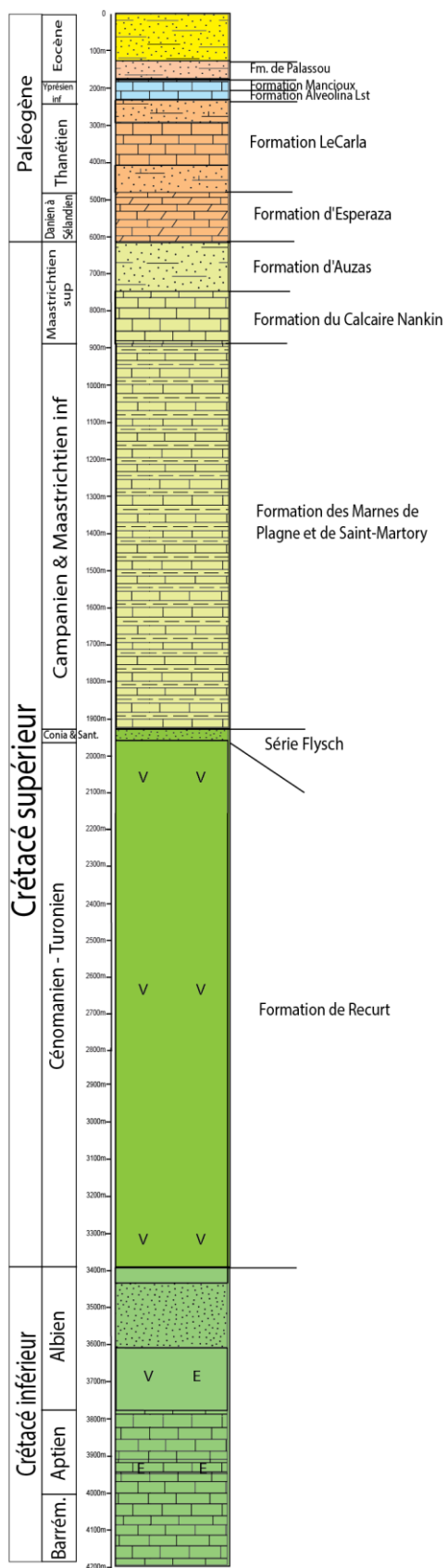
AG 1



M

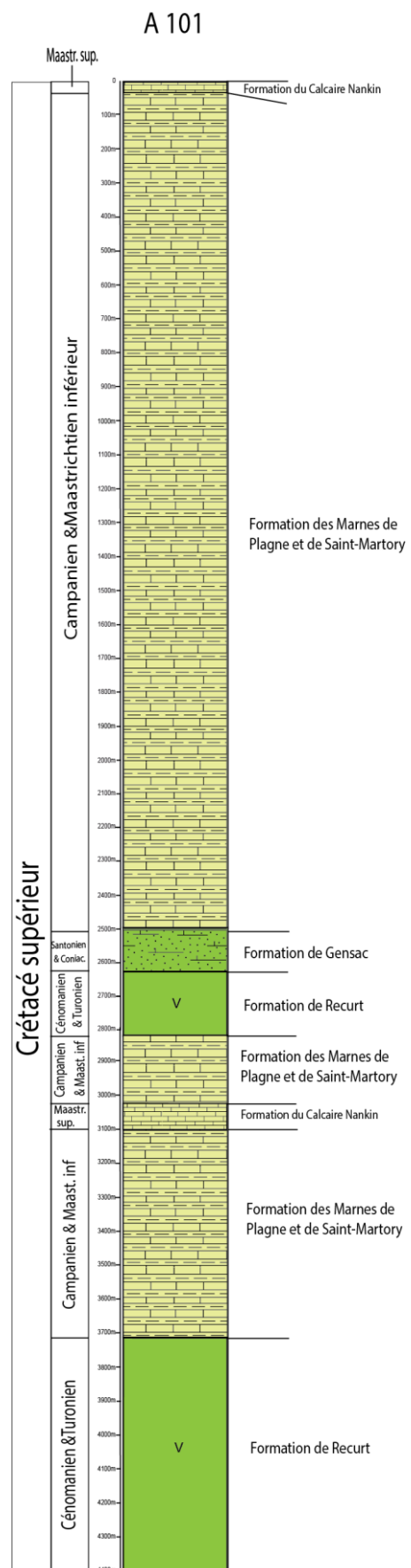
13- Lithostratigraphic log and detailed summary table for the borehole SA-1

SA 1



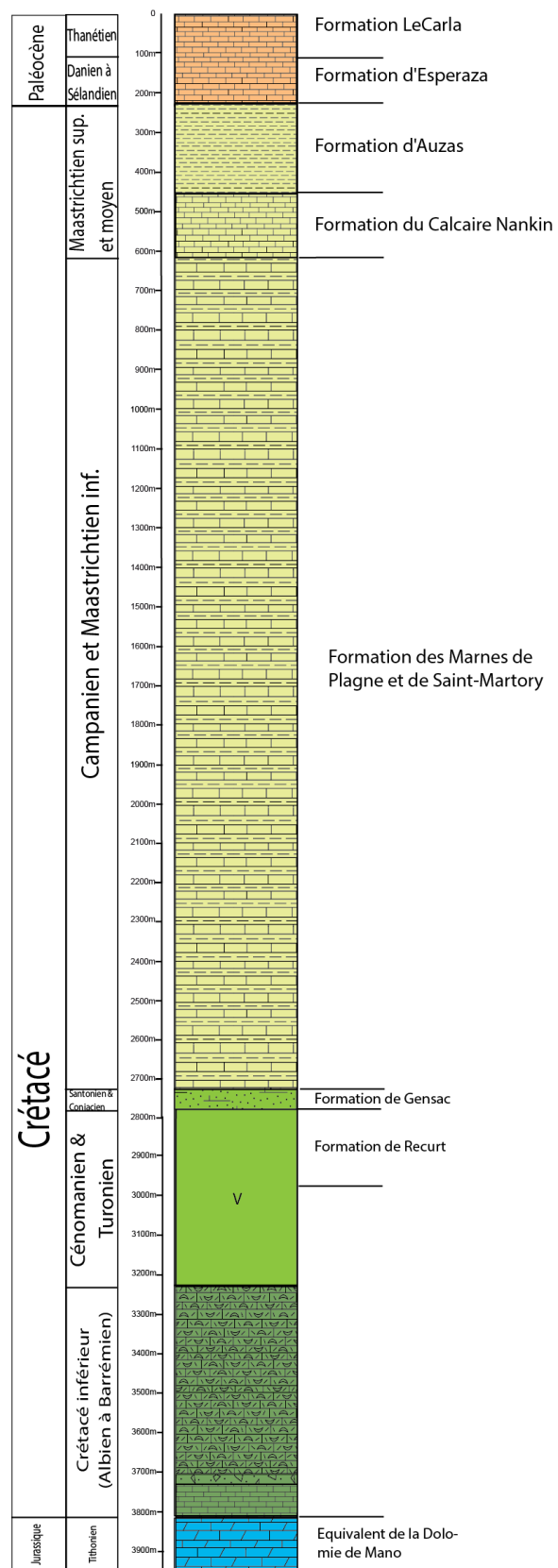
N

14- Lithostratigraphic log and detailed summary table for the borehole A-101



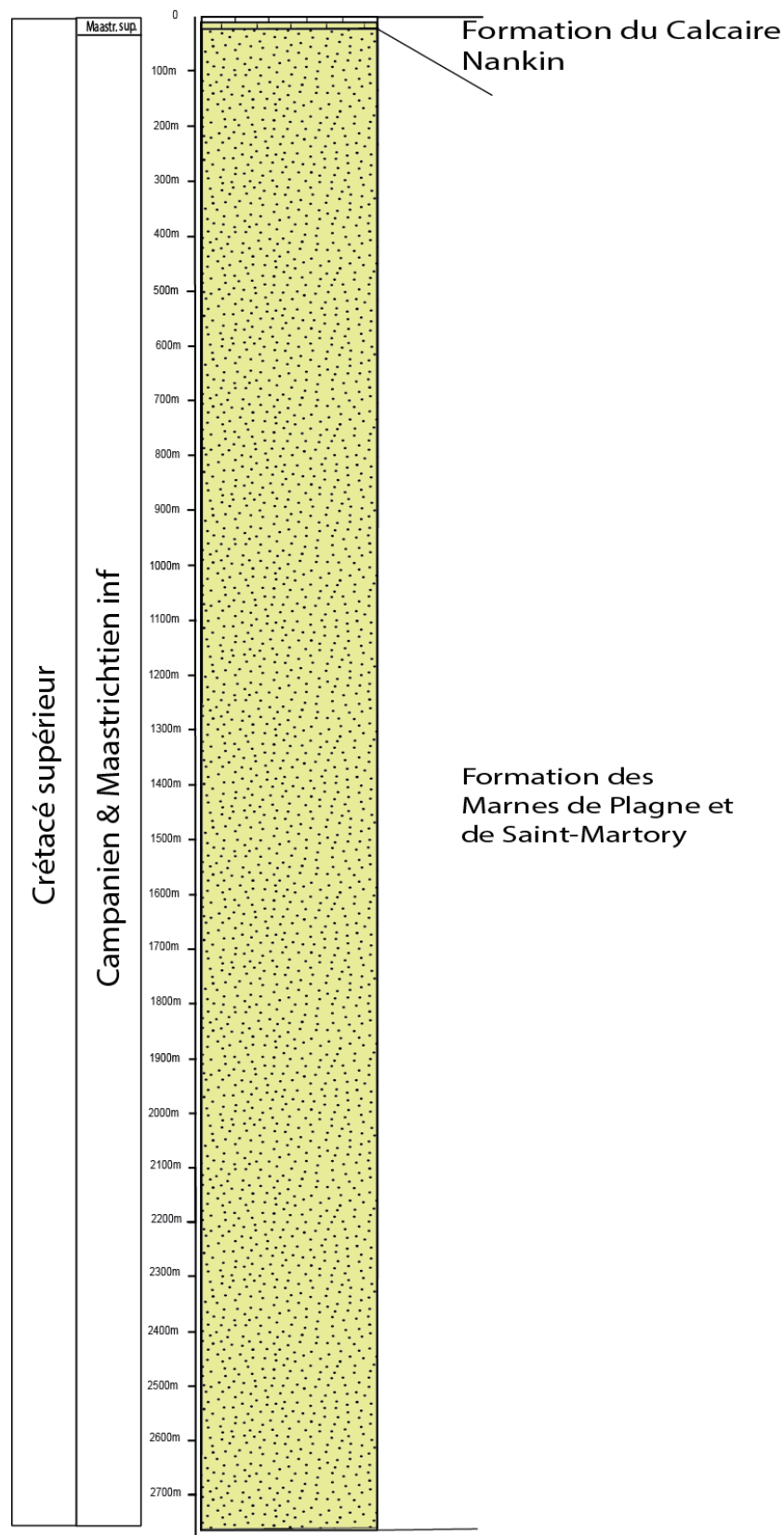
16- Lithostratigraphic log and detailed summary table for the borehole A-4

A 4



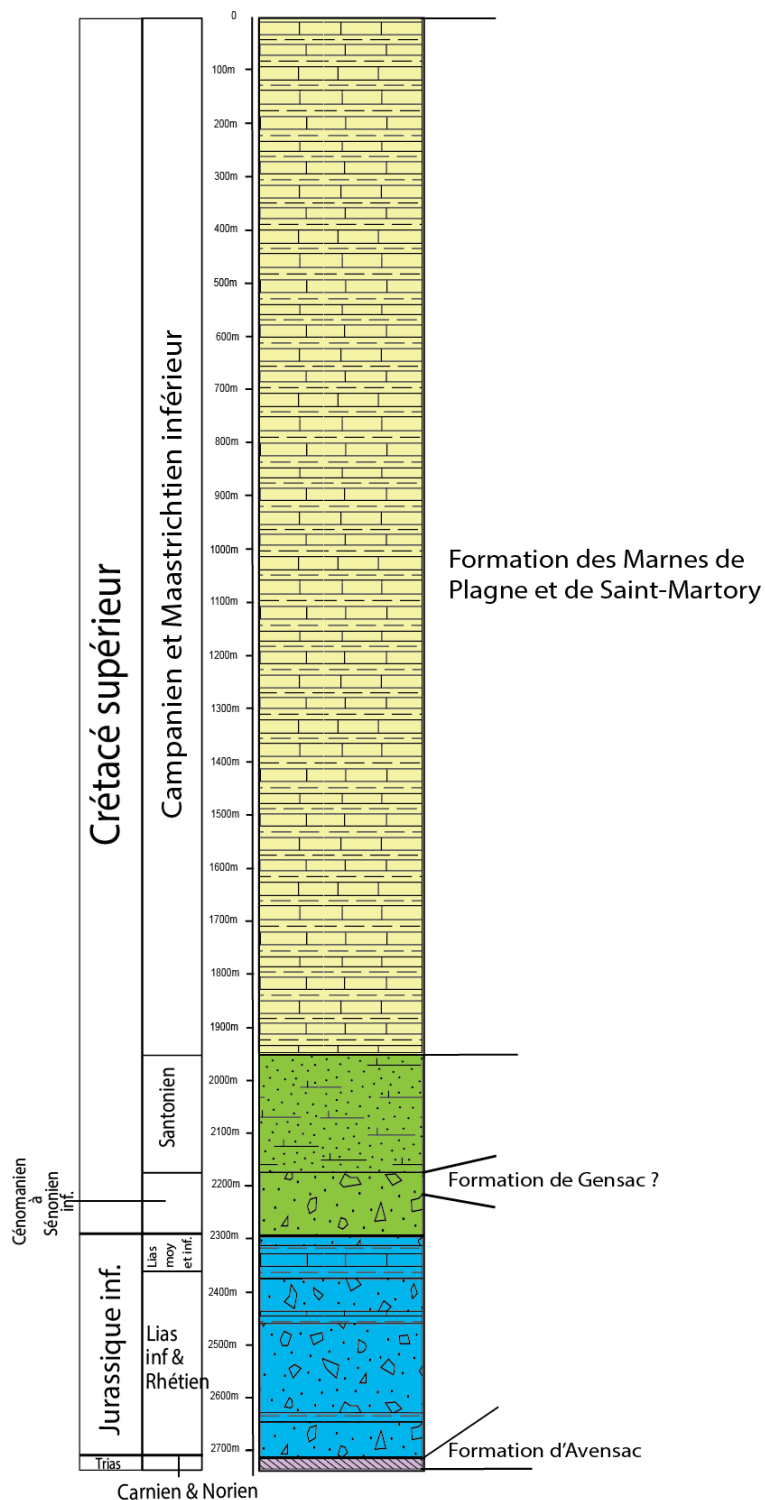
17- Lithostratigraphic log and detailed summary table for the borehole PR-3

PR 3



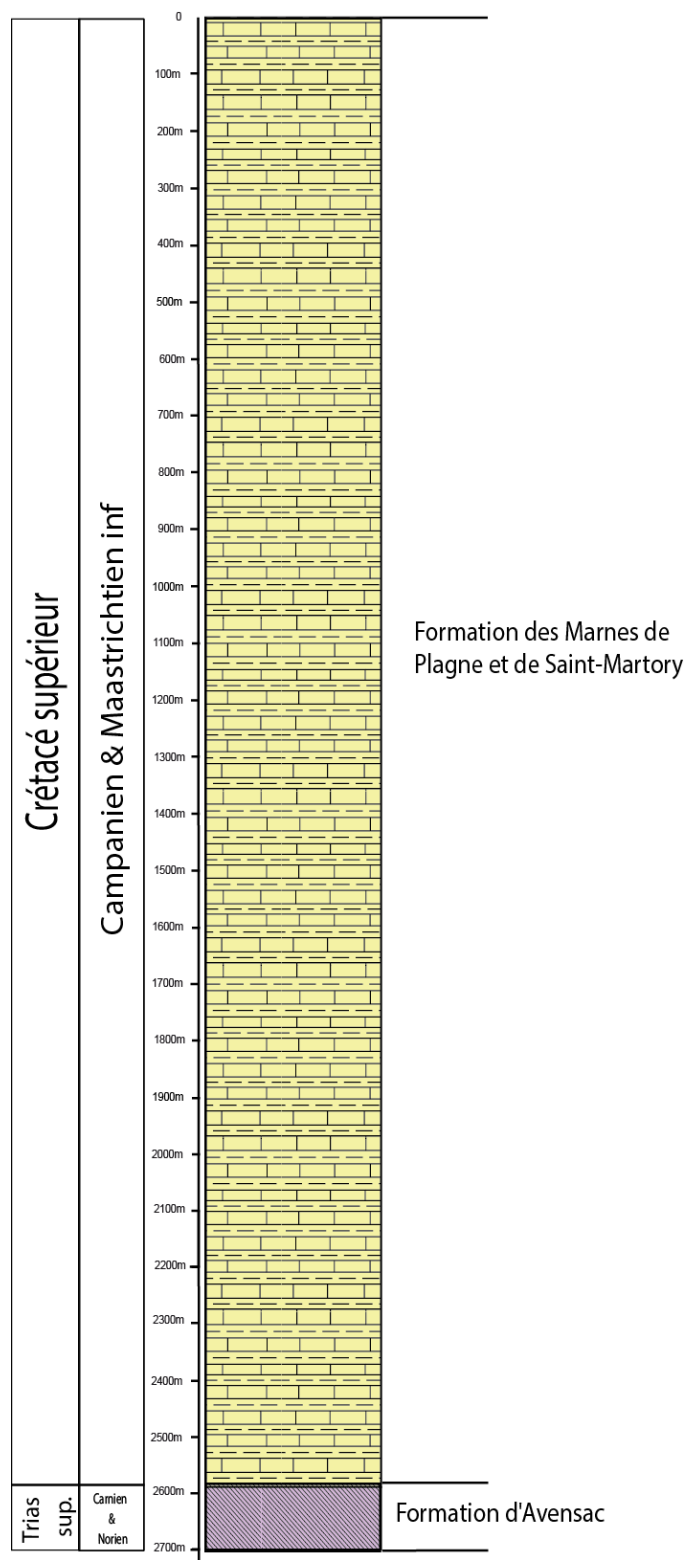
20- Lithostratigraphic log and detailed summary table for the borehole PR-2

PR 2

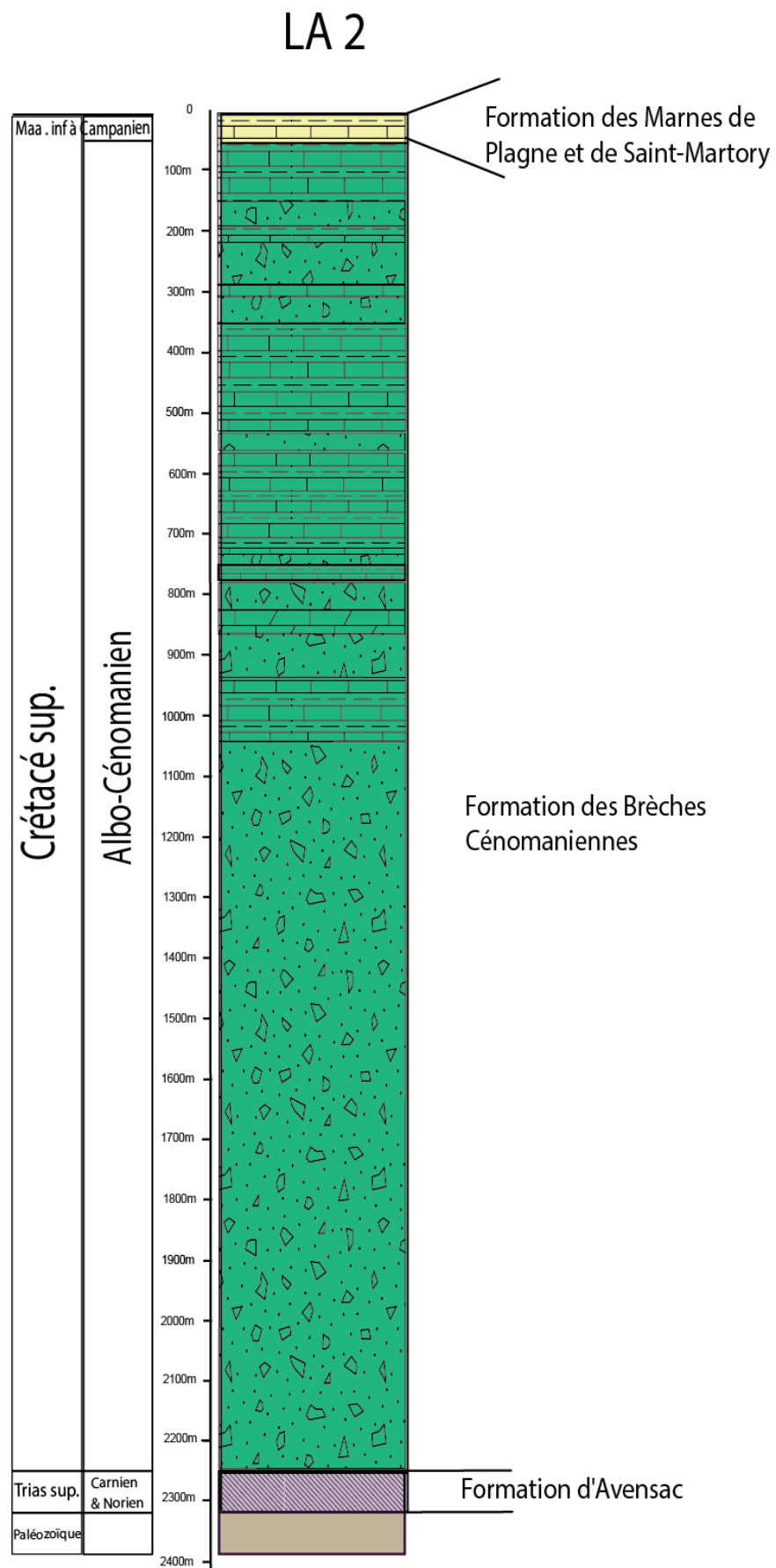


21- Lithostratigraphic log and detailed summary table for the borehole C-1

C 1

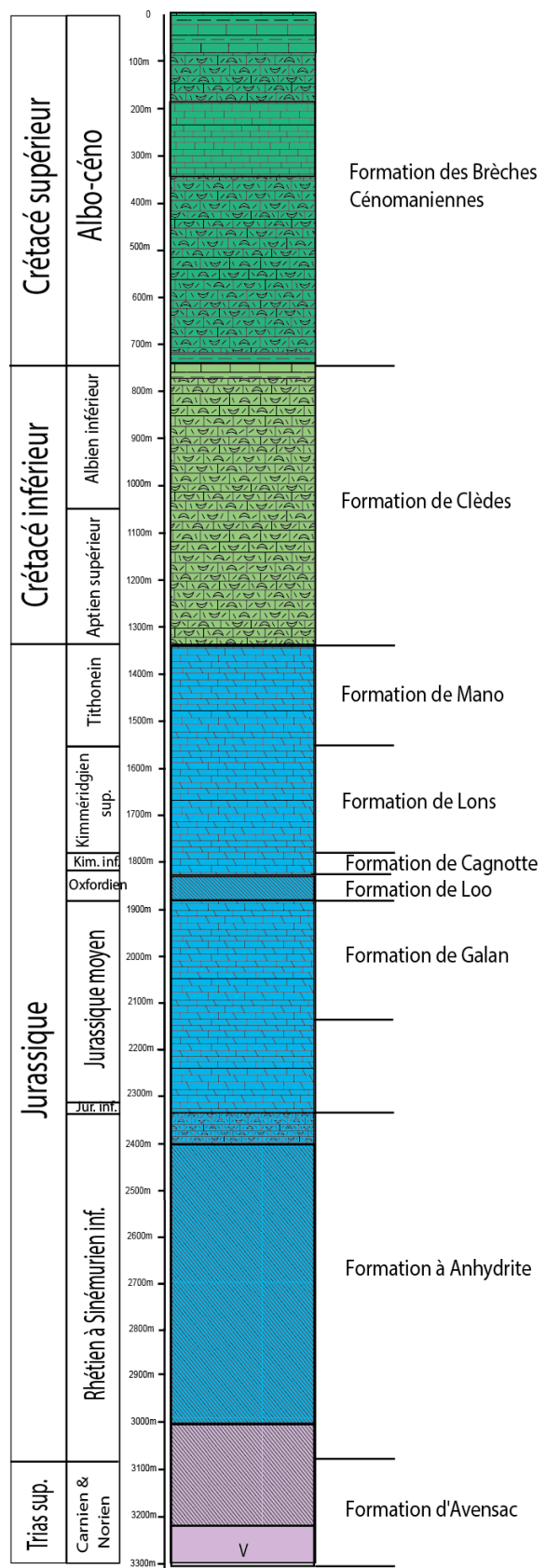


22- Lithostratigraphic log and detailed summary table for the borehole LA-2



23- Lithostratigraphic log and detailed summary table for the borehole PSI-1

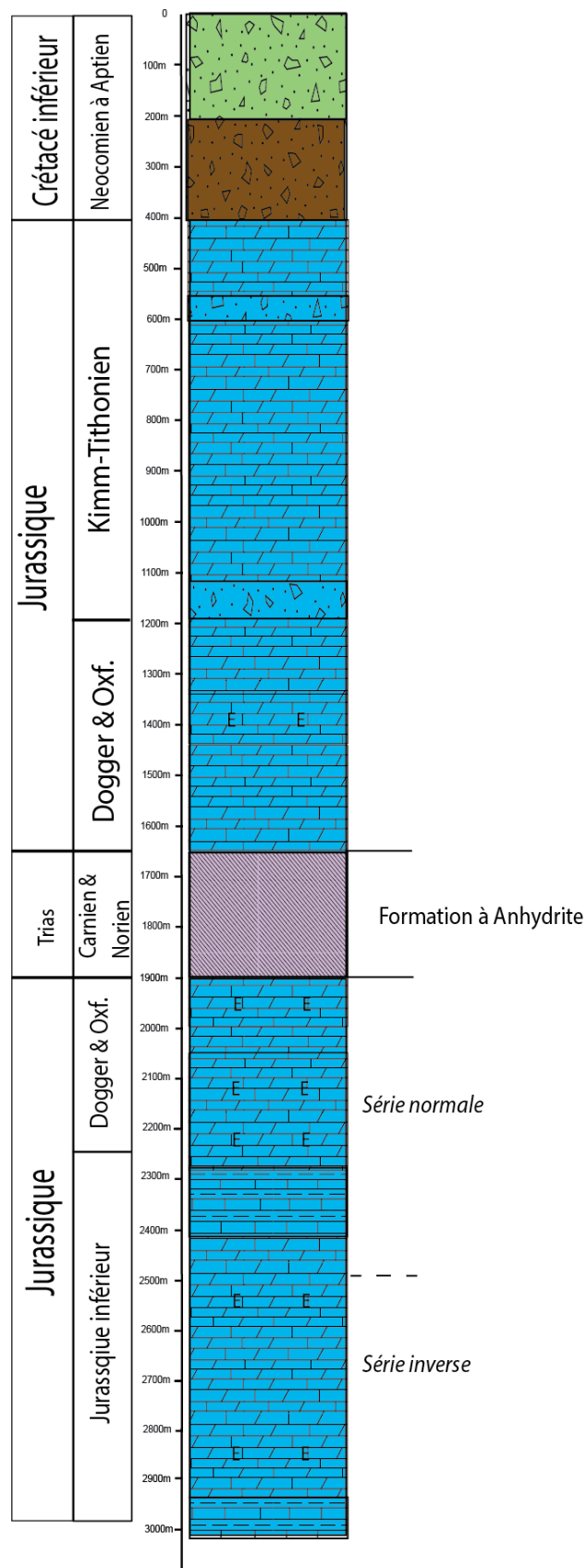
PSI 1



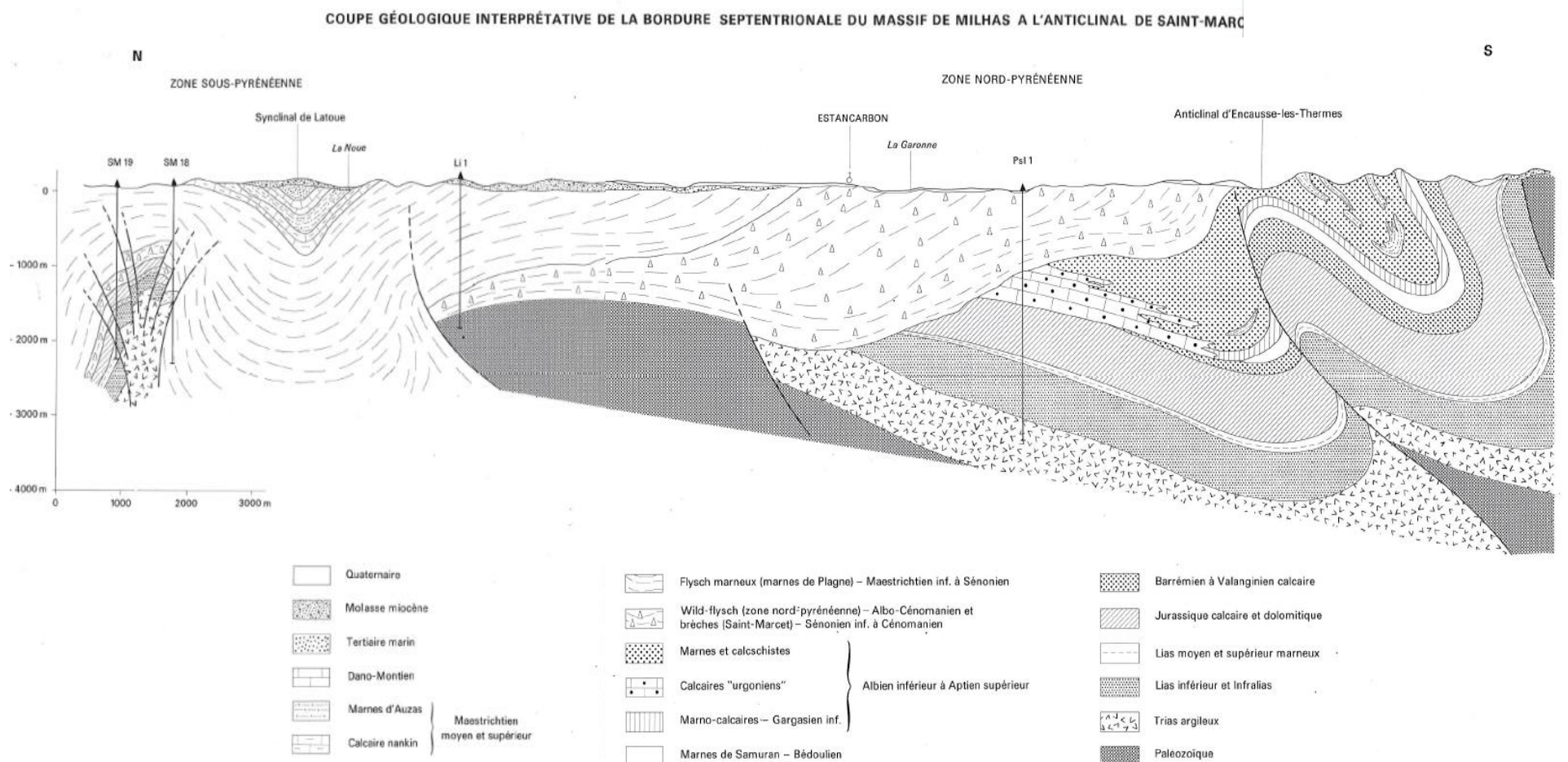
U

24- Lithostratigraphic log and detailed summary table for the borehole LOO-1

LOO 1

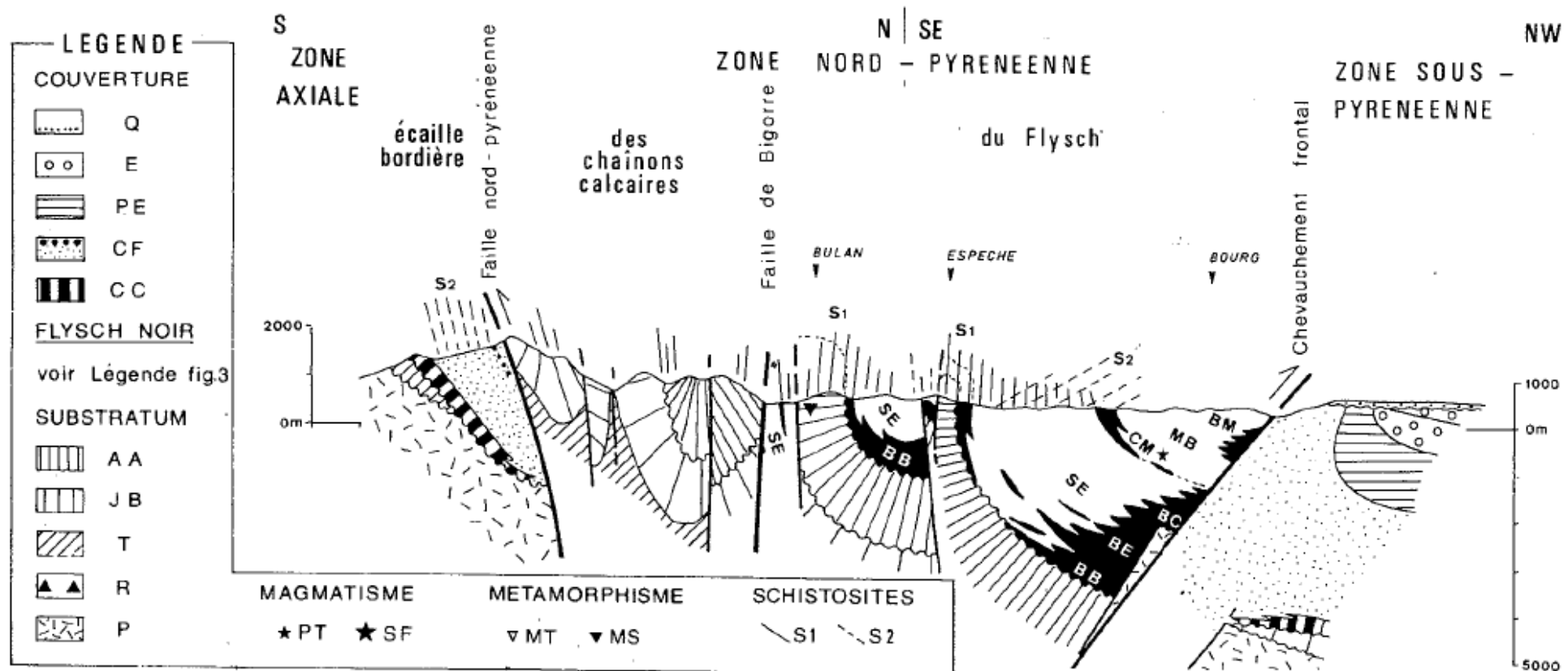


25- Structural cross-section of the south of the Petites Pyrenees and the northern part of the NPZ (Paris et al., 1971)

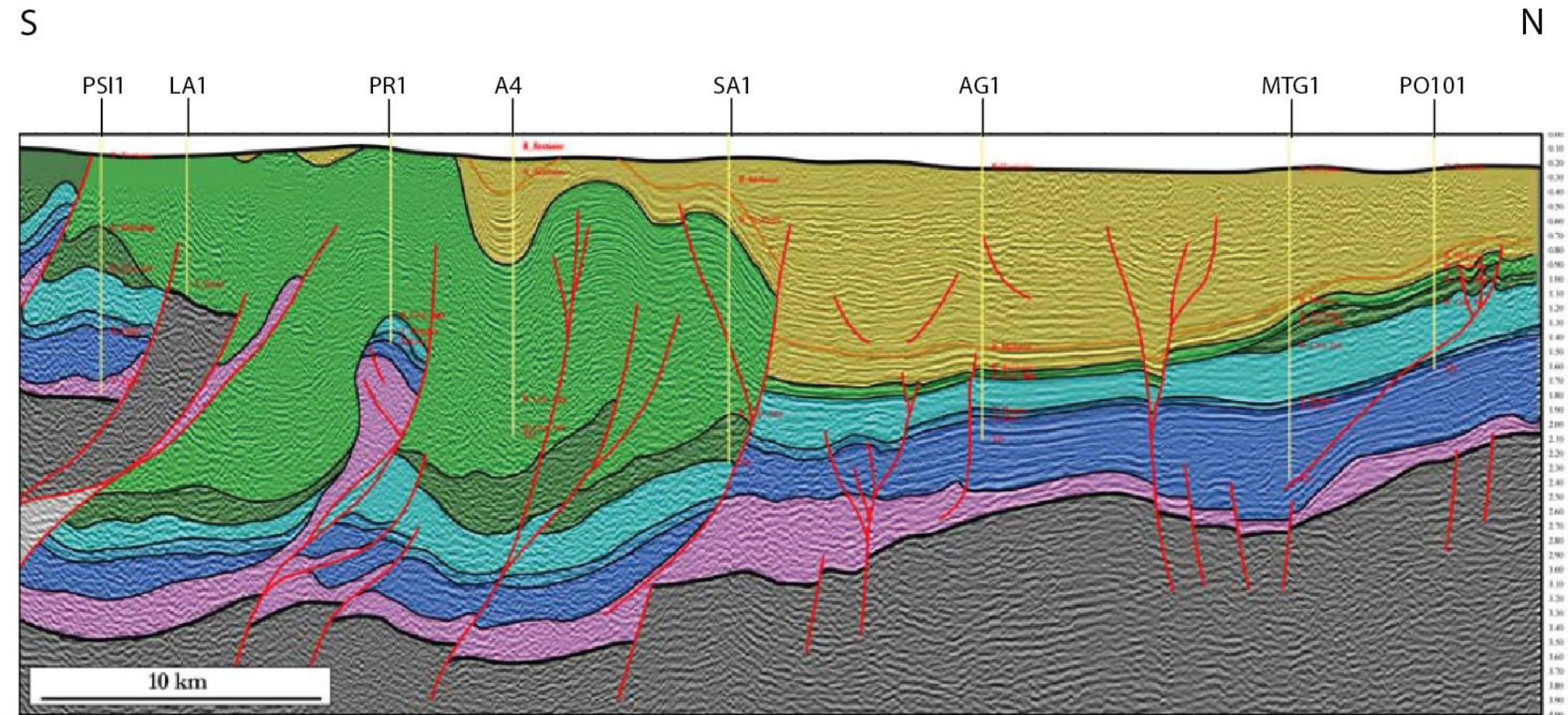


W

26- Structural cross-section of the NPZ (Debroas 1990)

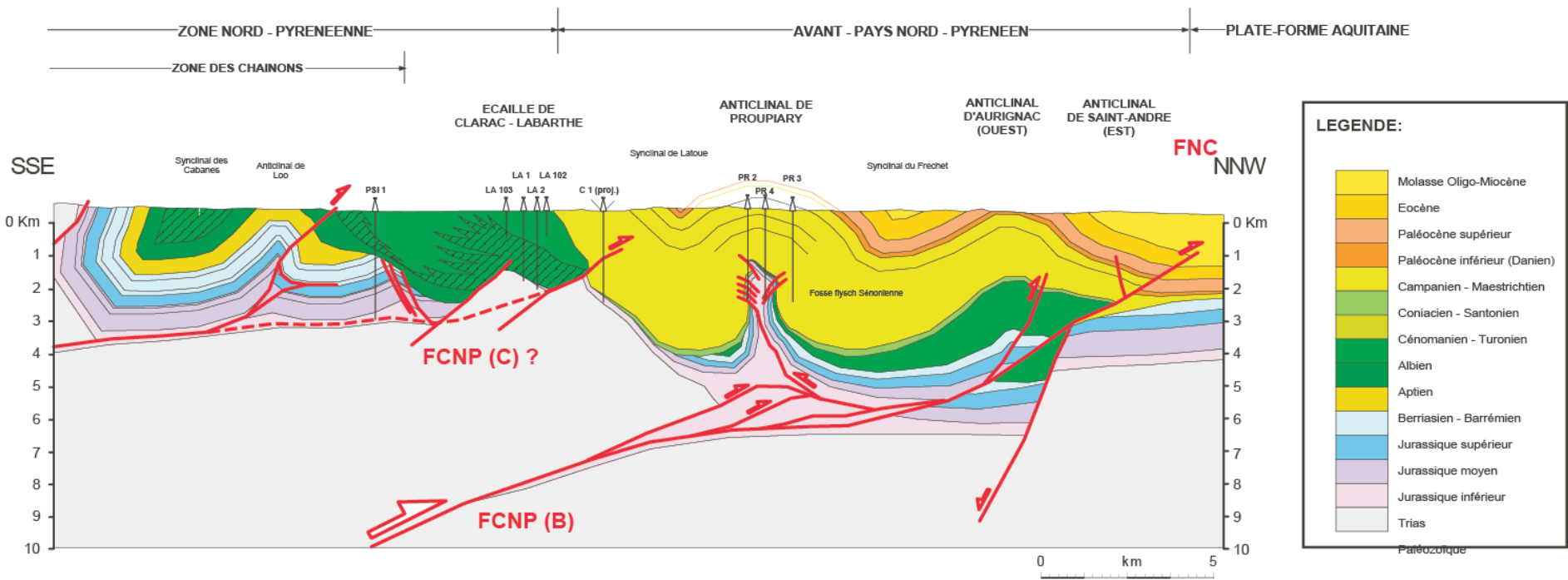


27- Interpreted seismic cross-section (Serrano et al. 2006)



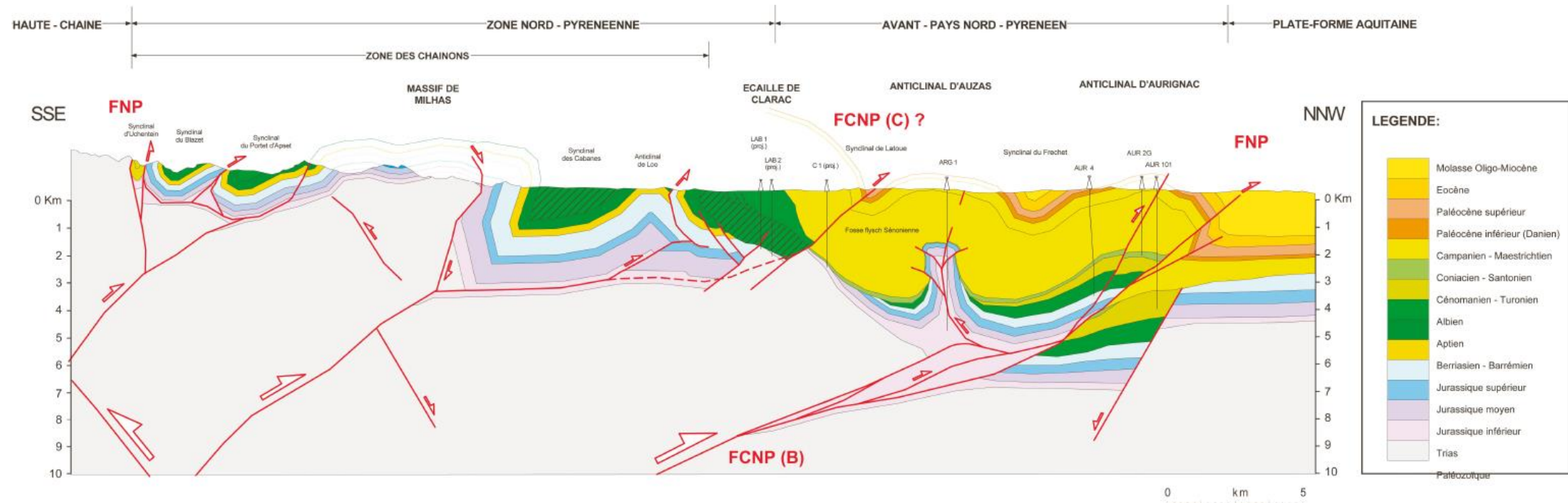
28- Structural cross-section of the NPZ, the Petites Pyrenees and the south of the platform (Total, 1998, n°13)

COUPE TRANSVERSALE n°13



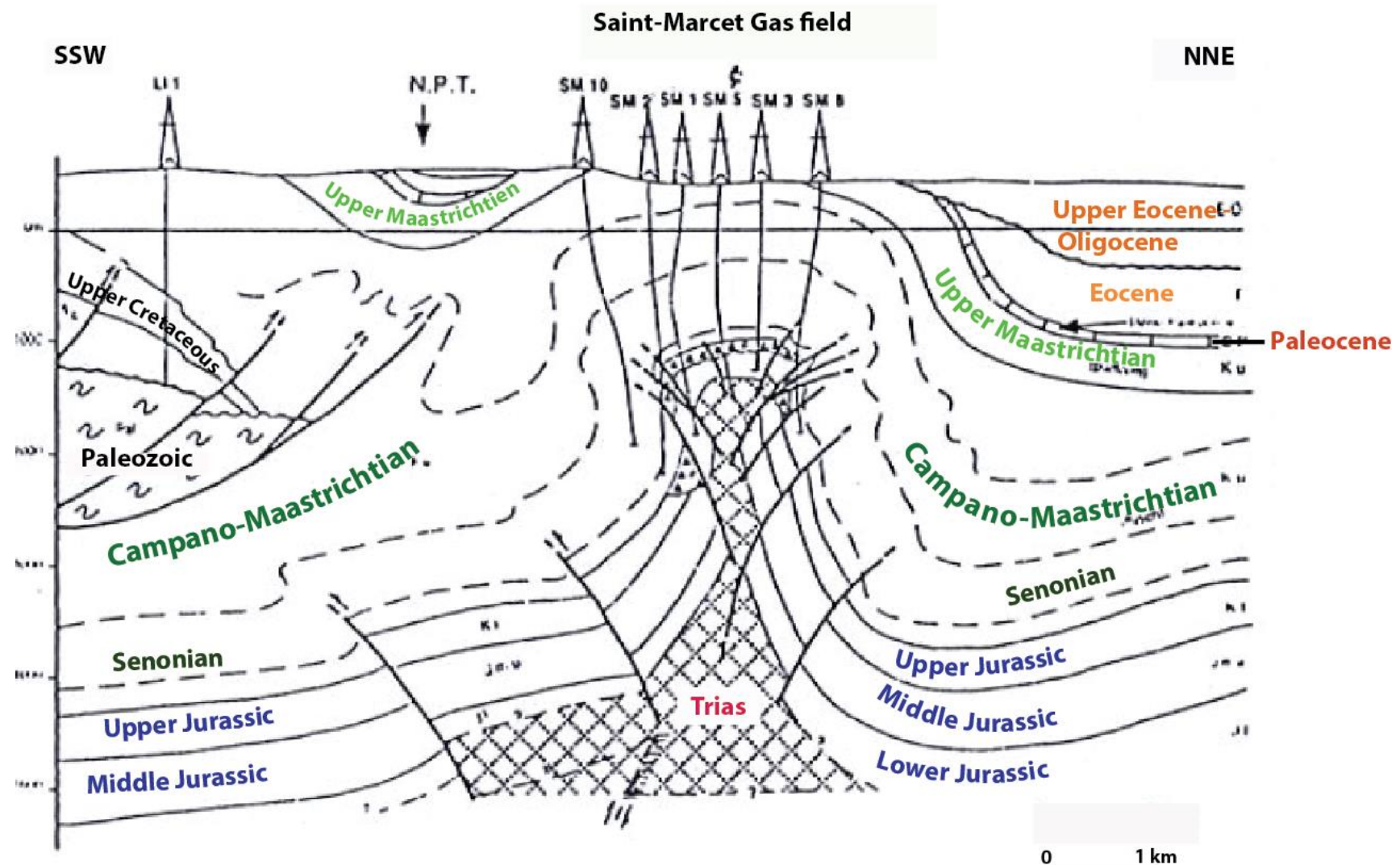
29- Structural cross-section of the NPZ, the Petites Pyrenees and the south of the platform (Total, 1998, n°14)

COUPE TRANSVERSALE n°14

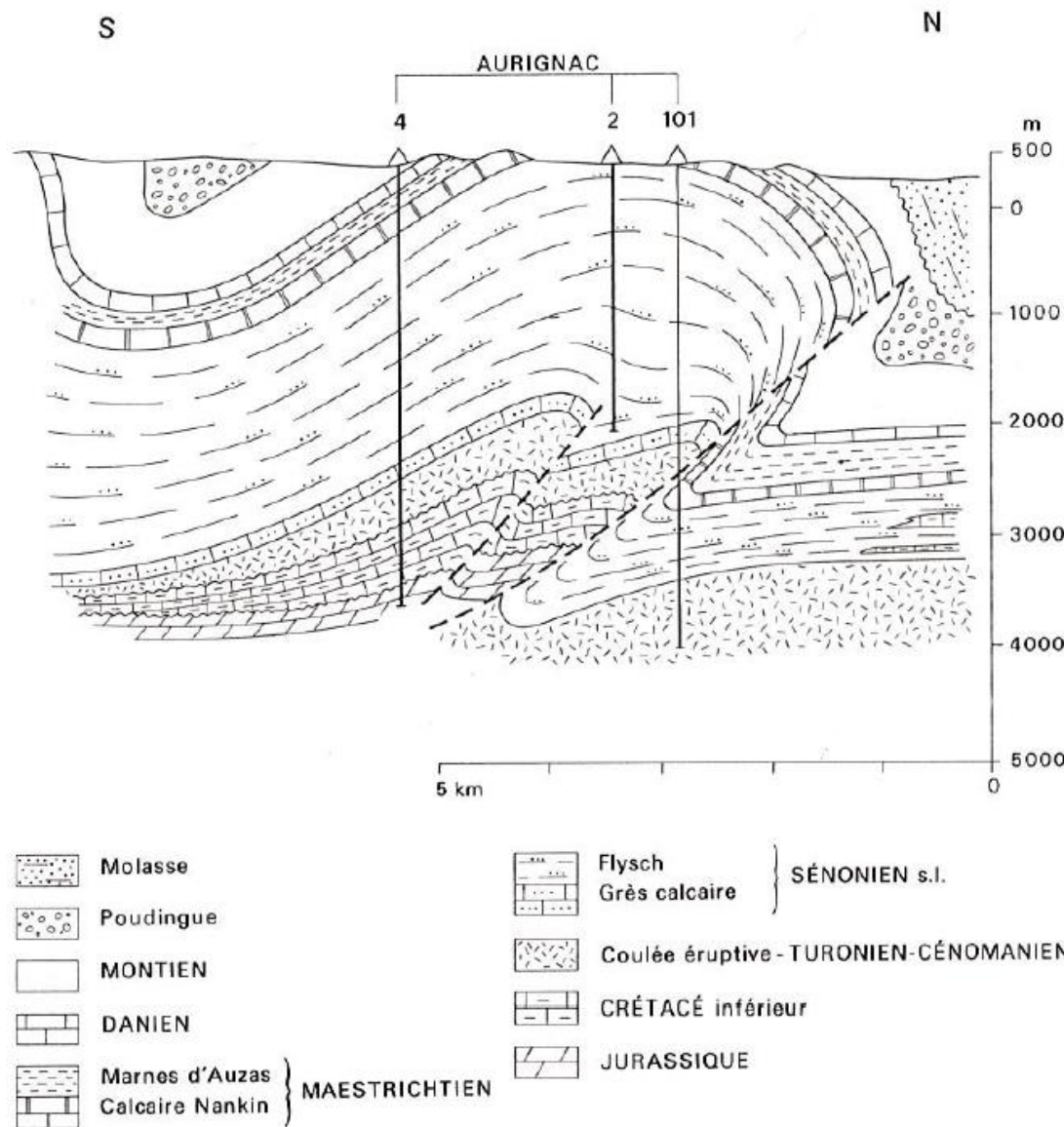


A A

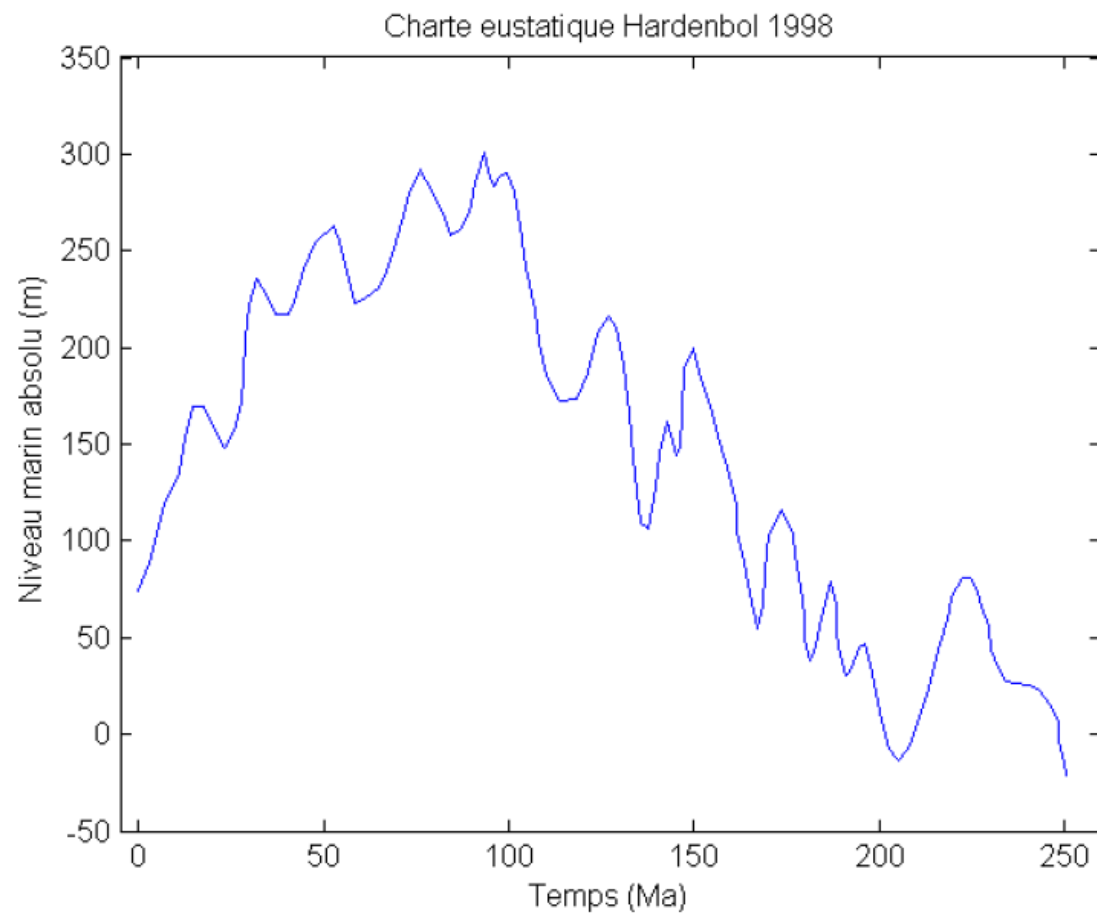
30- Structural cross-section of the Petites Pyrenees (Bourrouilh 1995)



31 - Structural cross-section of the Aurignac anticline (Heritier et al. 1972)



32- Eustatic chart used for the calculation of subsidence (Hardenbol et al., 1998)



Lithology	compaction coefficient (m^{-1})	initial porosity (%)	Bulk density ($kg.m^{-3}$)
Sandstone	0,00027	0,49	2600
Limestone	0,0007	0,5	2671
Anhydrite	0,0009	0,5	2850
Marl	0,00059	0,58	2500
Shale	0,0051	0,63	2500
Conglomerate	0,0003	0,5	2600
Evaporite	0,0009	0,5	2310
Volcanic	0,0004	0,5	2500

33- Coefficients used for the calculation of subsidence (from Vergès (1998) and Allen & Allen (2009))

Number of series	Series	Age top	Base m	Top m	compaction coefficient (m-1)	initial porosity (%)	volumic masse (kg m^- 3)	Paleobathymetry	Eustatism
1	S90A5Do5	237	2147	1850	0,000533	0,4975	2598,55	0	50
2	A55Anh10S5Ophite30	201,3	1850	1579	0,0030285	0,571	2540	0	0
3	C40Do50A10	195,05	1579	994	0,00114	0,513	2653,9	10	25
4	Do50Cs50	190,8	994	812	0,0007	0,5	2671	5	25
5	Cbio70M30	68,04	812	677	0,000667	0,524	2619,7	5	225
6	M50Cs45As5	66	677	641	0,0008435	0,546	2573,4	5	225
7	Do90S5C5	51,9	641	631	0,0006785	0,4995	2667,45	0	250
8	S90A5Gyp5	38	631	528	0,0005115	0,497	2595	0	215
9	M90S10	0	528	0	0,000558	0,571	2510	0	70

34- Calculation table used for the construction of the subsidence curves for the borehole AV-101

Number of series	Series	Age top	Base m	Top m	compaction coefficient (m-1)	initial porosity (%)	volumic masse (kg m^-3)	Paleobathymetry	Eustatism
1	Anhydrite100	200	5070	4470	0,0009	0,5	2850	0	0
2	Anh90Do5C2A3	190,8	4470	3482	0,001012	0,5039	2826,97	0	40
3	Cbio50M50	180	3482	3288	0,000645	0,54	2585,5	10	50
4	M90Do5Ca5	177	3288	3206	0,000601	0,572	2517,1	10	50
5	C60A10Do10Cbio10M10	174,1	3206	3187	0,000689	0,508	2653,9	10	60
6	Cbio70Do20A7Anh3	157,3	3187	2790	0,001014	0,5091	2664,4	5	140
7	C75Do10V10A5	152,1	2790	2393	0,00089	0,5065	2645,35	5	140
8	C75Do10Cbio10A5	145	2393	1963	0,00092	0,5065	2662,45	10	155
9	Cbio90S5A5	125	1963	1720	0,0008985	0,506	2658,9	10	215
10	Cbio90S5A2Do3	119	1720	1517	0,0007665	0,5021	2664,03	10	210
11	As95Do4Pyr1	66	1517	1438	0,004924	0,6248	2506,84	0	225
12	Dobio95A5	59,2	1438	1406	0,00092	0,5065	2662,45	0	215
13	S85Grv5M10	56	1406	1304	0,0003035	0,4995	2590	10	250
14	As100	51,9	1304	1289	0,0048585	0,623	2505	0	260
15	S80Cong15Grv5	38	1289	1247	0,000276	0,492	2600	5	230
16	M95Grv5	33,9	1247	1030	0,0005755	0,576	2505	0	175
17	M95Grv5	15,97	1030	0	0,0005755	0,576	2505	0	125

35 - Calculation table used for the construction of the subsidence curves for the borehole MTG - 1

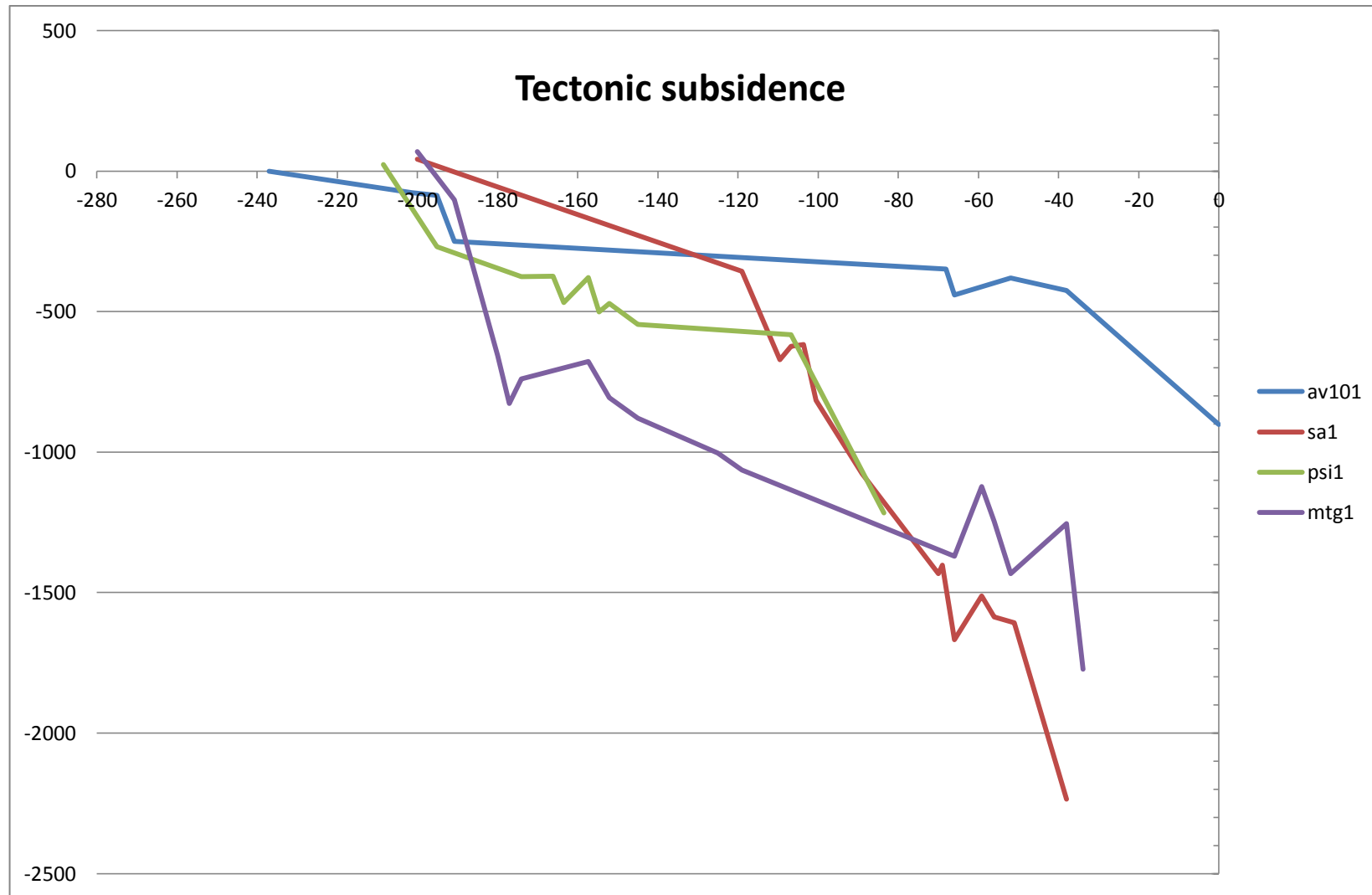
Number of series	Series	compaction coefficient (m-1)	initial porosity (%)	volumic masse (kg m^- 3)	Paleobathymetry	Eustatism	Age top	Base m	Top m
1	Anhydrite	0,0009	0,5	2850	5	0	200	5202	4202
2	Cs25Ca25Cm25Cb10Calcite5	0,000893	0,51	2650,35	10	190	119	4202	3793
3	basalte	0,0004	0,5	2500	0	210	109,5	3793	3615
4	Cs30Ca30C5M5G20Ciment5Anh5	0,0010255	0,514	2641,95	150	210	106,75	3615	3583
5	Cs40Ca40C10M10	0,0008875	0,514	2641,8	10	275	103,6	3583	3465
6	basalte	0,0004	0,5	2500	0	290	100,5	3465	3398
7	basalte	0,0004	0,5	2500	0	275	89	3398	1954
8	M70G10Cog10A5V5	0,000745	0,5615	2500	150	260	70	1954	1914
9	Mc80Ms10Cs5Ca5	0,0008215	0,562	2539,2	100	260	69	1914	886
10	M60Cs30Ms10	0,000564	0,5505	2549,2	0	225	66	886	611
11	C70Do20A10	0,00114	0,513	2653,9	0	220	59,2	611	486
12	G50Cs40A10	0,000925	0,508	2618,4	0	220	56	486	231
13	C40G10Cm50	0,000646	0,507	2646,8	5	250	51	231	182
14	A60Grv10Ms15Mc15	0,0032565	0,5935	2523,55	0	225	38	182	132
15	A60Grv10Ms15Mc15	0,0032565	0,5935	2523,55	0	150	15	132	0

36- Calculation table used for the construction of the subsidence curves for the borehole SA-1

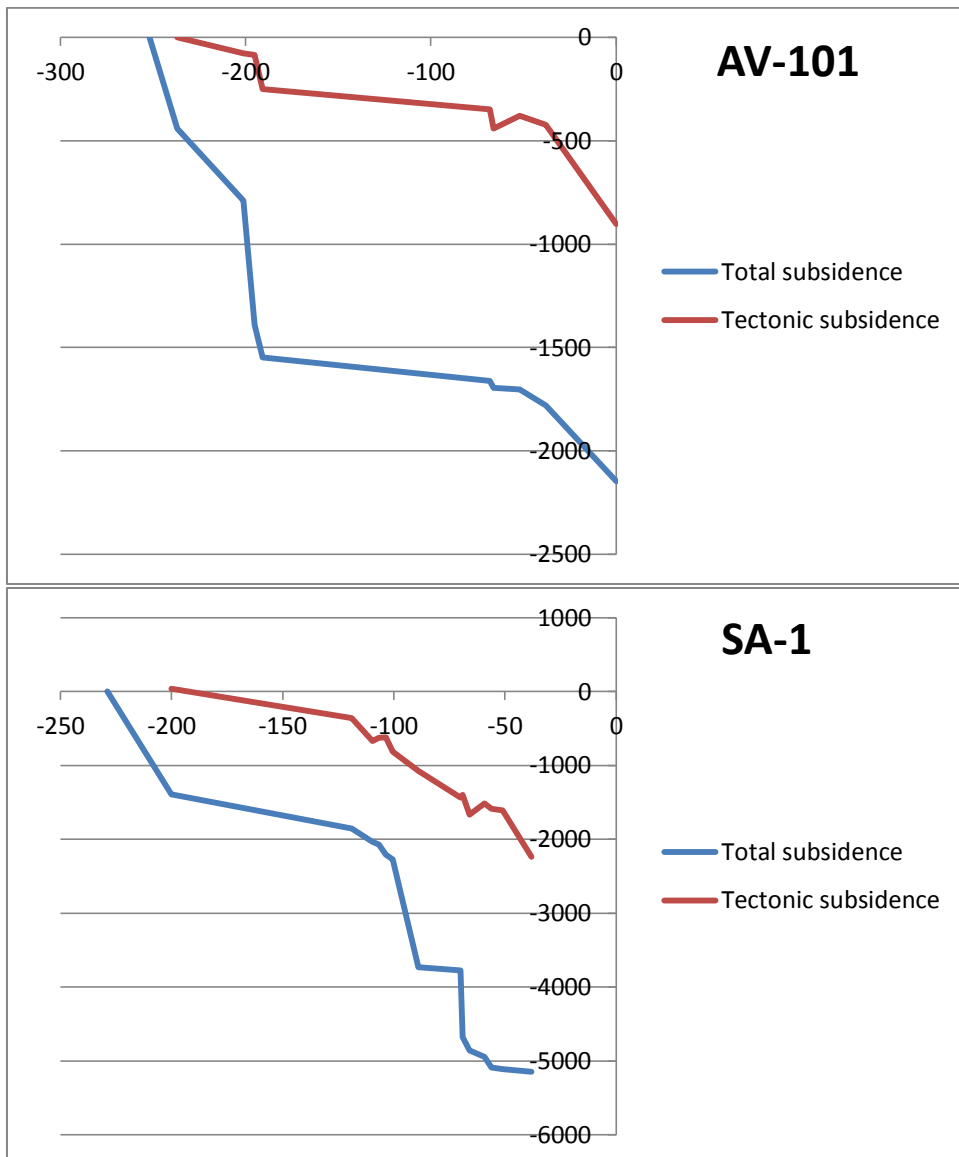
Number of series	Series	Age top	Base m	Top m	compaction coefficient (m- 1)	initial porosity (%)	volumic masse (kg m^-3)	Paleobathymetry	Eustatism
1	D010Anh80C5Ophite5	208,5	3290	2313	0,000845	0,5	2805,65	5	0
2	D010Anh80C5Ophite5	195,05	2313	2268	0,000845	0,5	2805,65	5	25
3	C70A30	174,1	2268	2109	0,00202	0,539	2619,7	10	75
4	Do90anh2C3As2Ablack3	166,1	2109	1873	0,000924	0,5065	2666,03	10	50
5	Do100	163,5	1873	1798	0,0007	0,5	2671	10	50
6	Anh90C5Do5	157,3	1798	1798	0,00088	0,5	2832,1	5	105
7	Cbio50Do50	154,7	1798	1769	0,0007	0,5	2671	5	105
8	Do60Cbio40	152,1	1769	1532	0,0007	0,5	2671	5	105
9	Do50Cbio50	145	1532	1332	0,0007	0,5	2671	5	155
10	C90A5Calcite2Anh3	106,75	1332	758	0,00093	0,5065	2671,4	5	275
11	A33M33S34	83,6	758	0	0,0019695	0,5659	2534	100	225

37- Calculation table used for the construction of the subsidence curves for the borehole PSI-1

38- Summarizing plot of the tectonic subsidence realized for the boreholes AV-101, MTG-1, SA-1 and PSI-1 with the software *subsidence.exe*



39- Subsidence curves pour les puits AV-101 et SA-1



40- Subsidence curves pour the boreholes PSI-1 and MTG-1

